When the Mean Is Not Enough: The Distribution of Inflation Expectations and Inflation Dynamics

Joy Bayan

October 13, 2026

Click here for the latest draft

Abstract

The representative-agent New Keynesian Phillips Curve assumes common inflation expectations across agents, while empirical applications typically summarize heterogeneous expectations by their mean. This paper asks whether the mean is a sufficient statistic for the role of expectations in inflation dynamics or whether the distribution of expectations also matters. Using individual responses from the University of Michigan Survey of Consumers from 1990 to 2025, I estimate inflation-expectation densities and use functional principal component analysis to characterize changes in their shape over time. Accounting for distributional features in the fixed-reference specification produces a steeper estimated aggregate Phillips Curve slope while reducing the explanatory role of the mean expectation. During the COVID inflation surge, the right tail of the distribution thickened before the entire distribution shifted rightward, suggesting that changes in the distribution can provide early signals of inflationary pressures. The results suggest that distributional information supplements mean expectations in explaining inflation dynamics, with additional predictive information during COVID.

JEL Codes: C4, C55, E31, E24, D84, C38
Keywords: Inflation expectations, New Keynesian Phillips Curve, heterogeneous beliefs, inflation, functional principal component analysis, survey data

1 Introduction

The representative-agent New Keynesian Phillips curve (NKPC) with full-information rational expectations relates current inflation to expected future inflation $E_t[\pi_{t+1}]$, economic slack x_t, and a cost-push shock ε_t:

$$\pi_t = \beta E_t[\pi_{t+1}] + \kappa x_t + \varepsilon_t. \tag{1}$$

The rational-expectations hypothesis links forecasts to model-implied predictions (Muth, 1961). Under the full-information benchmark above, agents share a common conditional forecast of aggregate inflation. Rational expectations alone, however, do not require identical forecasts when agents have different information. Meeks and Monti (2023) highlight a related aggregation problem: the cross-sectional average of individual expectations need not satisfy the law of iterated expectations even when each individual's expectations do. Replacing model expectations with a survey mean therefore requires additional assumptions. This paper examines whether the distribution of household inflation expectations contains information about inflation beyond its mean.

A related question is whether expectations only respond to macroeconomic developments or can also generate fluctuations. Following Ascari, Bonomolo, and Celani (2024), I allow for autonomous expectation innovations alongside endogenous adjustment. This motivates studying distributional movements as potential sources of subsequent inflation dynamics.

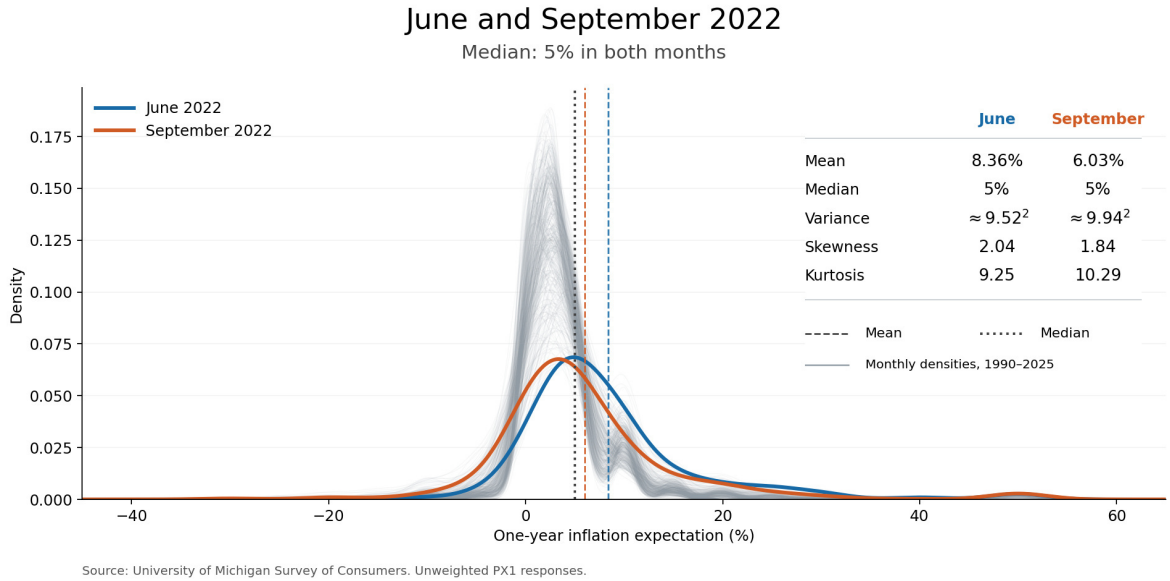


Figure 1.1: One-Year-Ahead Inflation Expectations: June and September 2022

Using monthly observations from the University of Michigan Survey of Consumers from 1990 to 2025, I distinguish between changes in average expectations and changes in where expectations are concentrated in Figure 1.1. Between June and September 2022, mean one-year-ahead inflation expectations fell from 8.36% to 6.03%, while the median

remained at 5%. The higher June mean alone does not establish whether expectations rose broadly across households or primarily among those reporting high inflation forecasts. Despite the lower mean, variance and kurtosis are higher in September. These moments alone do not show where probability mass changed. Examining the densities makes the location and direction of these changes visible.

These observations motivate three questions. Do rightward and leftward shifts, together with changes in the upper and lower tails of the expectations distribution, contain information about inflation beyond mean expectations? In what sequence do these distributional changes unfold during macroeconomic crises? What information do their dynamics provide about subsequent inflation?

The central finding is that the COVID-era adjustment in household inflation expectations began with upper-tail expansion before developing into a broader rightward shift. The share of respondents expecting inflation above 10 percent increased from 1.22 percent in February 2020 to 5.39 percent in April 2020, preceding the sustained rightward movement in 2021. COVID-period local projections show that rightward distributional movements are positively associated with subsequent inflation at horizons of one, three, six, and eight months, conditional on mean expectations and macroeconomic controls. The timing and direction differ from the Great Recession, when a leftward shift preceded lower-tail expansion.

I estimate each month's expectation density from individual survey responses using kernel density estimation (Silverman, 1986). The resulting functional time series tracks the population distribution across repeated cross-sections, without requiring a panel that follows the same households throughout the sample. Let $f_t(\pi^e)$ denote the cross-sectional density of one-year-ahead inflation expectations. Following the functional-data approach in Ramsay and Silverman (2005), I define a time-average reference density and measure monthly deviations from it:

$$\bar{f}(\pi^e) = \frac{1}{T}\sum_{t=1}^{T} f_t(\pi^e), \qquad \widetilde{f}_t(\pi^e) = f_t(\pi^e) - \bar{f}(\pi^e). \tag{2}$$

The reference density is fixed within the sample. Subtracting this common reference retains movements in location alongside changes in dispersion and tail behavior. Figure 1.2 illustrates the resulting deviations: positive values indicate more probability mass at a given expectation level than in the reference density, while negative values indicate less.

I summarize these deviations using functional principal component analysis (FPCA):

$$\widetilde{f}_t(\pi^e) \approx \sum_{k=1}^{3} \xi_{k,t}\phi_k(\pi^e), \tag{3}$$

where $\phi_k(\pi^e)$ are orthonormal basis functions and $\xi_{k,t}$ are their associated scores. The first three components explain approximately 96% of the temporal variation in the expectation densities. Their estimated shapes are interpreted as dispersion, directional shifts, and tail

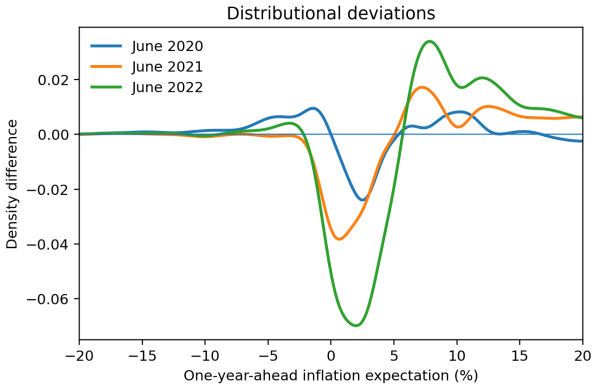


Figure 1.2: Distributional Deviations from the Time-Average Reference Density

behavior. Each score, together with its basis function, describes how probability mass moves relative to the reference density.

For a fixed number of components, FPCA minimizes the sample integrated squared reconstruction error over orthonormal bases (Ramsay and Silverman, 2005; Bosq, 2000). This property allows the main directions of density variation to be summarized with few regression coefficients. Economic interpretations follow from the estimated component shapes; their relevance for inflation is assessed through conditional regressions and forecasting exercises.

The empirical Phillips curve includes these scores alongside mean expectations:

$$\pi_t = a + \beta_e \bar{\pi}_t^e + \kappa x_t + \sum_{k=1}^{3} \alpha_k \xi_{k,t} + \delta' Z_t + u_t, \tag{4}$$

where $\bar{\pi}_t^e$ is mean one-year-ahead survey expectations and Z_t collects additional controls, including long-run expectations and supply factors. The survey mean is an observed regressor, distinct from the model expectation in the theoretical NKPC. The score terms approximate $\int \gamma(\pi^e)\widetilde{f}_t(\pi^e)\,d\pi^e$, where $\gamma(\pi^e)$ weights density changes across expectation levels and $\alpha_k = \int \gamma(\pi^e)\phi_k(\pi^e)\,d\pi^e$. Each α_k measures the component's association with inflation conditional on mean expectations and the remaining controls.

Results and contributions. The results are threefold. First, the distribution contains information about inflation beyond mean expectations. In the full-sample Phillips curve estimates, dispersion and the tail component are particularly relevant. Including the distributional components reduces the estimated coefficient and statistical significance of mean expectations and steepens the estimated inflation–slack relationship. The components remain jointly significant after controlling for the mean. Second, distributional adjustment differs across crises. During COVID, upper-tail expansion precedes a broader rightward shift; during the Great Recession, a leftward shift precedes lower-tail expansion. The decomposition distinguishes these sequences and allows their conditional relationships with inflation to be examined separately. Joint tests reject equality of the distributional coefficients between COVID and ordinary months. Third, distributional information is relevant for aggregate dynamics and forecasting. COVID-period local

projections show a short-run association between rightward movements and subsequent inflation conditional on mean expectations. The VAR evidence indicates that the components adjust at different speeds, while the forecasting exercise finds gains from including the tail component or all three components jointly.

Related literature. The closest related paper is Meeks and Monti (2023), who derive a heterogeneous-beliefs Phillips curve with an additional term reflecting the distribution of expectations. Their empirical results show that distributional information improves fit and, in several specifications, strengthens the estimated inflation-slack relationship, while mean expectations remain important. Their implementation centers individual forecasts around each period's mean, separating location movements from the centered distribution.

In contrast, I retain forecasts on their original scale and subtract a common time-average density. This representation allows upper-tail expansion and broader rightward adjustment to be traced within the same decomposition. I show that mean-centering does not consistently reduce the correlation with the mean in this sample. Mean-centering removes the common translation of each month's distribution before FPCA, but it does not mechanically separate distributional shape from movements in the mean over time. Indeed, the absolute correlations between the first three fixed-reference scores and mean expectations are 0.704, 0.531, and 0.301, compared with 0.678, 0.545, and 0.351 for the corresponding mean-centered scores over January 1990–January 2025. Mean-centering therefore does not consistently reduce the correlation between the functional scores and mean expectations in this sample. I consequently evaluate whether the functional components contain additional information conditional on mean expectations, rather than treating low correlation with the mean as a requirement for identifying distributional information.

My textbook methodology also builds on functional time-series econometrics (Ramsay and Silverman, 2005; Bosq, 2000; Hall and Horowitz, 2007; Park and Qian, 2012; Chang, Kim, and Park, 2016). Petersen and Müller (2016) develop invertible transformations for analyzing densities while respecting their non-negativity and unit-integral constraints when transformed back. I use untransformed density deviations so that the components directly describe movements of probability mass.

Chang, Chen, and Schorfheide (2024) and Chang, Kim, and Park (2025) develop models that jointly describe aggregate variables and cross-sectional distributions. Applications examine the distributional effects of monetary policy (Chang and Schorfheide, 2024) and economic uncertainty (Huber, Marcellino, and Tornese, 2024); the latter also develops functional local projections. Applied to inflation expectations, Chang, Gómez-Rodríguez, and Hong (2022) examine how economic shocks affect heterogeneous beliefs,

while Anderl and Caporale (2024) study functional shocks to expectations and real interest rates across forecast horizons. These functional shocks are jointly determined rather than individually analyzed like in my analysis.

Phillips curve estimation with distributional aggregation. Several theoretical approaches motivate extending the benchmark Phillips curve. Mankiw and Reis (2002) show how staggered information updating introduces a history of expectations into inflation dynamics. Meeks and Monti (2023) emphasize the aggregation of heterogeneous beliefs. Ascari and Sbordone (2014) and Cogley and Sbordone (2008) show that positive trend inflation changes the forward-looking terms in the linearized Phillips curve. A related empirical literature uses city- and state-level variation in inflation and labor-market conditions to estimate the Phillips curve (Hooper, Mishkin, and Sufi, 2020; Fitzgerald, Jones, Kulish, and Nicolini, 2024; McLeay and Tenreyro, 2020) and explain how regional variation within a common monetary regime can mitigate the identification problem created by endogenous monetary policy in aggregate data. Hazell, Herreño, Nakamura, and Steinsson (2022) show how time fixed effects absorb common movements in long-run inflation expectations and develop a multi-region model connecting regional estimates to the aggregate Phillips curve. Regional data also provide evidence on nonlinearities: Babb and Detmeister (2017) find a steeper inflation–unemployment relationship when unemployment is low. The treatment of expectations matters for these conclusions. Doser, Nunes, Rao, and Sheremirov (2023) find that controlling for consumer inflation expectations substantially weakens evidence of nonlinearity in both aggregate and regional data. Combining cross-city and aggregate evidence, Beaudry, Hou, and Portier (2026) likewise emphasize expectations controls and question the robustness of attributing recent inflation to tight labor markets operating through a nonlinear curve. These findings motivate my examination of how measuring expectations affects aggregate Phillips curve estimates.

The choice of slack measure and the economic environment also matter for this debate. Barnichon and Shapiro (2024) find that the vacancy-to-unemployment ratio and vacancy filling cost proxies explain inflation better than unemployment alone, emphasizing shifts in the Beveridge curve. Hottman and Reyes-Heroles (2023) examine how trade openness changes the slope and intercept of the Phillips curve. My analysis focuses on how measuring expectations affects this estimated relationship.

Information and expectation formation. Sims (2003) shows how limited capacity to process information can generate gradual responses to new information. Carroll (2003) studies the diffusion of information from professional forecasters to households. Coibion, Gorodnichenko, and Kamdar (2018) and Coibion and Gorodnichenko (2015) provide evidence on information rigidities that motivate departures from the full-information rational-expectations benchmark (Coibion, Gorodnichenko, and Weber, 2022). Personal inflation experiences (Malmendier and Nagel, 2016), learning from local price changes

(Łyziak, Pedersen, and Stanisławska, 2025), and political affiliation (Binder, Kamdar, and Ryngaert, 2024) also help explain differences in reported beliefs. Reviews synthesize evidence on the measurement, formation, and economic implications of subjective expectations (Coibion, Gorodnichenko, and Kamdar, 2018; Weber, D'Acunto, Gorodnichenko, and Coibion, 2022; D'Acunto, Malmendier, and Weber, 2023).

This literature explains how households obtain and process information when forming expectations. Changes in information exposure can move beliefs even when contemporaneous aggregate outcomes are unchanged. In a randomized information experiment, Coibion, Gorodnichenko, and Weber (2022) find revisions in household inflation expectations and subsequent spending effects. Such evidence supplies a mechanism for belief movements beyond observed macroeconomic conditions. Uneven updating across households can change tails or shift the distribution, the object summarized by my fixed-reference scores. Whether naturally occurring expectation innovations are exogenous remains an identification question.

Survey evidence documents substantial disagreement among households (Mankiw, Reis, and Wolfers, 2003) and firms (Coibion, Gorodnichenko, and Kumar, 2018). Łyziak and Sheng (2023) document differences in households' propensity to learn from professional forecasters and show how heterogeneous updating contributes to disagreement. Reis (2021b) relates disagreement to differences between survey and market-based expectations. Rich and Tracy (2021) distinguish disagreement across respondents from uncertainty within an individual's beliefs. Using a survey of economists, Mirkov and Steinhauer (2018) show that asymmetry in the aggregate forecast distribution mainly reflects disagreement across respondents rather than asymmetry in their individual forecast distributions. The densities studied here describe reported point forecasts: their dispersion measures cross-sectional disagreement, and their tails describe the prevalence of unusually high or low expectations.

Tail behavior and crisis episodes. Recent work emphasizes information contained in the tails of expectations distributions. Grishchenko and Wilcox (2024) examine probabilities of extreme inflation outcomes using professional forecasts. Ascari, Bonomolo, and Celani (2024) show that restricting attention to the first two moments can understate the macroeconomic effects of expectations shocks, with particularly large effects associated with left-tail perturbations. These findings motivate distinguishing movements in the upper and lower tails rather than summarizing both with a single measure of dispersion.

Autonomous movements in expectations. Ascari, Bonomolo, and Celani (2024) explicitly motivate shocks to expectations that arise independently of macroeconomic developments, while recognizing that expectations also respond endogenously. Their lagged-block analysis finds greater predictive relevance from expectations to macroeconomic variables than in the reverse direction. Their structural analysis uses survey and

data-release timing restrictions, while allowing immediate responses to oil prices and uncertainty. They also study right-tail disturbances and the COVID episode. These findings justify examining an autonomous component of expectation formation; they do not establish that all belief movements are exogenous.

My analysis connects this motivation to the sequencing of tail movements and broader shifts in the household expectation distribution. Retaining the original expectation scale allows both to be followed within the same fixed-reference representation. The regressions and local projections examine their information content conditional on the mean and macroeconomic controls; the VAR interpretations depend on the maintained identification restrictions. Orthogonal FPCA components alone do not identify exogenous expectations shocks.

The sequence of adjustment is also relevant. Reis (2021a) describes probability mass moving toward the right tail during 2020, followed by a thinning of the lower tail in early 2021, illustrating changes that averages alone can obscure. Reis (2022) describes increases in skewness and dispersion preceding a broader rise in household expectations during 2021–22. Historical evidence (Binder and Kamdar, 2022) and studies of the pandemic (Bae, Hodge, and Weber, 2024) further motivate examining expectations during periods of disruption. Binder (2020) finds that consumers expressing greater concern about COVID in early March 2020 also report higher expected inflation and a more pessimistic unemployment outlook. Such heterogeneous reactions help motivate examining where the distribution changes when a crisis begins. Armantier et al. (2021) document increases in uncertainty and disagreement alongside more limited adjustment in average expectations early in the pandemic. Armantier et al. (2023) subsequently show that elevated inflation coincided with increased deflation expectations at medium and longer horizons.

Predictive information. A further literature examines whether distributional features of expectations help predict inflation. Tsiaplias (2020) and Brandão-Marques et al. (2023) document predictive information beyond conventional measures of central tendency. Barrales-Ruiz, Islam, Mohammed, and Panovska (2026) examine how expectation moments relate to different parts of the inflation distribution. Doh and Smith (2022) link survey forecasts to VAR-implied forecasts through a Bayesian prior, improving forecasts of inflation tail risks. My local projections and forecasting exercises connect this literature to the measured paths of dispersion, directional shifts, and tails. Recursive VARs trace their joint dynamics with inflation and mean expectations under contemporaneous ordering restrictions (Kilian and Lütkepohl, 2017).

The remainder of the paper is organized as follows. Sections 2–4 present the data, methodology, and empirical strategy. Section 5 reports the aggregate results, and Section 6 concludes. Appendix A contains the regional theory and evidence. Mean-centered comparisons and supplementary dynamic evidence appear in the remaining appendices.

2 Data

The empirical analysis combines monthly national CPI inflation, the national unemployment gap, and measures of household inflation expectations from the University of Michigan Survey of Consumers. Individual one-year-ahead expectations are used to construct the national monthly expectation densities, computed moments, and FPCA scores. The mean longer-run expectation from PX5 enters as a separate control.

Table 1: Data Sources and Transformations

Variable	Source	Construction or use
Aggregate headline inflation	BLS, CPIAUCSL	Annualized monthly headline CPI inflation, $1200\Delta \log P_t$, using seasonally adjusted CPI.
Aggregate unemployment rate	BLS, UNRATE	Monthly civilian unemployment rate.
Aggregate Natural rate of unemployment	CBO, NROUST	Quarterly natural-rate series repeated within quarter. The aggregate unemployment gap is UNRATE minus NROUST.
One-year ahead inflation expectation mean	University of Michigan, PX1 microdata	Monthly mean of finite numerical responses to the one-year-ahead inflation expectation question.
Long-run inflation expectation	University of Michigan, PX5 microdata	Monthly mean of finite numerical responses to the longer-run inflation expectation question.
Expectation densities	Calculations from University of Michigan, PX1 microdata	Author-calculated monthly cross-sectional densities of one-year-ahead inflation expectations.
FPCA functional scores/moments	University of Michigan, PX1 microdata	Author-calculated functional principal-component scores.
Long-run inflation expectations	University of Michigan PX5 data	Long-run inflation expectations
Aggregate monetary policy surprises	Federal Reserve Bank of San Francisco, U.S. Monetary Policy Event-Study Database	Acosta et al. (2025): first principal component of high-frequency changes in money market futures rates over an approximately one-year horizon.
Aggregate oil supply news shocks	Oil Supply News Shock series	Känzig (2021): oil supply news shocks identified using high-frequency oil futures price changes around OPEC announcements.

3 Methodology

3.1 Constructing Inflation-Expectation Densities

Following the literature, I construct a national cross-sectional density of one-year-ahead inflation expectations for each month using individual responses from the University of Michigan Survey of Consumers. Let $f_t(\pi^e)$ denote this monthly density of one-year-ahead inflation expectations. The density function $f_t(\pi^e)$ is constructed with Gaussian kernel density estimator:

$$f_t(\pi^e) = \frac{1}{N_t h_t} \sum_{i=1}^{N_t} K\left(\frac{\pi^e - \pi^e_{i,t}}{h_t}\right), \tag{5}$$

where $\pi^e_{i,t}$ denotes the inflation expectation reported by individual i at time t, N_t is the number of respondents, $K(\cdot)$ is the Gaussian kernel, and h_t is the bandwidth selected using Silverman's rule-of-thumb for smoothing, with an example of f_t post-COVID:

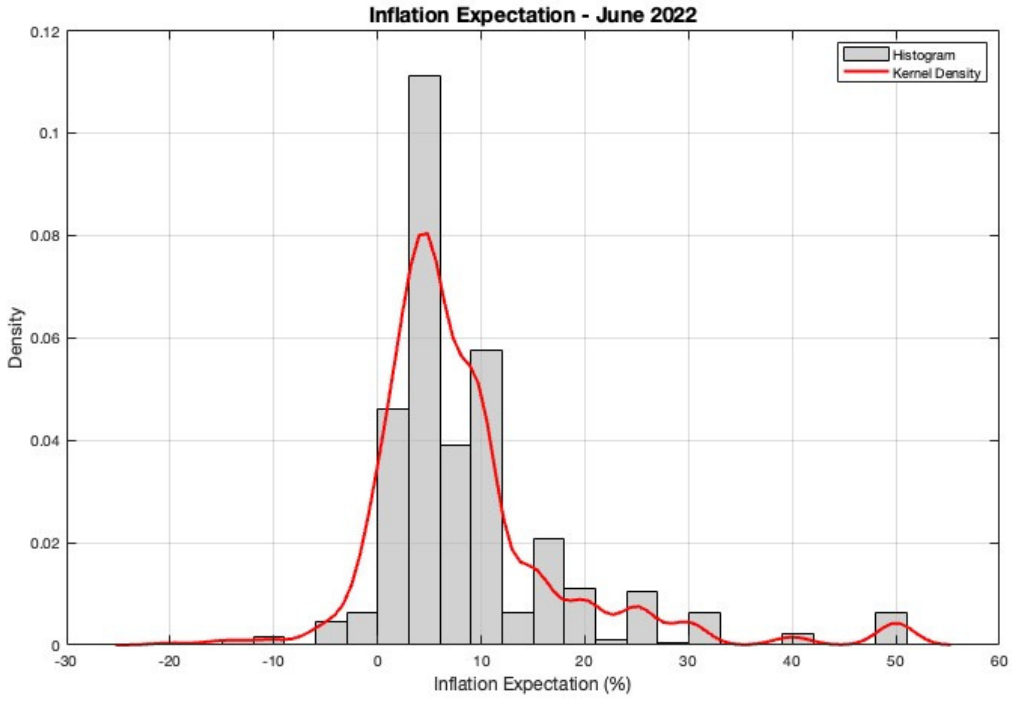


Figure 3.1: Individual Inflation Expectations and the Estimated Density: June 2022

Horizontal axis: individual one-year-ahead inflation expectation (PX1, %). Vertical axis: density. Bars show the histogram; the curve shows the kernel density estimate.

The monthly expectation distribution measured by a non-parametric kernel density itself is treated as the object of interest. Each month's distribution is decomposed into a time-average density and a distributional deviation, which allows me to track directional

changes in distributional shifts and tail behavior and evaluate whether distributional shifts contain information beyond average expectations:

$$\bar{f}(\pi^e) = \frac{1}{T}\sum_{t=1}^{T} f_t(\pi^e),$$
$$\widetilde{f}_t(\pi^e) = f_t(\pi^e) - \bar{f}(\pi^e).$$

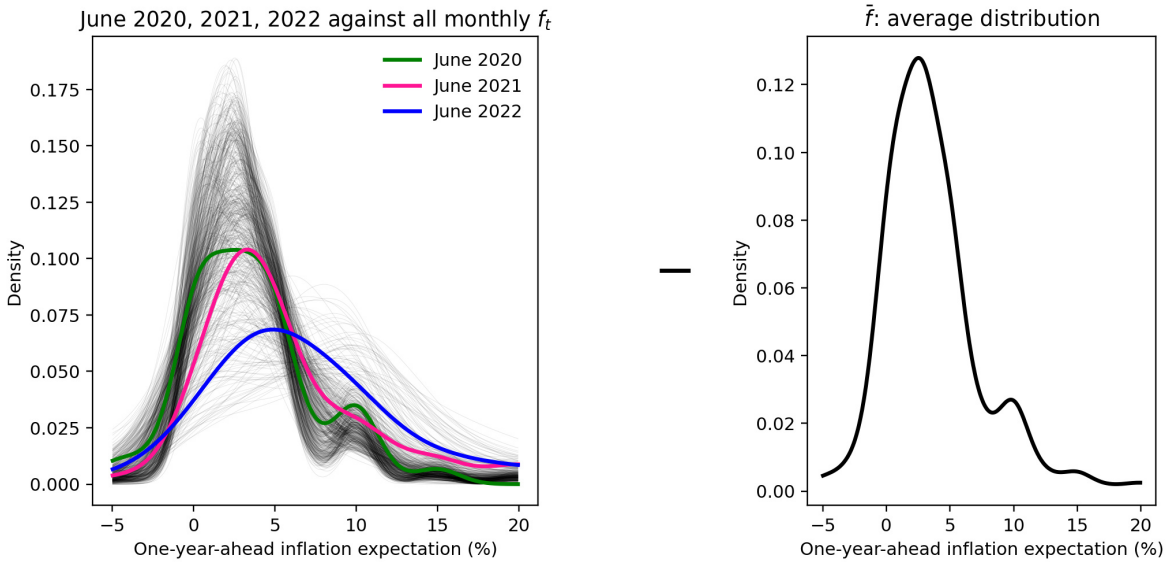


Figure 3.2: Monthly Densities and the Time-Average Reference Density

Left: monthly densities, highlighting June 2020, June 2021, and June 2022. Right: the time-average reference density $\bar{f}(\pi^e)$. The minus sign denotes the subtraction used to form distributional deviations.

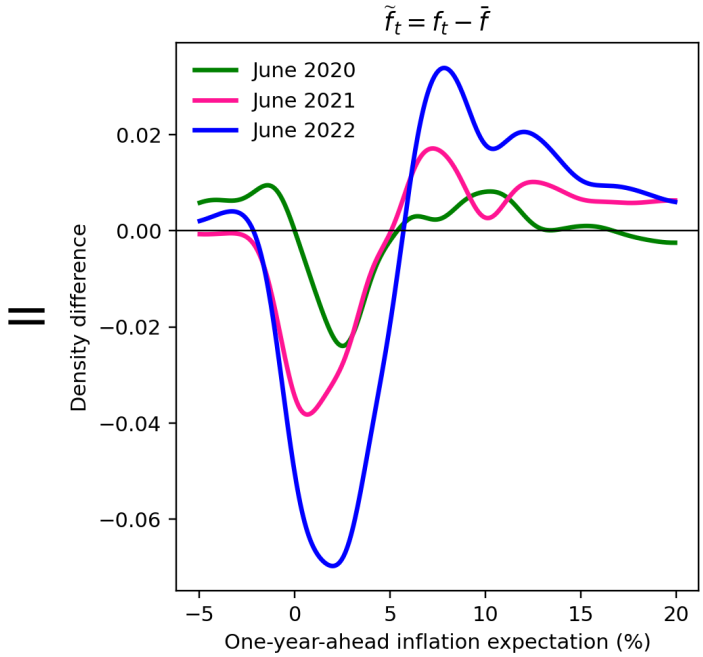


Figure 3.3: Distributional Deviations: June 2020, June 2021, and June 2022

Horizontal axis: one-year-ahead inflation expectation (%). Vertical axis: density deviation $\widetilde{f}_t(\pi^e) = f_t(\pi^e) - \bar{f}(\pi^e)$. Positive and negative values denote more and less density than the reference, respectively.

3.2 Functional Principal Components

Because each density is an infinite-dimensional object, I use functional principal component analysis (FPCA) to obtain a finite-dimensional representation of its variation over time. The Karhunen–Loève expansion expresses the density deviations as

$$\tilde{f}_t(\pi^e) = \sum_{k=1}^{\infty} \xi_{k,t}\phi_k(\pi^e) \approx \sum_{k=1}^{K} \xi_{k,t}\phi_k(\pi^e), \tag{6}$$

where $\phi_k(\pi^e)$ denotes the k-th eigenfunction of the covariance operator and $\xi_{k,t}$ is the score or loading of the associated functional principal component. The approximation retains the first K components. The eigenfunctions satisfy:

$$\int C(\pi^e, \pi^{e'})\phi_k(\pi^{e'})\, d\pi^{e'} = \lambda_k \phi_k(\pi^e), \tag{7}$$

where

$$C(\pi^e, \pi^{e'}) = \frac{1}{T}\sum_{t=1}^{T} \tilde{f}_t(\pi^e)\tilde{f}_t(\pi^{e'}) \tag{8}$$

Its eigenfunction bases are orthogonal, and each eigenvalue λ_k measures the variance captured by the corresponding score $\xi_{k,t}$. These scores summarize patterns of variation in the expectations distribution. The scree plot shows how much variation each component explains and guides the number of 3 scores as they explain 96% of the variation.

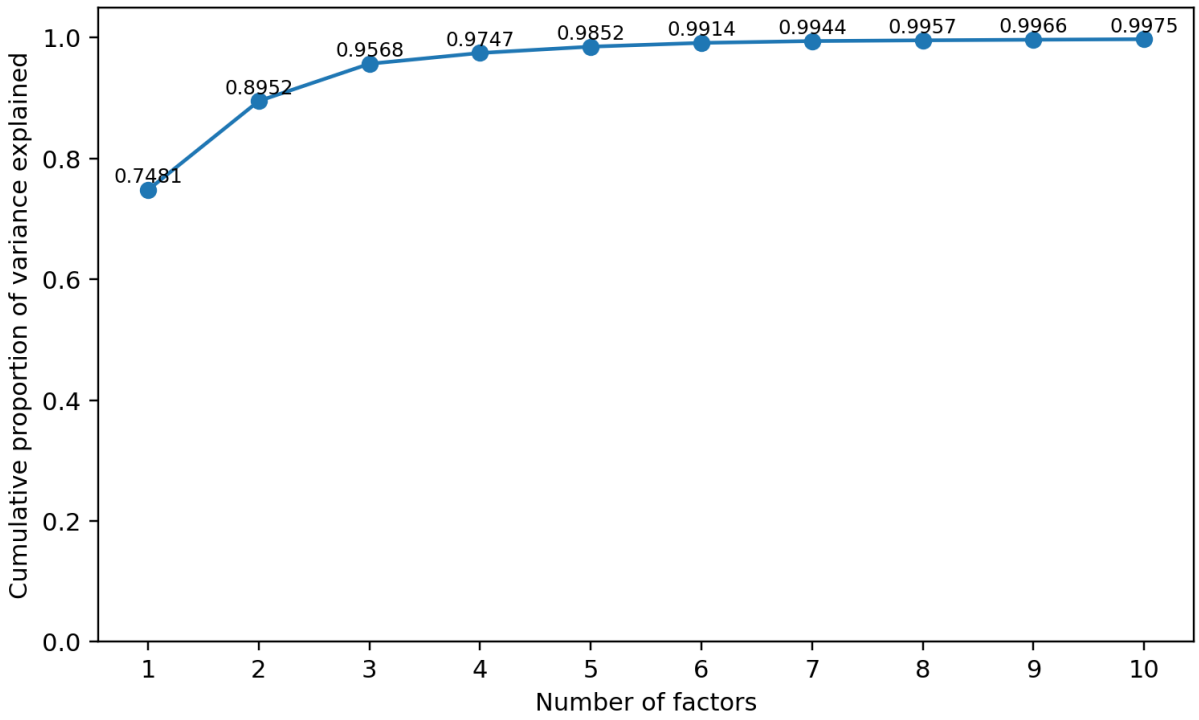


Figure 3.4: Cumulative Share of Density Variation Explained by FPCA Components
Horizontal axis: number of retained components. Vertical axis: cumulative proportion of variation explained. Numerical labels and the plotted values are unchanged.

3.3 Disagreement: High versus Low Dispersion

Two standard deviation perturbations of score $\xi_{1,t}$ along the first basis function $\phi_1(\pi^e)$ widen or narrow the distribution symmetrically around its center while leaving its location largely unchanged. Negative perturbations spread probability mass away from the modal inflation expectation, whereas positive perturbations concentrate probability mass around the center. Because the primary effect is to alter the dispersion of beliefs rather than their mean, the first component is interpreted as a measure of **dispersion**. The associated score therefore captures periods in which households exhibit high or low disagreement. High dispersion generally means high standard deviation (SD),so the first score relates to the high vs low variance or the second moment with correlation -0.819 as in Table 3.

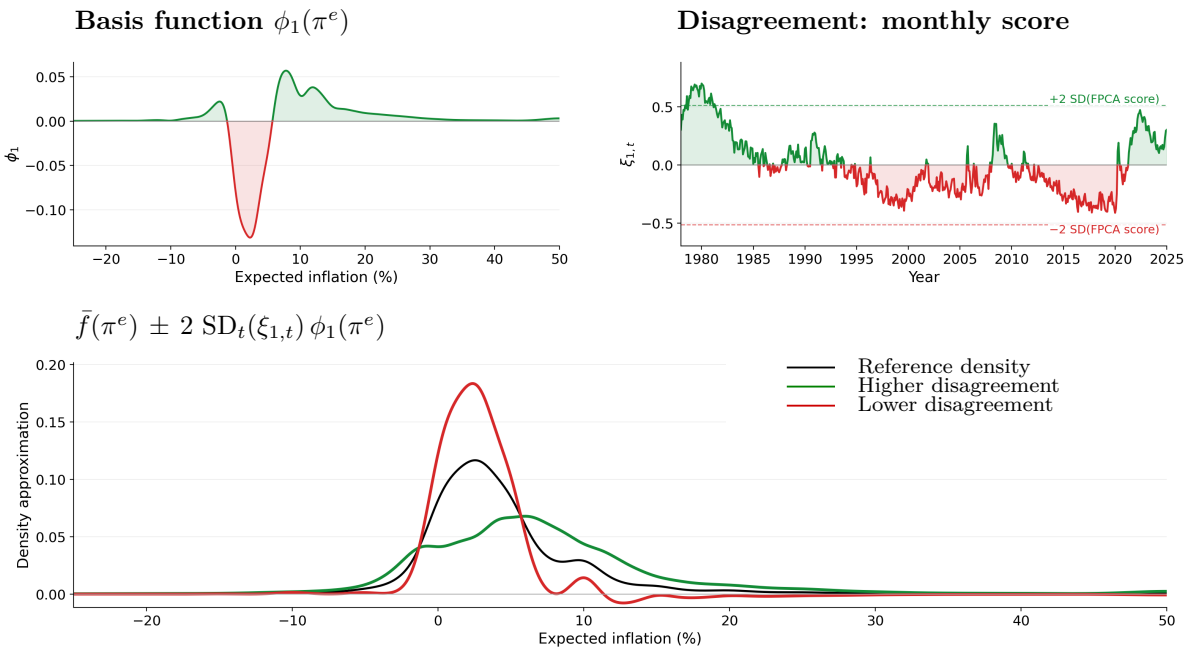


Figure 3.5: Disagreement: Basis Function, Monthly Score, and Density Perturbations

Lower panel: the reference density plus or minus twice the time-series standard deviation of the displayed score, multiplied by its basis function. Green shows higher disagreement; red shows lower disagreement.

3.4 Rightward and Leftward Distributional Shifts

Two-standard-deviation perturbations of the second FPCA score along the eigenfunction $\phi_2(\pi^e)$ redistribute probability mass toward lower or higher inflation expectations. A positive perturbation shifts the probability mass toward lower inflation expectations, corresponding to a Left shift in the distribution, whereas a negative perturbation shifts the probability mass toward higher inflation expectations, corresponding to a Right shift. Thus, this is rightward or leftward **distributional shift**.

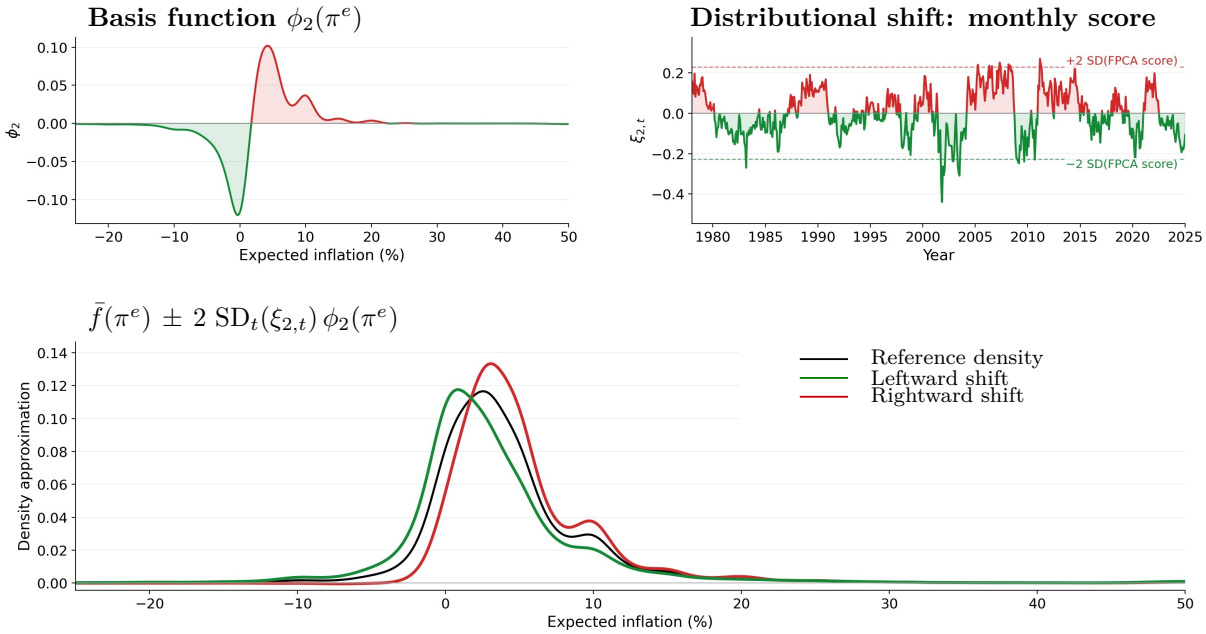


Figure 3.6: Distributional Shifts: Basis Function, Monthly Score, and Density Perturbations
Lower panel: the reference density plus or minus twice the time-series standard deviation of the displayed score, multiplied by its basis function. Red shows the rightward-shift perturbation; green shows the leftward-shift perturbation.

3.5 Right- and Left-Tail Thickening

Two standard deviation perturbations of score $\xi_{3,t}$ along the third basis function $\phi_3(\pi^e)$ mainly redistribute the probability mass between the left and right tails of inflation expectations, while leaving the center largely unchanged. Positive realizations of the component increase the relative weight of the right tail, corresponding to a higher share of households reporting unusually high inflation expectations, while reducing the mass in the left tail. Negative realizations produce the opposite pattern, increasing the relative importance of deflationary expectations. Here, probability mass refers to the cross-sectional distribution of reported expectations, not to probabilities assigned by individual respondents. Economically, this component measures shifts in the balance between upside and downside inflation risks increasing and is interpreted as **tail risk**.

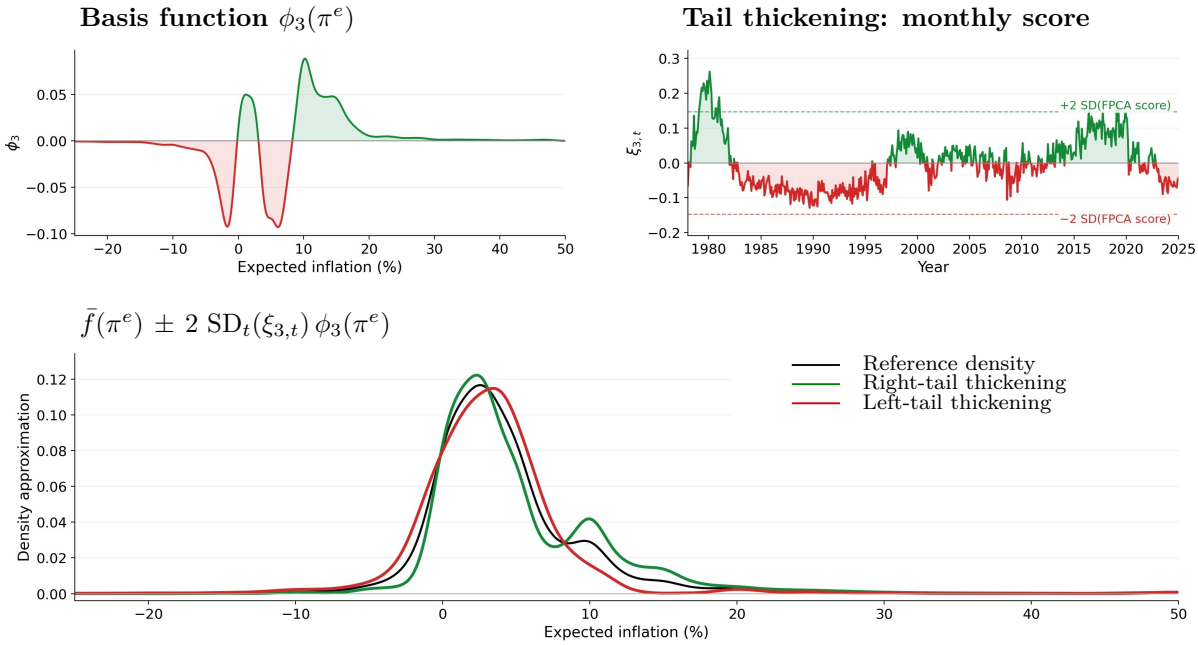


Figure 3.7: Tail Thickening: Basis Function, Monthly Score, and Density Perturbations
Lower panel: the reference density plus or minus twice the time-series standard deviation of the displayed score, multiplied by its basis function. Green shows right-tail thickening; red shows left-tail thickening.

3.6 Distributional Features vs Distributional Moments

3.6.1 Construction of Moments from the Expectations Distribution

For each month, computed moments summarize the national expectations density $f_t(\pi^e)$. Variance(m2), skewness(m3), and kurtosis(m4) are obtained from these computed moments as:

$$\begin{aligned} m_{2,t} &= \int (\pi^e - \mu_t)^2 f_t(\pi^e)\, d\pi^e, \\ m_{3,t} &= \int (\pi^e - \mu_t)^3 f_t(\pi^e)\, d\pi^e, \\ m_{4,t} &= \int (\pi^e - \mu_t)^4 f_t(\pi^e)\, d\pi^e. \end{aligned} \tag{9}$$

The integrals are evaluated numerically over the support of the estimated density. Skewness and kurtosis likewise summarize the monthly density f_t.

3.6.2 Correlation among computed moments

Table 2 shows substantial overlap between some computed moments. Skewness and kurtosis are strongly correlated ($\rho = 0.767$), while mean and variance have a correlation of 0.576. These relationships indicate that movements in individual moments do not represent entirely separate changes in the expectation distribution.

Table 2: Correlations among computed Moments

	Mean	Variance	Skewness	Kurtosis
Mean	1.000			
Variance	**0.576**	1.000		
Skewness	0.344	0.327	1.000	
Kurtosis	0.137	0.368	**0.767**	1.000

3.6.3 Relationship between distributional features and moments

Table 3 shows that the distributional features proxy computed moments but are not interchangeable with them. Correlation is expected because both approaches summarize the same expectation distribution. Their construction nevertheless differs: moments measure collapsed distributional characteristics as point forecasts, whereas functional components identify patterns of density variation from the data. Orthogonality of the functional basis does not imply independence from computed moments. Because both are constructed from the same underlying density, the FPCA scores naturally retain information related to computed moments while capturing broader patterns of distributional variation.

Figure 3.8 illustrates these relationships using standardized series.

Table 3: Correlations between Distributional Features and Moments

	Mean	Variance	Skewness	Kurtosis
FPCA score1	0.704	**-0.819**	0.153	0.202
FPCA score2	-0.531	0.194	**-0.161**	0.039
FPCA score3	-0.301	-0.543	-0.449	**-0.639**

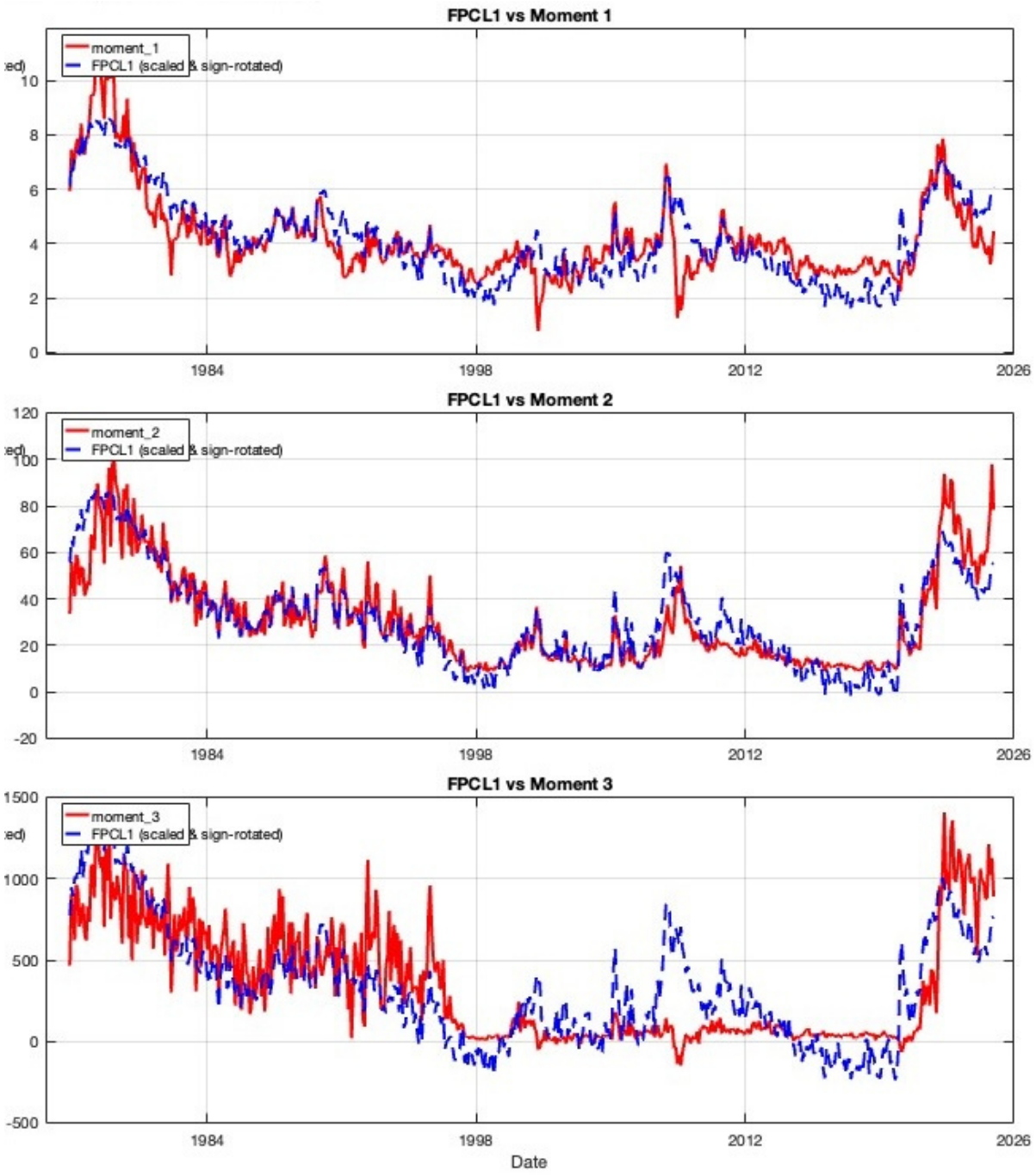


Figure 3.8: Aggregate Distributional Shape Features and computed Moments. The corresponding correlations are 0.819, −0.161, and −0.639.

The image retains its original panel labels and its rescaled, sign-matched score series. The printed panel identities are not reassigned to different FPCA components here.

3.7 Time Variation in Disagreement, Shifts, and Tail Thickening

Figure 3.9 traces the aggregate monthly scores in the regression sample. Under the empirical sign convention, positive values of scores correspond, respectively, to higher disagreement, a leftward direction, and a right-tail direction. The score level records a deviation from the reference density. The distributional shift is below zero throughout March 2021–June 2022, whereas it is above zero in nine of the ten months from September 2008 to June 2009. These contrasting paths motivate the episode comparisons in the empirical analysis.

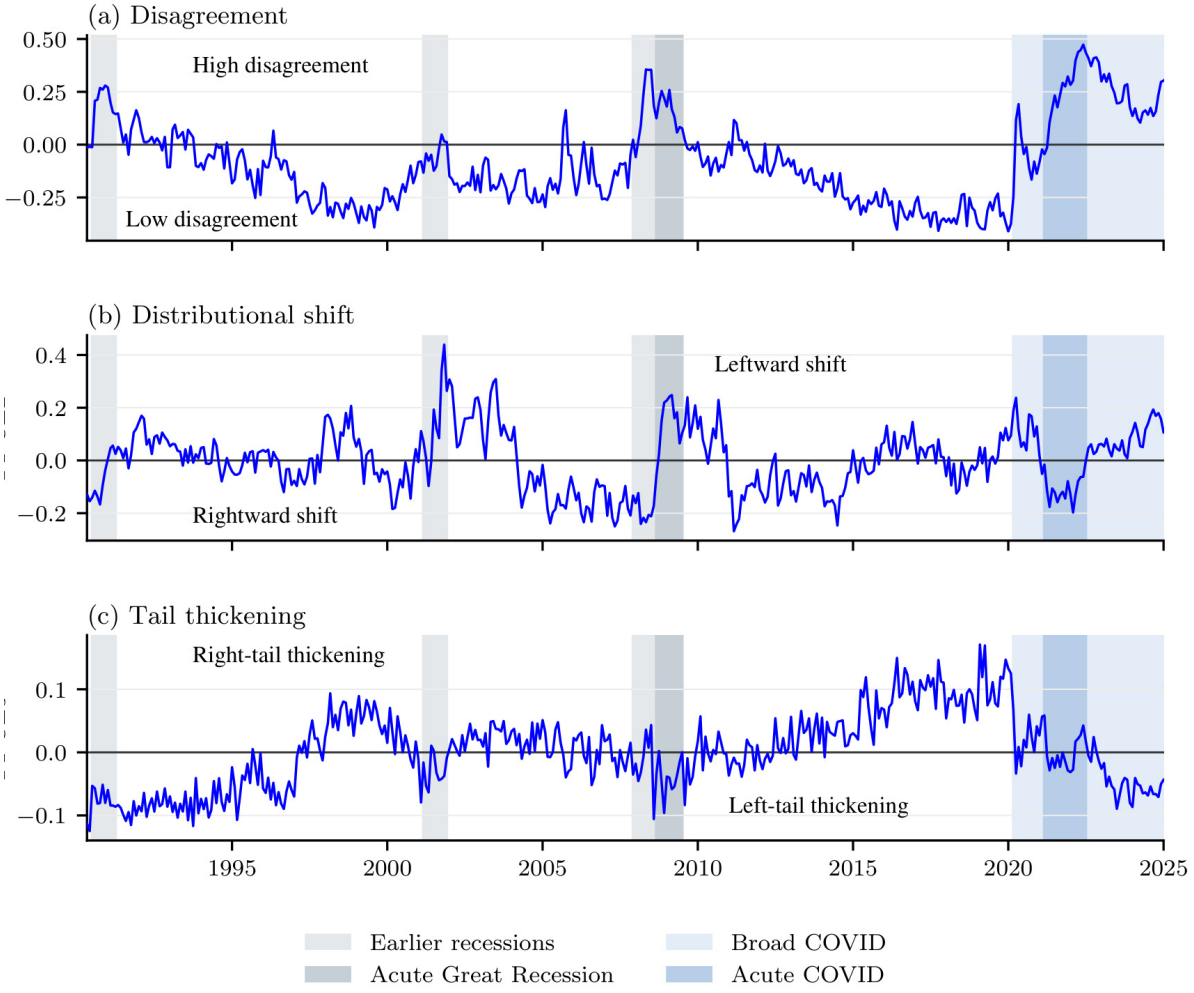


Figure 3.9: Observed Fixed-Reference FPCA Scores, May 1990–January 2025
Notes: Light gray shading marks the earlier recession windows; darker gray marks September 2008–June 2009. Light blue marks March 2020–January 2025; darker blue marks March 2021–June 2022.
Panels (a)–(c) show disagreement, distributional shift, and tail thickening in the displayed source orientation. Horizontal axis: calendar year. Vertical axes: monthly FPCA scores; scales differ by panel.

4 Empirical Strategy

The empirical analysis addresses three questions using national time-series variation. First, do distributional features of inflation expectations contain information about aggregate inflation beyond the mean forecast and computed moments? Second, how do these relationships and distributional movements differ across major macroeconomic episodes? Third, what do VARs and aggregate local projections reveal about the dynamics of inflation and the expectations distribution?

4.1 Information Beyond a Mean Forecast

I compare four representations of inflation expectations while holding the common controls and estimation sample fixed. The benchmark includes no distributional measures. The moments specification adds variance, skewness, and kurtosis. The FPCA specification adds the first three functional principal-component scores. The combined specification includes both the moments and FPCA scores. For the aggregate density, define the standardized FPCA score vector and moments as

$$\boldsymbol{\xi}_t^* = \left(\frac{\xi_{1,t}}{\sigma_1}, \frac{\xi_{2,t}}{\sigma_2}, \frac{\xi_{3,t}}{\sigma_3} \right)', \quad \mathbf{m}_t = (\mathrm{Var}_t, \mathrm{Skew}_t, \mathrm{Kurt}_t)'$$

Here, $\mathbf{m}_t$ contains the computed moments. The scores summarize the distributional deviations defined in the methodology section. The standard deviations σ_k are calculated over the January 1990–January 2025 source sample and held fixed across specifications. For economic interpretation, the signs of the scores are oriented in the reported tables toward disagreement, rightward or leftward shifts, and the relevant tail direction. Reorientation changes the sign of a coefficient but not the fitted values, standard errors, or joint tests.

4.1.1 Aggregate Phillips Curve

Let π_t denote annualized monthly CPI inflation, $\widehat{u}_t$ the unemployment gap, π_t^e the mean one-year-ahead inflation expectation, and $\pi_t^{e,LR}$ the mean long-run inflation expectation. The aggregate specification without episode interactions is

$$\pi_t = a + \kappa \widehat{u}_t + \beta \pi_t^e + \lambda \pi_t^{e,LR} + \boldsymbol{\gamma}' \mathbf{s}_t + \boldsymbol{\theta}' \boldsymbol{\xi}_t^* + \boldsymbol{\delta}' \mathbf{m}_t + \varepsilon_t, \tag{10}$$

where $\mathbf{s}_t$ contains the observed monetary-policy and supply-shock controls. The estimates in Tables 4 and 5 use the episode-interaction specification in equation (11), which augments this equation with episode indicators and interactions with the included distributional controls.

4.2 Evolution Across Major Macroeconomic Episodes

Let D_t^C denote an indicator for broad COVID (March 2020–January 2025), and let D_t^R denote an indicator for the pooled earlier recessions: July 1990–March 1991, March–November 2001, and December 2007–June 2009. Months outside both sets of windows form the reference period.

Aggregate Phillips Curve with time dummies I estimate a joint specification containing both COVID and earlier-recession indicators and their interactions with the distributional components and moment controls:

$$\begin{aligned}\pi_t = a + \kappa \widehat{u}_t + \beta \pi_t^e + \lambda \pi_t^{e,LR} + \boldsymbol{\gamma}' \mathbf{s}_t + \eta_C D_t^C + \eta_R D_t^R \\ + \left(\boldsymbol{\theta}_0 + D_t^C \boldsymbol{\theta}_C + D_t^R \boldsymbol{\theta}_R\right)' \boldsymbol{\xi}_t^* \\ + \left(\boldsymbol{\delta}_0 + D_t^C \boldsymbol{\delta}_C + D_t^R \boldsymbol{\delta}_R\right)' \mathbf{m}_t + \varepsilon_t.\end{aligned} \tag{11}$$

The reported FPCA coefficients are $\boldsymbol{\theta}_0$ outside the episode windows, $\boldsymbol{\theta}_0 + \boldsymbol{\theta}_C$ post-COVID, and $\boldsymbol{\theta}_0 + \boldsymbol{\theta}_R$ during earlier recessions. Joint tests evaluate whether each within-period coefficient vector is zero.

4.3 Dynamic Evidence: Full sample and post-COVID

I use two VAR specifications. The first includes observed monetary-policy and supply-shock series as regressors:

$$\mathbf{v}_t = \mathbf{a} + \sum_{j=1}^{p} \mathbf{A}_j \mathbf{v}_{t-j} + \mathbf{B}\mathbf{s}_t + \boldsymbol{\varepsilon}_t, \qquad \mathbf{v}_t = (\pi_t^e, \xi_{1,t}, \xi_{2,t}, \xi_{3,t})'. \tag{12}$$

The COVID specific VAR is a recursive VAR ordered as

$$\mathbf{y}_t = (\widehat{u}_t, \pi_t, \pi_t^e, \xi_{1,t}, \xi_{2,t}, \xi_{3,t})'. \tag{13}$$

For 2020–2025, I compare this macro-first ordering with an alternative that places the FPCA scores first. The comparison assesses sensitivity to the contemporaneous restrictions; neither ordering is interpreted as uniquely causal.

4.3.1 Aggregate Local Projections post-COVID

For horizons $h = 1, \ldots, 20$, I estimate local projections using only observations from March 2020 through January 2025:

$$\pi_{t+h} = a_h + \beta_h \pi_t^e + \boldsymbol{\theta}_h' \boldsymbol{\xi}_t^* + \boldsymbol{\Gamma}_h' \mathbf{X}_t + \varepsilon_{t+h}. \tag{14}$$

All three current FPCA scores enter jointly with the mean expectation. The controls $\mathbf{X}_t$ include current inflation, the current unemployment gap, and one lag each of inflation and mean expectations. Both predictor and outcome dates lie within the COVID sample; the available observations decline with the horizon. The reference density and FPCA basis are estimated over January 1990–December 2019 and held fixed when constructing the COVID scores. Scores are standardized using that pre-COVID period. The LP regressions themselves use only COVID observations. Inference uses Newey–West HAC standard errors with 12 lags, a finite-sample correction, and a t reference distribution.

4.3.2 Out-of-Sample Forecast Evaluation post-COVID

I evaluate whether distributional features improve forecasts of aggregate inflation beyond mean expectations using the COVID only period for the forecast after Jan 2025. For each horizon $h = 1, \ldots, 12$, I compare a benchmark with an augmented specification:

$$\pi_{t+h} = a_h + \mathbf{b}_h' \mathbf{X}_t + c_{0,h} \xi^*_{k,t} + c_{1,h} \xi^*_{k,t-1} + u_{t+h}. \tag{15}$$

The benchmark imposes $c_{0,h} = c_{1,h} = 0$. The control vector includes current inflation and three lags, the current unemployment gap and one lag, current mean one-year expectations and one lag, lagged PX5, and current monetary-policy and supply-shock controls. The outcome is annualized monthly CPI inflation at $t + h$, not cumulative inflation.

5 Results

5.1 Shifts and Tails across COVID and the Great Recession

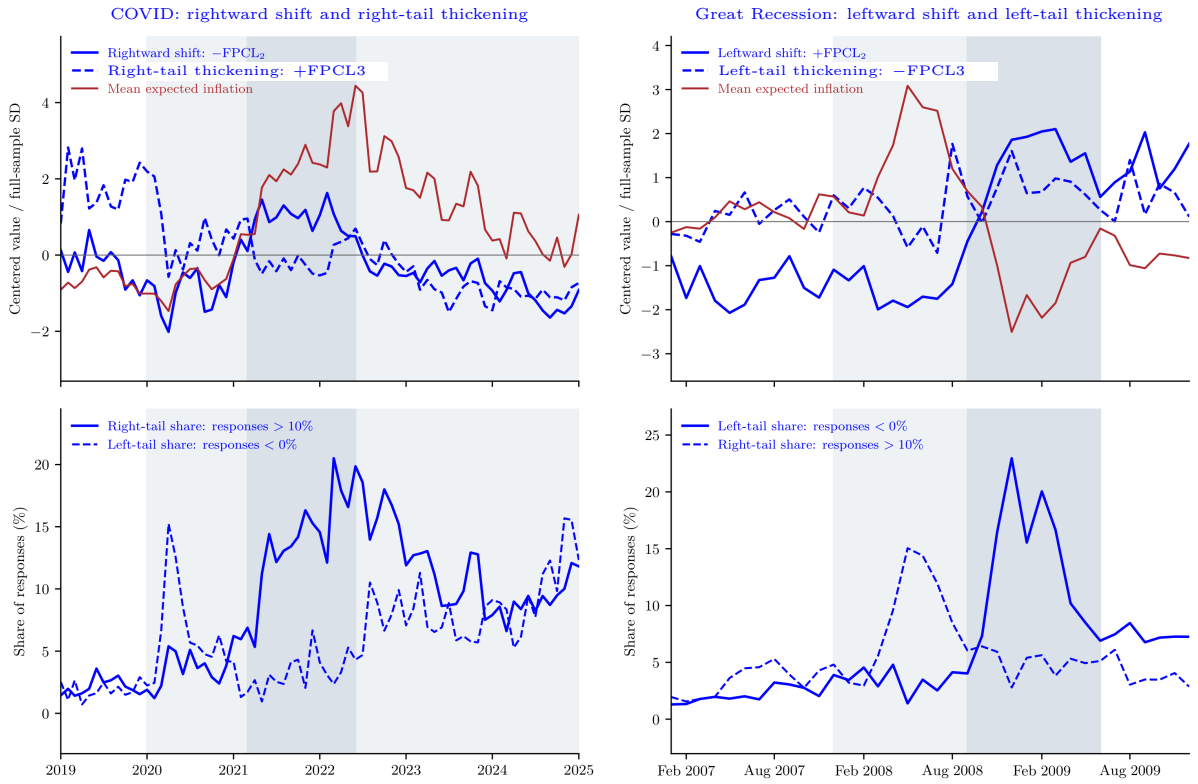


Figure 5.1: Distributional Shifts and Tail Frequencies: COVID and the Great Recession
Upper panels: the displayed shift score, tail score, and mean expectation, centered and divided by their full-sample standard deviations. Lower panels: shares of individual responses above 10% or below 0% (percent of responses). The lower-panel series are tail frequencies, not FPCA scores.

COVID Upper-tail expansion precedes the rightward shift. Figure 5.1 places the broad and acute episodes together. The share of respondents expecting inflation above 10 percent rises from 1.22 percent in February 2020 to 5.39 percent in April 2020, before the sustained rightward movement evident in 2021. By February 2021 the rightward-shift score is above its full-sample mean, and the share above 10 percent subsequently reaches 11.22 percent in May and 14.42 percent in June. The chronology is consistent with upper-tail expansion preceding the broader rightward adjustment.

Great Recession: leftward shifts followed by left-tail expansion. The Great Recession has an early rightward phase during the 2008 commodity price run-up, followed by a marked leftward reversal. The standardized leftward score rises from −1.42 in August 2008 to −0.45 in September and 0.23 in October. The large lower-tail expansion follows: the negative expectation share rises from 4.03 percent in September to 16.44 percent in November and 22.96 percent in December. Thus the leftward reversal precedes the pronounced lower-tail expansion late in 2008.

5.2 Aggregate Phillips Curve with Fixed-Reference Distributional Components

The fixed-reference specification is presented here; the mean-centered comparisons are retained in Appendix B.

The aggregate regressions provide evidence that distributional features of inflation expectations contain information about inflation beyond the mean forecast, conditional on the included macroeconomic controls. Once distributional features of inflation expectations are incorporated, the mean expectations becomes statistically insignificant, while the distributional features remain jointly significant. This suggests that information contained in the distribution of beliefs is associated with inflation beyond the mean forecast.

The estimated role of mean inflation expectations is highly sensitive to whether the shape of the expectations distribution is taken into account, even after controlling for long-run inflation expectations. In the benchmark specification, the coefficient on mean expectations is 1.743 and highly significant. Once the FPCA distributional components are included, the coefficient falls to 0.427 and becomes statistically insignificant.

The slope increases in absolute magnitude from -0.282 in the mean benchmark to -0.456 with computed moments and -0.358 with FPCA components; when both representations are included, the estimated slope is -0.387. Thus, accounting for expectation heterogeneity does not eliminate the Phillips Curve. Instead, the benchmark specification that summarizes expectations primarily by their mean produces the flattest estimated slope.

Table 4: Full Sample: Aggregate Phillips Curve: Mean and Distributional Controls

	Dependent variable: Annualized monthly CPI inflation			
	(1) Mean	(2) Mean+Moments	(3) Mean+FPCA	(4) All
Unemployment gap (κ)	-0.282***	-0.456***	-0.358***	-0.387***
	(0.081)	(0.107)	(0.104)	(0.117)
Mean expectation	1.743***	1.495***	0.427	0.137
	(0.214)	(0.294)	(0.636)	(0.700)
FPCA coefficients: one-SD effects				
Dispersion score (ξ_1)	–	–	1.342***	1.535**
	–	–	(0.460)	(0.719)
Rightward shift ($-\xi_2$)	–	–	0.277	0.331
	–	–	(0.244)	(0.265)
Right-tail risk (ξ_3)	–	–	0.935***	0.738**
	–	–	(0.277)	(0.293)
FPCA joint-test p-value	–	–	0.006	0.038
Moments joint-test p-value	–	0.263	–	0.975
Supply and monetary-policy shocks	Yes	Yes	Yes	Yes
Five-year long-run expectation (PX5)	Yes	Yes	Yes	Yes
COVID and recession time dummies	Yes	Yes	Yes	Yes
R^2	0.408	0.443	0.473	0.484
Observations	417	417	417	417

* $p < 0.10$, ** $p < 0.05$, *** $p < 0.01$.

Table 5: Full sample Aggregate Phillips Curve: Distributional Coefficients Across Episodes

	Dependent variable: Annualized monthly CPI inflation			
	(1) Mean	(2) Mean+Moments	(3) Mean+FPCA	(4) All
Unemployment gap (κ)	-0.282***	-0.456***	-0.358***	-0.387***
	(0.081)	(0.107)	(0.104)	(0.117)
Mean expectation	1.743***	1.495***	0.427	0.137
	(0.214)	(0.294)	(0.636)	(0.700)
Broad COVID: March 2020–January 2025; total one-SD effects				
Disagreement	–	–	-0.390	-0.648
	–	–	(0.625)	(1.545)
Rightward shift	–	–	2.054***	2.237***
	–	–	(0.529)	(0.739)
Right-tail thickening	–	–	1.897***	1.720**
	–	–	(0.598)	(0.700)
FPCA joint-test p-value	–	–	< 0.001	0.003
Moments joint-test p-value	–	0.264	–	0.979
Earlier recession windows: total one-SD effects				
Disagreement	–	–	-0.603	-2.420
	–	–	(0.665)	(1.587)
Leftward shift	–	–	-1.066**	-1.562**
	–	–	(0.513)	(0.648)
Left-tail thickening	–	–	-1.544**	-3.003***
	–	–	(0.756)	(0.965)
FPCA joint-test p-value	–	–	0.008	0.005
Moments joint-test p-value	–	0.198	–	0.075
Supply and monetary-policy shocks	Yes	Yes	Yes	Yes
Five-year expectation (PX5)	Yes	Yes	Yes	Yes
COVID and recession time dummies	Yes	Yes	Yes	Yes
R^2	0.408	0.443	0.473	0.484
Observations	417	417	417	417

Earlier recession windows are July 1990–March 1991, March–November 2001, and December 2007–June 2009. The omitted state excludes COVID and these recession windows. Joint tests evaluate the three total coefficients in each block. * $p < 0.10$, ** $p < 0.05$, *** $p < 0.01$.

The distribution of inflation expectations matters for inflation, and the distributional shift differs sharply between crisis episodes. During the post-COVID period, higher inflation is associated with rightward distributional shifts and increases in the right-tail component, conditional on mean expectations and the other controls. As shown in Table 5, a one-standard-deviation rightward shift in expectations is associated with 2.24 percentage points higher annualized monthly inflation, while a one-standard-deviation increase in right-tail risk is associated with 1.72 percentage points higher inflation in the full specification. I also assess whether the relationship between the expectations distribution and inflation varies across periods, and find that they do.

These results imply that the post-pandemic inflation surge was not merely characterized by an increase in average inflation expectations. Rather, inflation accelerated when the entire cross-sectional distribution shifted toward higher expected inflation and when the upper tail placed greater weight on unusually high reported inflation expectations. Consistent with this interpretation, the coefficient on the mean expectation becomes economically small and statistically insignificant once the distributional shifts are included. The relevant information appears to reside in the shape of the expectations distribution rather than in its average alone. These coefficients must be interpreted conditionally. Fixed-reference FPCA retains shifts in location, so its scores can share variation with the mean. Including them can reduce the variation available to estimate a separate mean coefficient.

5.2.1 Do Distributional Coefficients Change across Periods?

To assess whether the relationship between the expectations distribution and inflation varies across periods, I test the episode-interaction coefficients directly. The distributional contribution to the regression in column (4) of Table 5 can be written as

$$\left(\boldsymbol{\theta}_0 + D_t^C \boldsymbol{\theta}_C + D_t^R \boldsymbol{\theta}_R\right)' \boldsymbol{\xi}_t^*, \tag{16}$$

where $\boldsymbol{\xi}_t^*$ contains the three standardized FPCA scores. The vectors $\boldsymbol{\theta}_C$ and $\boldsymbol{\theta}_R$ measure changes relative to months outside COVID and the earlier recession windows. A constant relationship across periods implies

$$H_0 : \quad \boldsymbol{\theta}_C = \boldsymbol{\theta}_R = \mathbf{0}. \tag{17}$$

This is a joint test of six restrictions. Pairwise tests impose $\boldsymbol{\theta}_C = \mathbf{0}$, $\boldsymbol{\theta}_R = \mathbf{0}$, or $\boldsymbol{\theta}_C = \boldsymbol{\theta}_R$. These tests evaluate differences across periods, separately from tests of whether the coefficients within a period are jointly zero.

Table 6: Tests of Equality of Distributional Coefficients across Periods

	p-value	
Null hypothesis	Conventional OLS	HAC(12)
A. Fixed-reference distributional components		
Equal coefficients across all periods	**0.0049**	**0.0058**
COVID equals ordinary months	**0.0174**	**0.0014**
Earlier recessions equal ordinary months	**0.0259**	0.2392
COVID equals earlier recessions	0.2251	0.5670
B. Mean-centered distributional components		
Equal coefficients across all periods	0.3447	0.4581
COVID equals ordinary months	0.5845	0.2988
Earlier recessions equal ordinary months	0.1154	0.3696
COVID equals earlier recessions	0.7445	0.8551

Notes: Both panels use 417 monthly observations and the combined specification with PX1, moments, and the same macroeconomic controls and episode interactions. Ordinary months exclude COVID and the earlier recession windows defined in Table 5. Panel B recomputes three FPCA components after centering each month's responses around their arithmetic mean. Conventional inference uses OLS F-tests; HAC(12) uses Wald tests with a Newey–West covariance estimator and 12 lags. Reported p-values are unadjusted for multiple testing; bold entries indicate rejection at the 5% level.

Table 6 rejects equality across periods in the fixed-reference specification, with evidence of a difference between COVID and ordinary months under both inference methods. Equality between COVID and earlier recessions is not rejected. Thus, the evidence supports changes in the conditional distribution–inflation relationship within the fixed-reference specification, but the conclusion is sensitive to how the distribution is represented.

5.3 Dynamic Evidence

5.3.1 Aggregate Local Projection of Distributional Features post-COVID

The local projections examine whether distributional shifts in inflation expectations contain information about future inflation during the post-pandemic inflation episode. Table 7 reports COVID-only coefficients on the three standardized FPCA scores at selected horizons between one and twelve months.

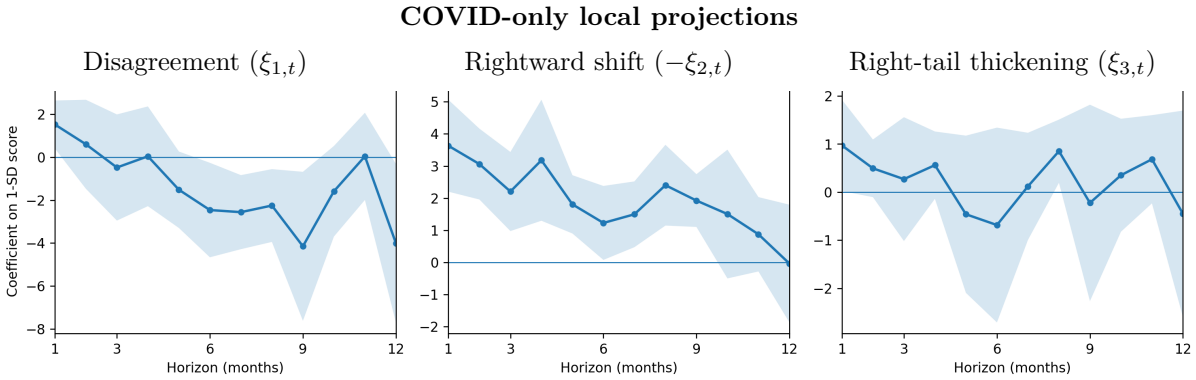


Figure 5.2: COVID-Only Local Projections: Distributional Scores and Subsequent Inflation

Horizontal axis: forecast horizon in months. Vertical axis: coefficient for annualized monthly CPI inflation, in percentage points per one-standard-deviation score movement. Panels show disagreement, rightward shift, and right-tail thickening. The sample is March 2020–January 2025; the specification and inference are in Table 7.

Table 7: COVID-only Local Projections: March 2020–January 2025

Horizon (months)	1	3	6	8	12
Dispersion	1.528^{***}	-0.477	-2.461^{**}	-2.250^{**}	-4.007^{**}
	(0.556)	(1.229)	(1.092)	(0.840)	(1.824)
Rightward shift	3.630^{***}	2.206^{***}	1.229^{**}	2.403^{***}	-0.036
	(0.710)	(0.611)	(0.570)	(0.622)	(0.904)
Tail component	0.971^{**}	0.270	-0.685	0.852^{**}	-0.451
	(0.472)	(0.640)	(1.005)	(0.325)	(1.060)

Notes: Local projections estimated only on March 2020–January 2025 observations. Controls are current inflation, the current unemployment gap, the current mean expectation, and one lag each of inflation and mean expectations; all three current FPCA scores enter jointly. The reference density, basis, and score standardization use January 1990–December 2019 and are held fixed. The outcome is annualized monthly CPI inflation at the indicated horizon. Newey–West standard errors use 12 lags, a finite-sample correction, and a t reference distribution. $^{*}p < 0.10$, $^{**}p < 0.05$, $^{***}p < 0.01$.

The rightward-shift is positively associated with future inflation at one, three, six, and eight months, with statistically significant coefficients at these reported horizons. Its coefficient is close to zero and statistically insignificant at twelve months. Dispersion is positively associated with inflation at one month and negatively associated at six, eight, and twelve months. The tail component is positively associated with inflation at one and eight months, but is not statistically significant at the other reported horizons. These

are conditional predictive associations within the COVID sample, controlling for mean expectations, current inflation, labor-market slack, and lagged inflation and expectations.

5.3.2 Responses to monetary-policy and supply shocks

Monetary-policy shocks primarily affect the central expectation measure, whereas supply shocks induce broader changes in the distribution of beliefs, including disagreement and tail risk. This difference highlights why the mean expectation alone cannot fully characterize the evolution of inflation expectations following major macroeconomic disturbances. Supply-shock responses indicate that macroeconomic disturbances affect multiple dimensions of the expectation distribution simultaneously. Following a positive oil supply shock, inflation expectations increase, the dispersion rises, and tail-risk perceptions become more pronounced. These results suggest that supply disturbances influence not only the mean but also the distribution. Households respond through changes in disagreement, distributional shifts, and tail risk rather than through a revision of expectations alone.

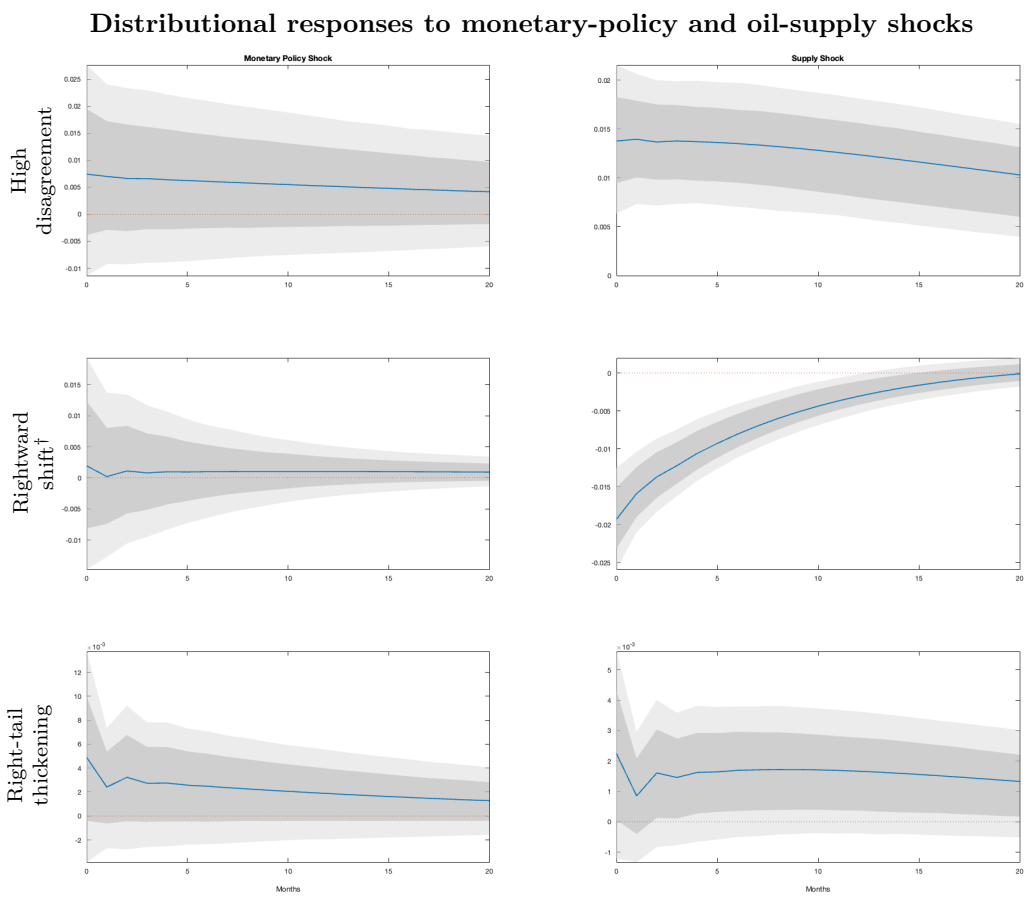


Figure 5.3: High Disagreement, Rightward Shift, and Right-Tail Thickening: Responses to Monetary-Policy and Oil-Supply Shocks

Columns: monetary-policy shock (left) and supply shock (right). Rows: high disagreement, rightward shift†, and right-tail thickening. Horizontal axes: months after the shock. Vertical axes: responses in the displayed score units. Lines and uncertainty bands are retained from the source graphic.

†*Sign convention.* Rightward shift is $-\xi_{2,t}$ in the main text. The original ξ_2 panels are retained: converting a shift response or a shift shock to rightward-shift units reverses its sign; converting both leaves the own-response panel unchanged.

5.4 Distributional-Shape-Augmented Recursive VAR

The VAR shows that dispersion, directional shifts, and tail risk are dynamically distinct features of the expectations distribution. Directional shifts adjust relatively quickly, whereas dispersion and tail risk are more persistent, and shocks to the three components are associated with different inflation responses.

These heterogeneous responses provide dynamic evidence that the expectations distribution cannot be adequately represented by a single summary statistic: disagreement, directional shifts, and tail risk capture distinct aspects of household beliefs. Taken together, the VAR evidence shows that the three distributional features capture distinct dynamic dimensions of household inflation expectations.

Following an inflation shock, the directional-shift component reverts relatively quickly, whereas dispersion and tail risk remain more persistent. Conversely, shocks to the distributional components generate different inflation responses: inflation falls following a dispersion shock, changes sign following a directional-shift shock, and initially rises following a right-tail-risk shock before gradually reverting. These differences show that the mean of expectations and distributional shapes are not interchangeable.

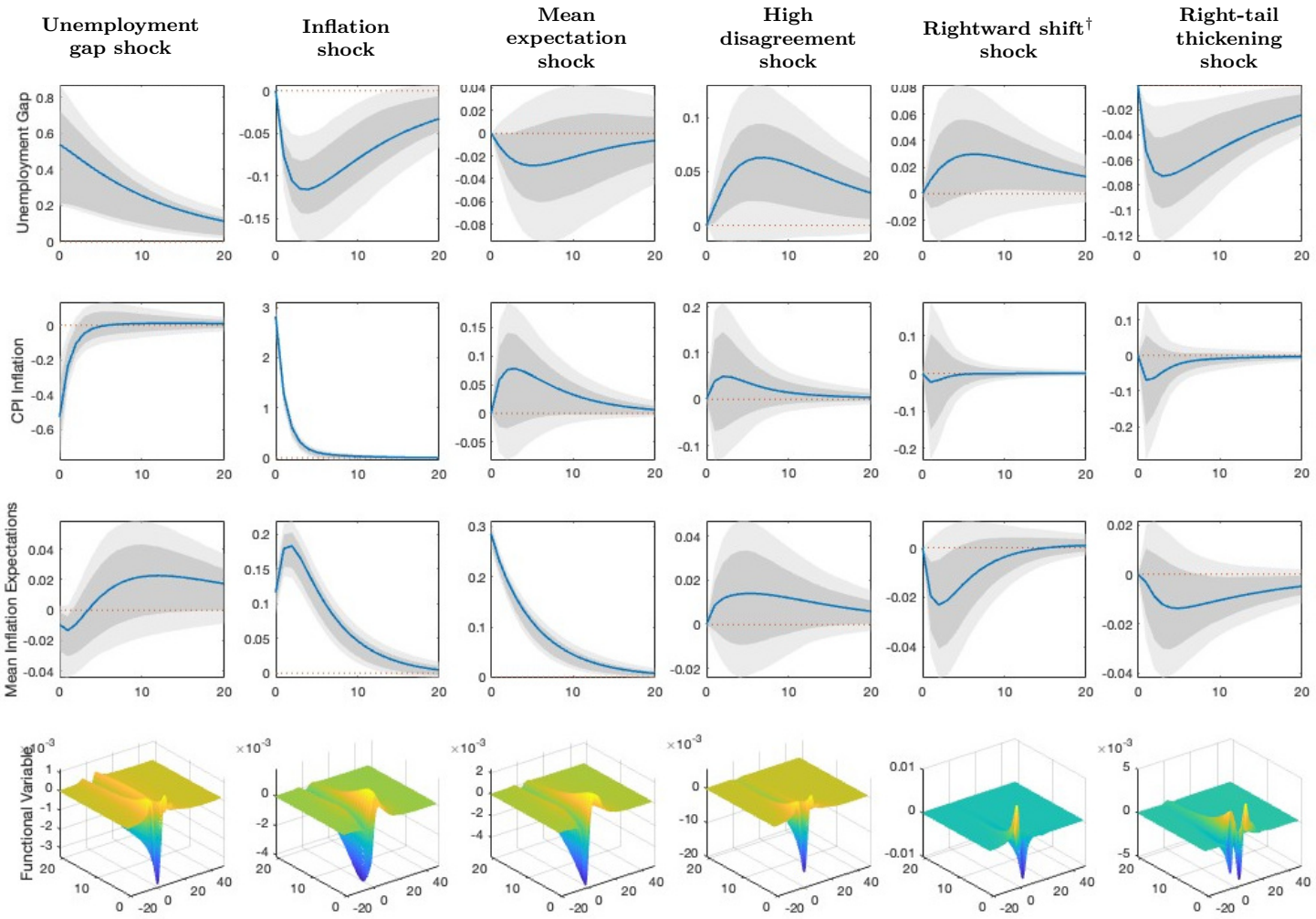


Figure 5.4: MVAR Responses of Macroeconomic Variables and the Expectation Distribution

Columns identify the displayed shocks; rows show the unemployment gap, inflation, mean expectations, and the functional-density response. Horizontal axes of the two-dimensional panels are months after the shock. The three-dimensional panels retain their original axes and scales.

†*Sign convention.* Rightward shift is $-\xi_{2,t}$ in the main text. The original ξ_2 panels are retained: converting a shift response or a shift shock to rightward-shift units reverses its sign; converting both leaves the own-response panel unchanged.

5.4.1 Recursive VAR: heterogeneous responses and persistence

The joint system of both functional and aggregate variables in equation (13) evolve together. The recursive VAR shows that shocks to the distributional features of inflation expectations have heterogeneous dynamic effects. After the CPI inflation shock, dispersion and tail risk rise and fall. The directional-shift tends to revert relatively quickly, whereas the dispersion and tail-risk components are more persistent. Inflation also responds differently to the three shocks. Inflation falls after a positive dispersion shock; its response to positive distributional shift changes sign, and its initial positive response to the tail risk decays with wider later bands. The evidence suggests that the expectations distribution cannot be summarized by a single statistic, as distinct distributional features contain separate dynamic information about inflation.

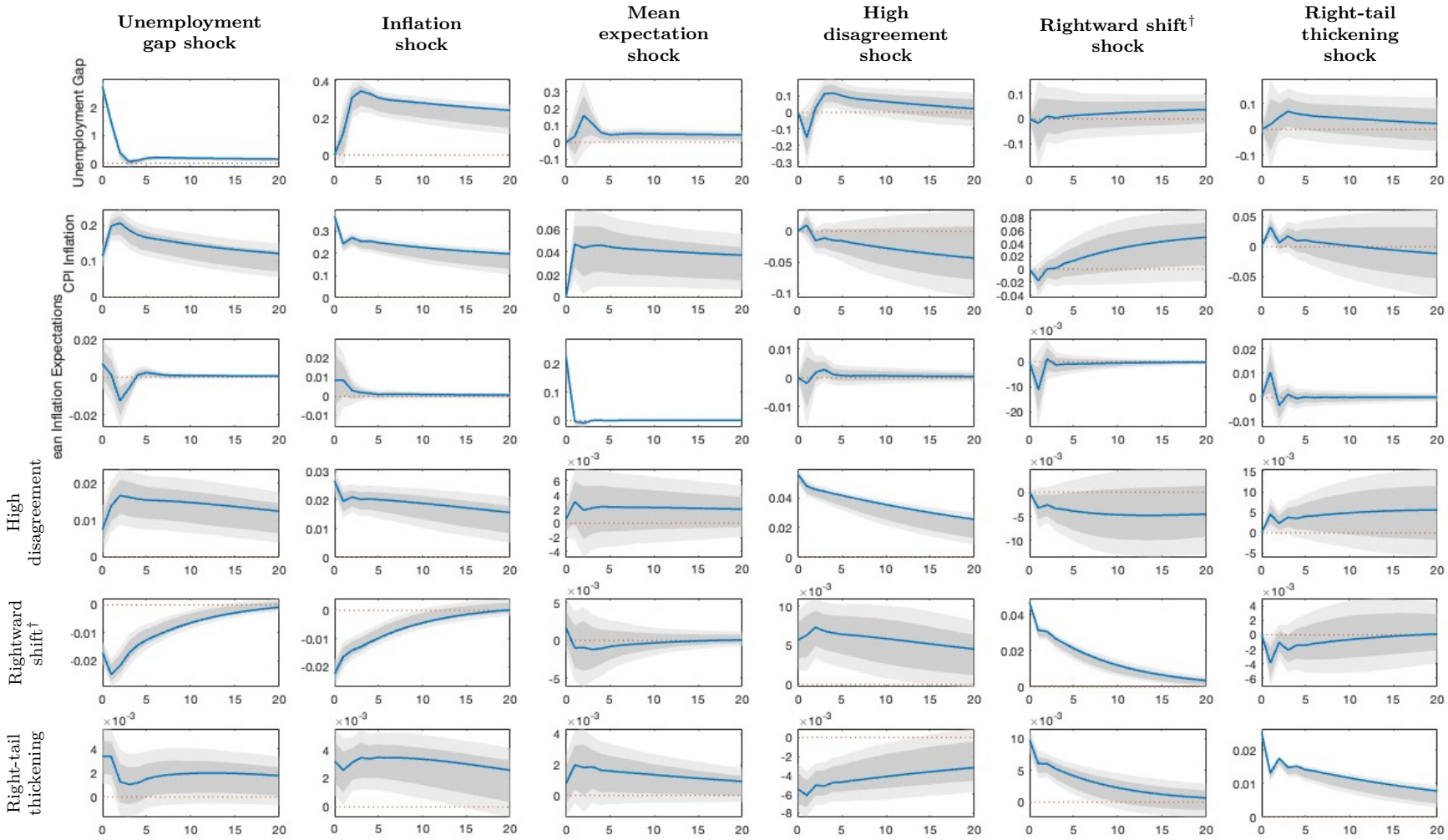


Figure 5.5: Recursive VAR: Macroeconomic and Distributional Responses

Columns identify shocks and rows identify response variables, ordered as unemployment gap, CPI inflation, mean expectations, and high disagreement, rightward shift†, and right-tail thickening. Horizontal axes are months after the shock. FPCA scores are not reoriented; vertical scales differ by panel.

†*Sign convention.* Rightward shift is $-\xi_{2,t}$ in the main text. The original ξ_2 panels are retained: converting a shift response or a shift shock to rightward-shift units reverses its sign; converting both leaves the own-response panel unchanged.

The heterogeneous responses and persistence patterns suggest that the three distributional features capture distinct dimensions of household beliefs rather than alternative measures of the same expectation process. Shocks to distributional shifts dissipate relatively quickly, whereas shocks to dispersion and tail risk remain elevated for longer horizons. The differing inflation responses further indicate that changes in disagreement, directional movements, and perceived inflation risks are associated with different channels through which expectations evolve. Taken together, the VAR evidence is consistent with the paper's central argument that the mean expectation is not a sufficient statistics.

5.4.2 Crisis VAR: impulse responses during 2020–2025

Figure 5.6 examines the joint dynamics of inflation, expectations, and the distributional features during the 2020–2025 period. Following a positive inflation shock, both the dispersion and tail-risk increase, while the directional-shift declines. The responses exhibit different persistence patterns: the directional-shift reverts relatively quickly, whereas the dispersion and tail-risk components remain elevated for longer horizons. These results suggest that inflation disturbances affect multiple dimensions of the expectations distribution simultaneously, but that the resulting adjustments occur at different speeds. The distributional features also generate heterogeneous responses to inflation. Inflation declines following a positive dispersion shock, exhibits a sign-changing response after a directional-shift shock, and initially rises following a tail-risk shock before gradually reverting.

Taken together, the results indicate that disagreement, distributional shifts, and tail risk capture distinct aspects of expectation formation during the post-pandemic period rather than alternative measures of the same underlying belief process.

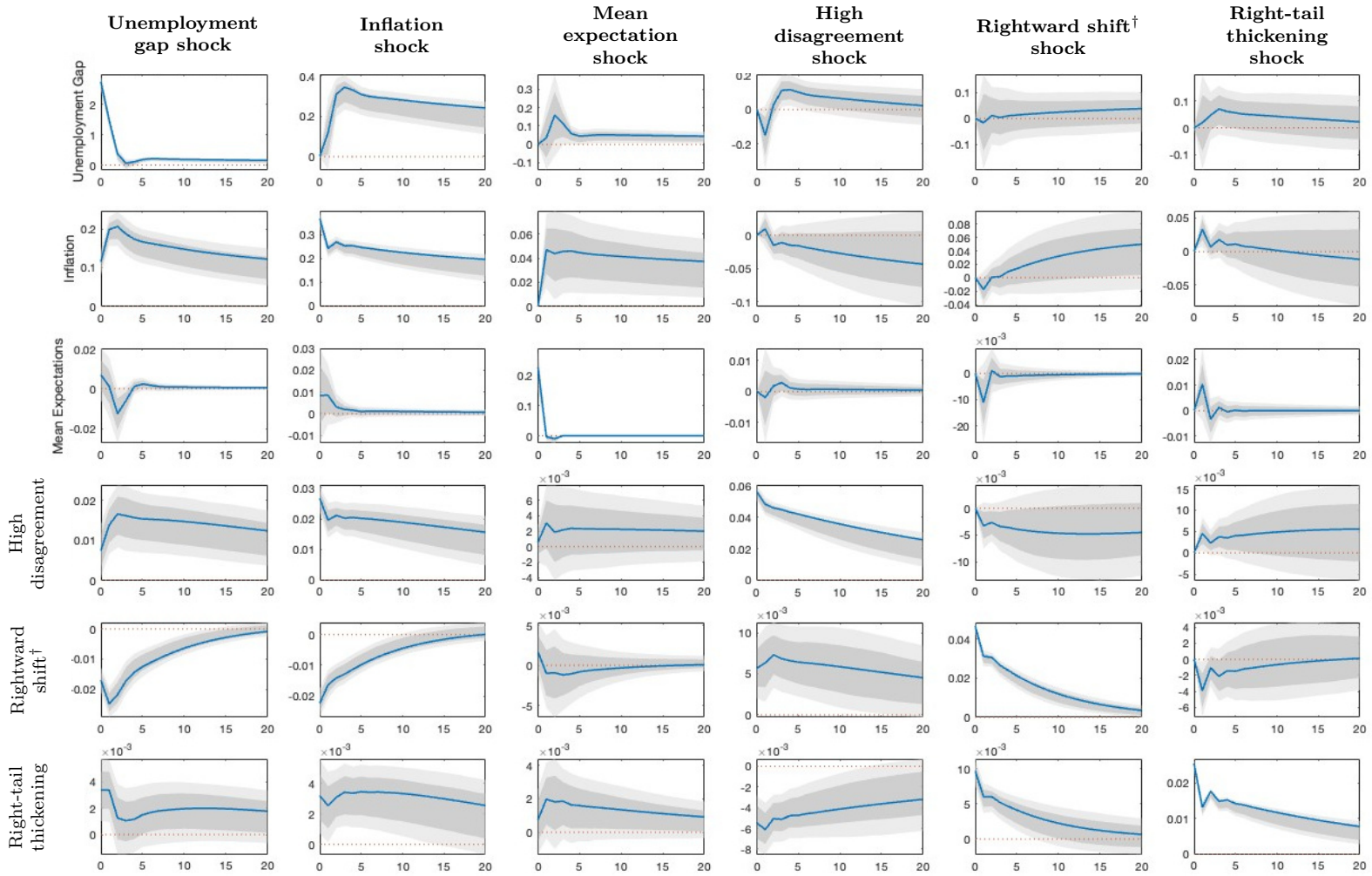


Figure 5.6: Crisis VAR, 2020–2025: Macroeconomic Variables before Distributional Scores

Columns identify shocks; rows identify response variables. Both follow the displayed order: unemployment gap, inflation, mean expectations, and high disagreement, rightward shift†, and right-tail thickening. Horizontal axes are months after the shock. Blue curves and gray uncertainty bands are unchanged.

†*Sign convention.* Rightward shift is $-\xi_{2,t}$ in the main text. The original ξ_2 panels are retained: converting a shift response or a shift shock to rightward-shift units reverses its sign; converting both leaves the own-response panel unchanged.

What changes with the reverse ordering? Figure 5.7 instead places the distributional features first and unemployment last. Under this ordering, inflation can respond contemporaneously to distributional innovations. Several impulse responses differ from those in Figure 5.6, including the sign and magnitude of the inflation response to the distributional features. These differences indicate that the estimated short-run dynamics are sensitive to the maintained contemporaneous restrictions. Despite these differences, one result is common across both orderings. The distributional features exhibit substantially greater persistence than the central expectation measure, whose own response decays more quickly. The evidence therefore suggests that disagreement, distributional shifts, and tail risk evolve on different time scales and contain dynamic information beyond a single summary statistic. Because the crisis sample is short and the responses depend on the maintained ordering, the figures are interpreted as evidence on persistence and dynamic adjustment rather than as uniquely identified causal effects.

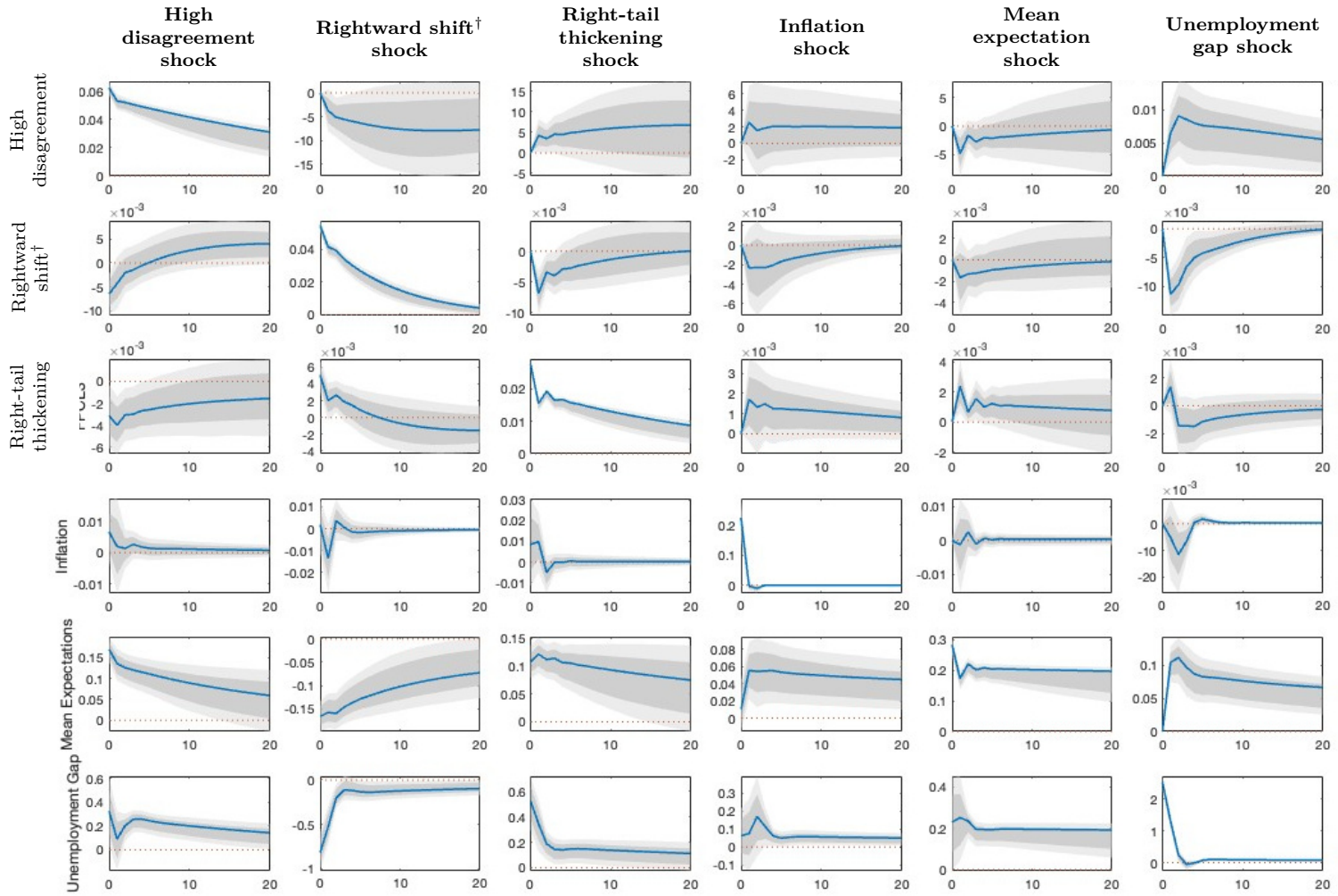


Figure 5.7: Crisis VAR, 2020–2025: Distributional Scores before Macroeconomic Variables

Columns identify shocks; rows identify responses. The displayed order is high disagreement, rightward shift†, right-tail thickening, inflation, mean expectations, and unemployment gap. Horizontal axes are months after the shock. Original signs, scales, curves, and uncertainty bands are retained.

Notes: Rows and columns follow the displayed alternative recursive order. The response to a rightward-shift shock is the sign reversal of its displayed column. Blue curves are point estimates; gray shading shows the reported uncertainty bands. Panel scales differ.

†*Sign convention.* Rightward shift is $-\xi_{2,t}$ in the main text. The original ξ_2 panels are retained: converting a shift response or a shift shock to rightward-shift units reverses its sign; converting both leaves the own-response panel unchanged.

5.5 Forecast-Error Variance Decomposition

Figure 5.8 reports forecast-error variance decompositions for the MVAR. Unemployment and CPI inflation are primarily explained by their own innovations. Interestingly, the mean expectations reflect both expectation and inflation shocks. In contrast, the functional evaluations are dominated by functional shocks at the 10th percentile or at the tail. Only a comparatively small fraction of their forecast-error variance is attributable to inflation, unemployment, or mean-expectation shocks. This result suggests that the distributional features are not merely passive reflections of movements in aggregate inflation or the average expectation. Rather, they contain an important independent source of variation within the expectations distribution itself. However, the 50th percentile and the 90th percentile are still informative about inflation and inflation expectations.

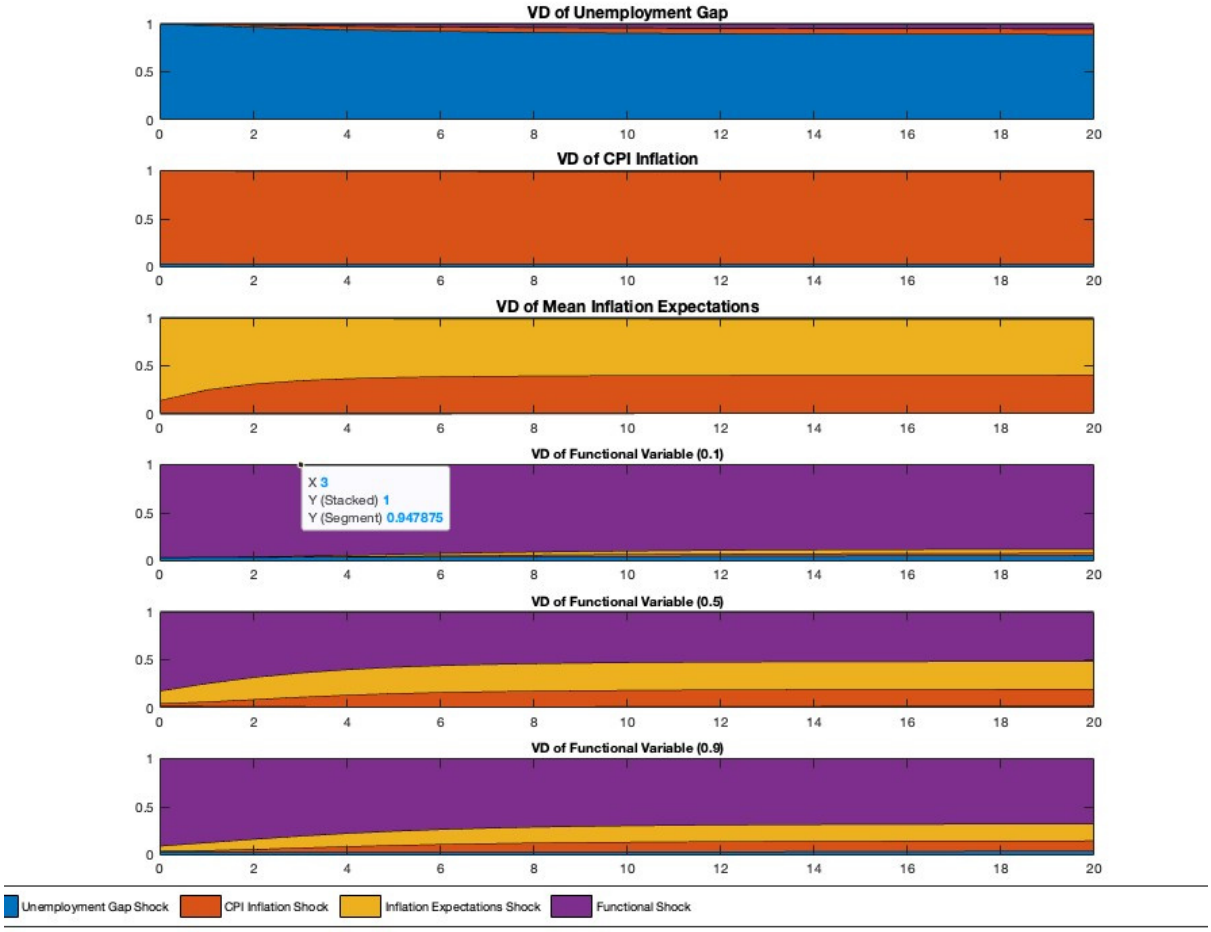


Figure 5.8: MVAR Forecast-Error Variance Decomposition

Notes:Functional shocks are reported as one category; the three functional evaluations retain the displayed source labels 0.1, 0.5, and 0.9.

Horizontal axes: forecast horizon in months. Vertical axes: shares of forecast-error variance. The three lower panels retain the source labels 0.1, 0.5, and 0.9 for the functional evaluations; functional shocks are grouped.

5.5.1 Historical Decompositions of Aggregate Variables

Figures below decomposes the historical paths of unemployment gap, CPI inflation, and one-year-ahead inflation expectations into the contributions of the identified shock categories. Unemployment movements are primarily explained by unemployment shocks, particularly during the Great Recession and the sharp increase in 2020. Inflation fluctuations are largely driven by inflation shocks, although expectation and functional shocks also contribute during major macroeconomic episodes.

The expectations decomposition in Figure 5.9 reveals a larger role for expectation and functional shocks, particularly during the 2021–2023 inflation surge. Functional shocks sometimes amplify and sometimes offset the contributions of inflation and expectation shocks, indicating that movements in the expectations distribution are not simply passive responses to aggregate inflation.

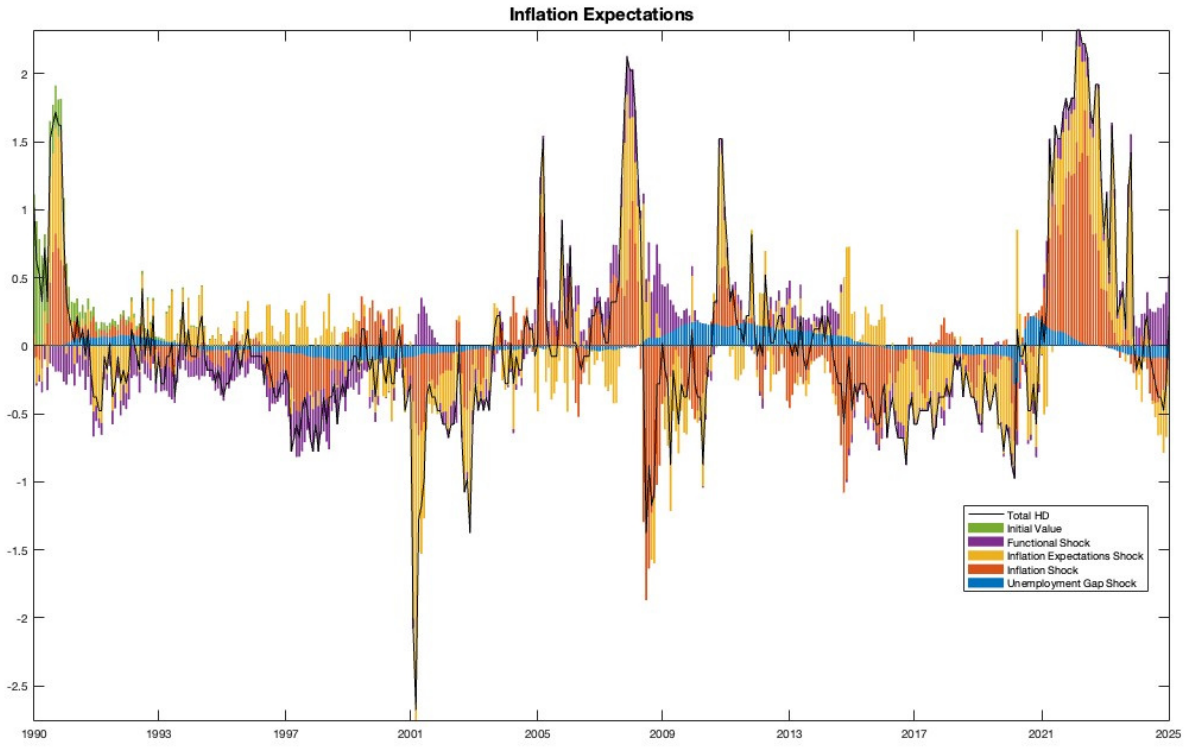
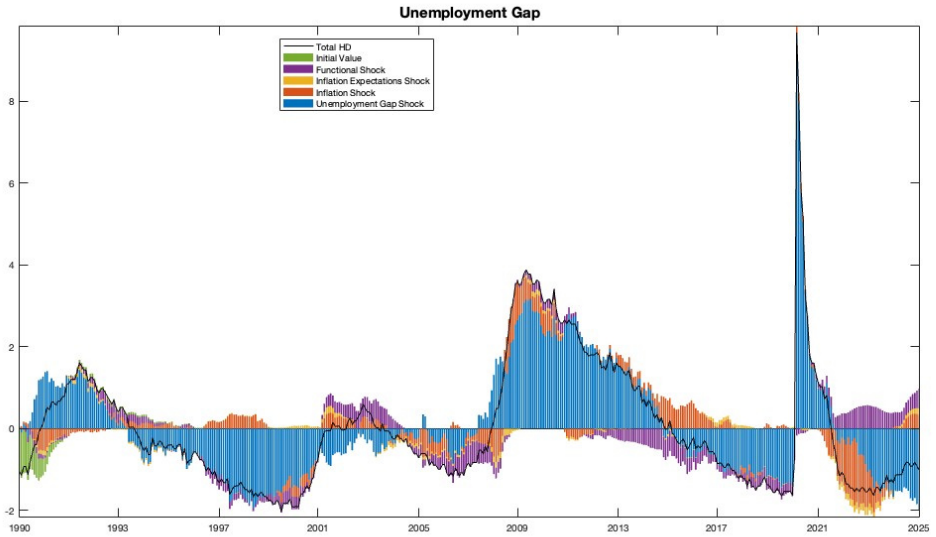
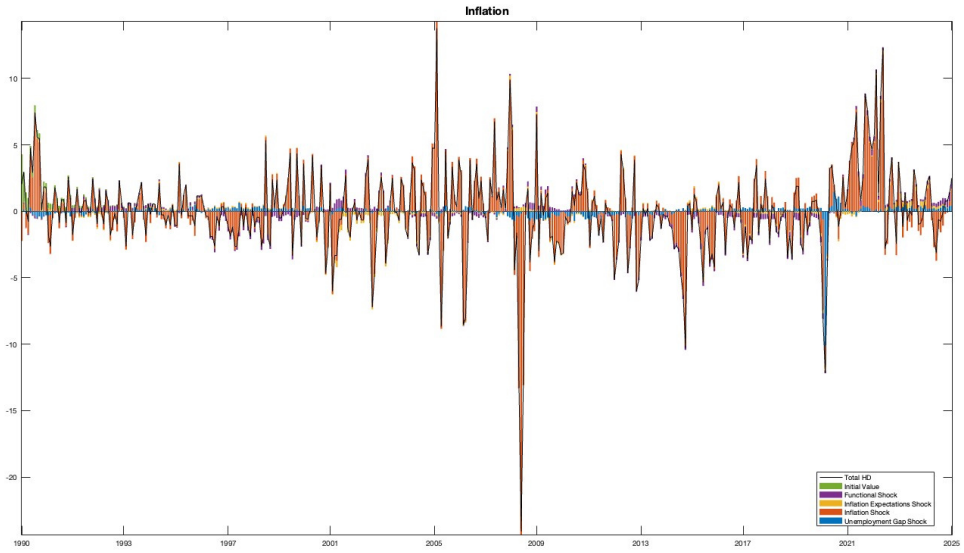


Figure 5.9: Historical Contributions to One-Year-Ahead Inflation Expectations

Horizontal axis: calendar year. The black line and colored contributions retain the supplied decomposition. Contributions are signed, not variance shares.



(a) Unemployment gap



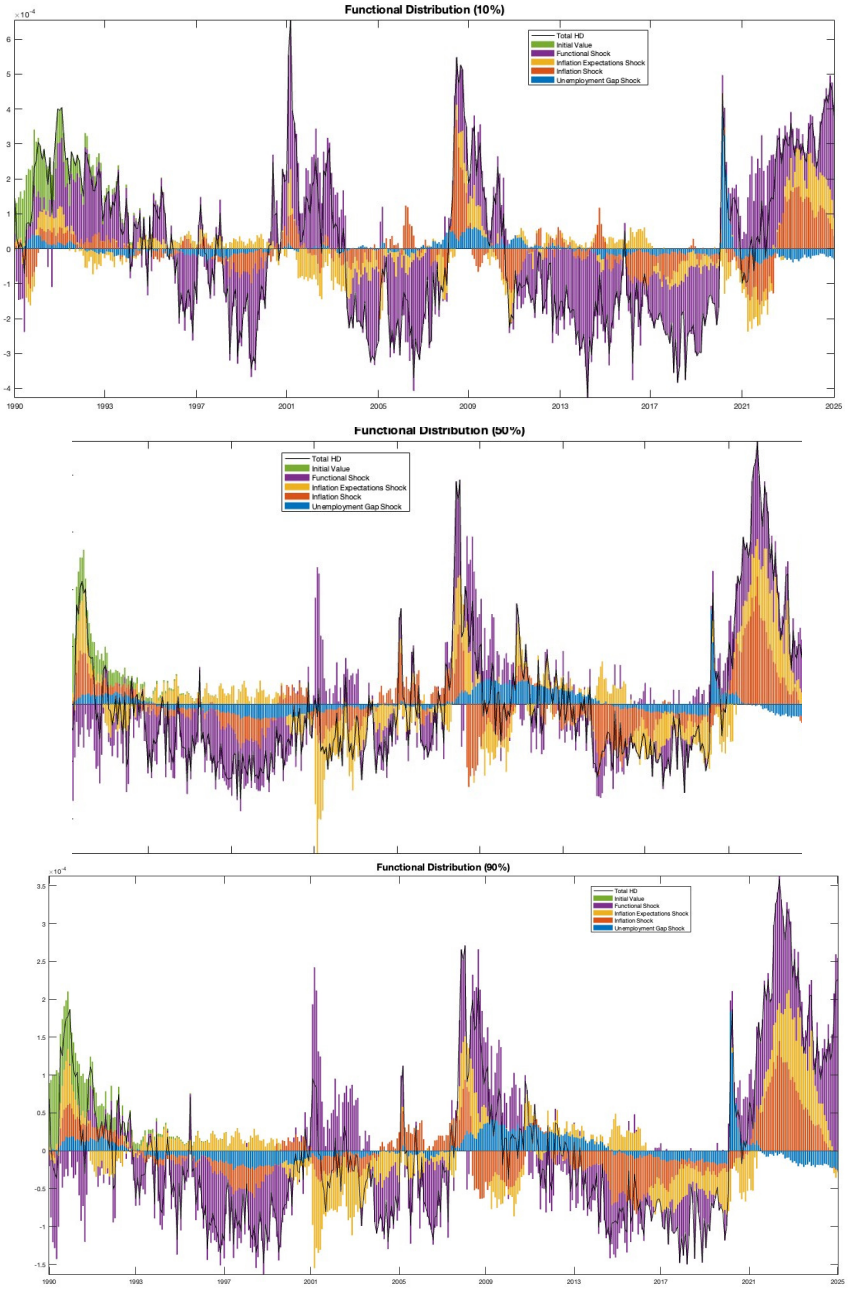
(b) Inflation

Figure 5.10: Historical Decompositions of Aggregate Variables

[a]

[a] Black lines are total historical decompositions. Colored bars show the signed contributions of unemployment-gap, inflation, expectations and functional shocks; green denotes the initial-value component. Dates follow the supplied figures, 1990–2025. "Functional Shock" is a grouped contribution; these panels do not separately identify the historical shares of Dispersion , shifts and tail risk. Contributions depend on the maintained recursive identification and are not forecast-error variance shares.

These are signed contributions conditional on the recursive model. A large movement in the expectation distribution need not imply a large historical contribution to inflation in the same model. The grouped functional bars also cannot tell us which individual feature accounts for a given episode.



(a) Historical Contributions at the Three Displayed Functional Evaluations

Figure 5.11: Historical Decomposition of the Functional Variable

Top to bottom: functional evaluations labeled 10%, 50%, and 90% in the supplied images. Horizontal axes: calendar year. Separate vertical scales and scientific-notation multipliers are retained.

5.6 Forecasting Inflation Beyond the Estimation Sample

I evaluate whether the FPCA scores improve forecasts of inflation beyond January 2025. Using a fixed January 2025 forecast origin, I estimate separate direct forecasting regressions for horizons of one to twelve months. The benchmark includes inflation lags, mean expectations, labor-market slack, long-run expectations, and shock controls. Alternative specifications add each FPCA score individually or all three jointly, including their first lags. Estimation uses no inflation outcomes after January 2025. Figure 5.12 compares the benchmark, shift, tail, and joint forecasts with observed annualized monthly CPI inflation from February 2025 through January 2026.

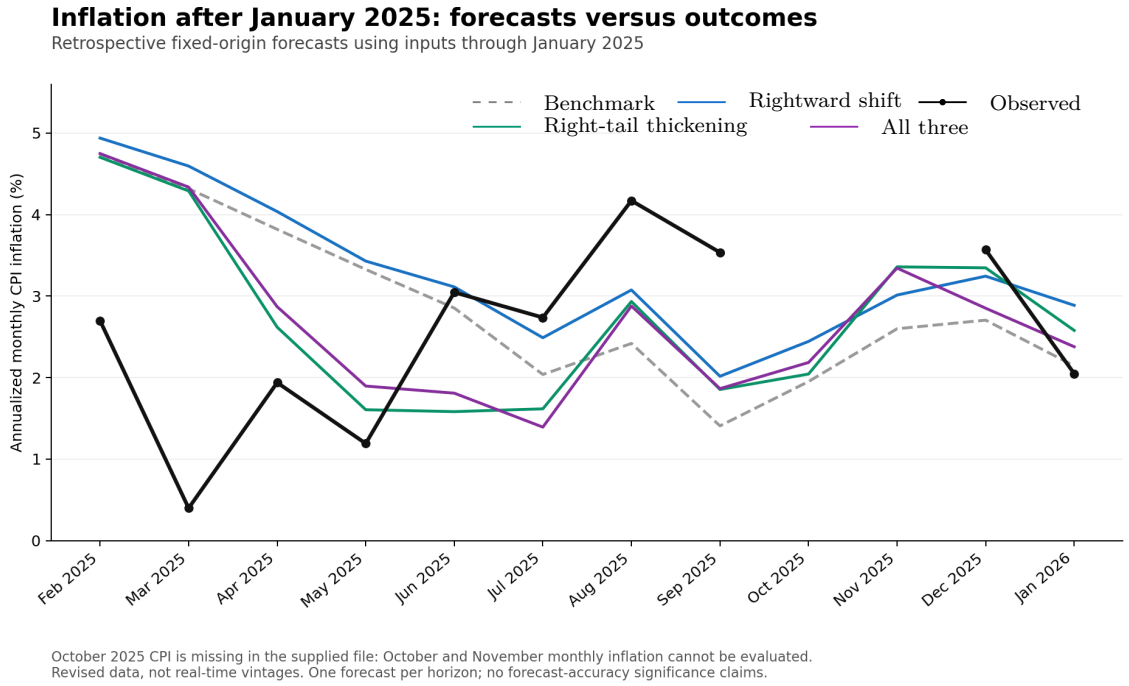


Figure 5.12: Inflation Forecasts from January 2025 and Subsequent Outcomes
Notes: The rightward-shift specification adds the second component and the right-tail-thickening specification adds the third; "All three" includes disagreement, shift, and tail thickening jointly. Forecasts use a fixed January 2025 origin. Gaps in observed inflation reflect missing CPI data.
Horizontal axis: outcome month. Vertical axis: annualized monthly CPI inflation (%). Benchmark excludes FPCA scores; Rightward shift adds the second component; right-tail thickening adds the third; All three includes all three components. Forecast curves, observed outcomes, and gaps are unchanged.

The improvement is a reduction in root mean squared error (RMSE) for forecasts of annualized monthly CPI inflation relative to the benchmark with mean expectations and macroeconomic controls. Over the ten available outcomes, adding tail lowers RMSE from 1.912 to 1.670 percentage points, a 12.6% reduction. Adding all three shape features jointly lowers it to 1.718, a 10.1% reduction. Shift alone lowers RMSE by only 0.1%, while dispersion alone raises it by 5.9%. Thus, the forecast gains in this exercise come from tail and the joint specification.

6 Conclusion

6.1 Summary of the contribution

This paper examines whether the mean inflation expectation is sufficient to characterize inflation dynamics, more specifically concentrating on the distributional shift during COVID. Using monthly individual responses from the University of Michigan Survey of Consumers, I summarize distributional deviations from a time-average reference density through dispersion, directional distributional shifts, and tail risk.

In the aggregate Phillips Curve, including these distributional features reduces the estimated coefficient on mean expectations and increases the absolute magnitude of the unemployment-gap coefficient. The distribution therefore contains information about inflation beyond that captured by average expectations and the other included controls.

The crisis period reveals distributional shifts that differ across macroeconomic episodes. During the acute phase of the post-COVID inflation surge, changes were concentrated in the upper tail of the expectations distribution, reflecting unusually high reported inflation expectations. These tail movements preceded a broader rightward shift in the distribution. During the Great Recession, the leftward reversal toward lower expected inflation preceded the expansion of the lower tail. These periods show that the distributional shifts and tail risk can be interconnected.

The dynamic and forecasting exercises show how these features relate to subsequent inflation. In the post-COVID local projections, rightward shift contains information about future inflation conditional on mean expectations, the other distributional scores, and macroeconomic controls. In the out-of-sample forecasting exercise using forecasts from January 2025, the tail score reduces inflation forecast RMSE by 12.6%, while all three scores jointly reduce it by 10.1%, relative to the benchmark. These forecast gains are specific to the crisis period. Together, the findings show that different parts of the expectations distribution matter at different stages of inflation dynamics.

More broadly, the results suggest that inflation expectations are not adequately summarized by their average level. Changes in disagreement, directional distributional shifts, and tail risk contain distinct information about inflation dynamics, and the relevance of these features varies across episodes and across locations. During periods of macroeconomic stress, movements in the tails of the distribution and subsequent shifts in its overall location provide signals that are not captured by the mean expectation alone. These findings imply that models and policy analyses that focus exclusively on average expectations may overlook important information contained in the distribution of beliefs. Monitoring the full distribution of inflation expectations therefore provides a richer characterization of inflation pressures and their evolution over time.

6.2 Policy Implication

The findings suggest that changes in the tails of inflation expectations may provide early warning signals of emerging inflation pressures before expectations shift more broadly. During the post-COVID inflation surge, upper-tail expansion preceded a broad rightward shift in the distribution. Monitoring the share of households reporting unusually high inflation expectations could therefore help policymakers detect emerging concerns at an early stage. Tracking whether these movements persist and spread toward the center of the distribution would then help assess whether those concerns are becoming more widespread. The predictive information contained in the tail component provides additional motivation for incorporating such signals into inflation monitoring and forecasting.

The Great Recession illustrates that the sequence of adjustment can differ across episodes: a broad leftward shift preceded lower-tail expansion. An early warning framework should therefore monitor both directional shifts and tail movements, rather than rely on a single indicator. For policymakers, the practical implication is to examine where changes in expectations first appear and how they subsequently spread across the distribution. This approach could supplement mean expectations and conventional inflation forecasts, providing earlier information about the direction and breadth of changes in inflation beliefs.

The findings support monitoring the distribution of inflation expectations alongside its mean and other moments, although moments are less informative in my analysis. Dispersion, directional shifts, and tail movements describe different aspects of how beliefs adjust. During the post-COVID inflation surge, upper-tail expansion preceded a broad rightward shift, whereas the Great Recession exhibited a leftward shift before lower-tail expansion. Monitoring both extreme forecasts and broader distributional movements can therefore help policymakers distinguish changes concentrated among a small share of respondents from changes that have become more widespread.

The results also have implications for the use of reduced-form Phillips curve in policy analysis. Including distributional information produces a steeper estimated relationship between inflation and the unemployment gap. Assessments of inflation pressures should therefore consider how the estimated slope depends on the representation of expectations. Distributional components may also supplement inflation forecasting, although their usefulness requires evaluation across additional periods. These findings inform the measurement and monitoring of inflation pressures; they do not establish an optimal monetary policy response to a particular distributional movement.

6.3 Future direction and limitations

The analysis documents conditional and predictive relationships, but identifying the causal effects of changes in expectations remains a task for future research. Inflation and expectations may respond to common economic shocks, and the VAR results depend on identification assumptions. Moreover, observing tail expansion before a broader distributional shift does not establish that the former causes the latter. Future work could use plausibly exogenous changes in information or expectations to investigate the mechanisms connecting distributional movements to inflation.

A second limitation concerns the interpretation of the survey data. The analysis uses household inflation expectations, whereas firms make price-setting decisions. Combining firm expectations with pricing data would provide a more direct assessment of the relationship between heterogeneous beliefs and price adjustment. In addition, the estimated densities describe the cross-sectional distribution of point forecasts. Their tails measure the prevalence of extreme reported expectations, rather than the probabilities that individual respondents assign to extreme inflation outcomes.

Finally, the functional components summarize statistical patterns whose interpretation depends on the reference distribution, sample, and density construction. Further analysis could examine the stability of these patterns across survey sources and estimation periods. The out-of-sample forecast comparison also covers a short evaluation window. Extending it to multiple forecast origins and different inflation environments, with all density and score estimates constructed from information available at each origin, would provide stronger evidence on the components' usefulness for real-time forecasting.

Appendix contents

Click a section title or page number to jump to it.

Appendix section	Page
A Regional Theory and Evidence	**48**
A.1 Heterogeneous-Beliefs Regional Phillips Curves	48
A.2 Overview	50
A.3 Regional data and geographic assignment	50
A.4 Regional empirical specifications	51
A.5 Regional results	53
A.6 Pooled full-sample and crisis comparisons	54
A.7 Local Projection estimates	58
A.8 Additional Regional Analysis	59
A.9 Mean-centered regional robustness	67
B Mean-Centered FPCA and Aggregate Estimates	**69**
B.1 Aggregate Phillips Curve: Mean-Centered Comparison	69
B.2 Measurement and Distributional Summaries	73
B.3 Additional Aggregate Estimates	75
C Additional Dynamic Evidence	**78**
C.1 Inflation responses and recursive ordering	78
C.2 Responses associated with observed shocks	81
C.3 Predictive distributional effects during COVID	81
C.4 Historical shock contributions	82
D Robustness Checks	**84**
D.1 Mean-centered aggregate robustness	84
D.2 Robustness of the dynamic results	85
E Historical Distributions	**87**
E.1 Monthly Densities across Historical Episodes	87

A Regional Theory and Evidence

Back to appendix contents

A.1 Heterogeneous-Beliefs Regional Phillips Curves

Firm-Level Price Setting: Following Meeks and Monti (2023), consider a continuum of firms indexed by j located in the metropolitan area r. Firms operate under monopolistic competition and face Calvo price rigidity: in each period, a firm can reset its price with probability $1-\theta$ and otherwise keep its existing price. Firms may hold heterogeneous beliefs about future economic conditions. Let $E^j_{r,t}[\cdot]$ denote the expectation operator of firm j at time t. The firm's optimal reset price is

$$p^*_{j,r,t} = (1-\beta\theta)\sum_{k=0}^{\infty}(\beta\theta)^k E^j_{r,t}\left[mc_{r,t+k} + p_{r,t+k}\right], \tag{18}$$

where $mc_{r,t}$ denotes real marginal cost and $p_{r,t}$ denotes the aggregate price level. Define the firm's relative reset price by subtracting:$q_{j,r,t} \equiv p^*_{j,r,t} - p_{r,t}$. Assuming that firms' beliefs satisfy the law of iterated expectations, equation (18) can be written recursively:

$$q_{j,r,t} = (1-\beta\theta)mc_{r,t} + \beta\theta E^j_{r,t}\left[q_{j,r,t+1} + \pi_{r,t+1}\right], \quad \pi_{r,t+1} \equiv p_{r,t+1} - p_{r,t} \tag{19}$$

Equation (19) implies that firms' desired prices depend on expectations of future inflation and future relative prices. When firms hold heterogeneous beliefs, they may choose different desired reset prices even if they face the same economic conditions.

Aggregation and the Heterogeneous-Beliefs Phillips Curves: Let $q_{r,t} = \mathbb{E}_j[q_{j,r,t}]$ denote the average relative reset price across firms. Adding and subtracting the average future reset price yields $q_{j,r,t+1} = q_{r,t+1} + (q_{j,r,t+1} - q_{r,t+1})$ Substituting this decomposition into equation (19) and averaging across firms gives

$$q_{r,t} = (1-\beta\theta)mc_{r,t} + \beta\theta E_{r,t}\left[q_{r,t+1} + \pi_{r,t+1}\right] + \beta\theta\Delta_{r,t}, \tag{20}$$

where

$$E_{r,t}[X] \equiv \mathbb{E}_j\left[E^j_{r,t}[X]\right] \tag{21}$$

denotes the average expectation across firms, and

$$\Delta_{r,t} \equiv \mathbb{E}_j\left[E^j_{r,t}\left(q_{j,r,t+1} - q_{r,t+1}\right)\right] \tag{22}$$

captures the effect of heterogeneous beliefs. If all firms hold identical expectations, then $\Delta_{r,t} = 0$. Under Calvo aggregation,

$$\pi_{r,t} = \frac{1-\theta}{\theta} q_{r,t}. \tag{23}$$

Substituting equation (23) into equation (20) and rearranging yields

$$\pi_{r,t} = \frac{(1-\beta\theta)(1-\theta)}{\theta} mc_{r,t} + \beta E_{r,t}\left[\pi_{r,t+1}\right] + \beta(1-\theta)\Delta_{r,t}. \tag{24}$$

Equation (24) is the heterogeneous-beliefs Phillips curve. The first term captures the effect of current marginal costs, the second captures expected future inflation, and the third captures the influence of heterogeneous beliefs on firms' pricing decisions.

Measuring the Heterogeneous-Beliefs Wedge: Departure from Monti-Meeks The theoretical wedge $\Delta_{r,t}$ depends on firms' beliefs about future relative reset prices, which are not directly observed. Following Meeks and Monti (2023), I use the cross-sectional distribution of survey inflation expectations as an empirical proxy for the underlying heterogeneity in beliefs relevant for pricing decisions. This constitutes a measurement assumption linking observed survey expectations to the unobserved firm-level belief wedge.

I depart from Meeks and Monti (2023) in the distributional object used for this mapping. Rather than centering individual expectations around the contemporaneous mean and retaining only the disagreement distribution, I retain the expectation density on its original support. This allows movements in the location of probability mass, as well as changes in dispersion and the tails, to enter the empirical counterpart of the heterogeneous-beliefs wedge.

Let $R = g(r)$ denote the survey region assigned to metropolitan area r. Because expectation densities are observed at the broader survey-region level, the density in $g(r)$ is used as an empirical proxy for the local belief distribution. This measurement assumption uses the geographic crosswalk described in Section A.3.

Define the region-specific average density as

$$\bar{f}_R(\pi^e) = \frac{1}{T}\sum_{t=1}^{T} f_{R,t}(\pi^e), \tag{25}$$

and define the density deviation

$$\widetilde{f}_{R,t}(\pi^e) = f_{R,t}(\pi^e) - \bar{f}_R(\pi^e). \tag{26}$$

I approximate the heterogeneous-beliefs wedge using a functional of these density deviations,

$$\Delta_{r,t} \approx \widetilde{\mathcal{G}}_{R,t}, \tag{27}$$

where

$$\widetilde{\mathcal{G}}_{R,t} = \int \gamma(\pi^e)\widetilde{f}_{R,t}(\pi^e)\, d\pi^e. \tag{28}$$

Substituting into equation (24) yields

$$\pi_{r,t} = \kappa mc_{r,t} + \beta E_{r,t}\left[\pi_{r,t+1}\right] + \beta(1-\theta)\widetilde{\mathcal{G}}_{R,t}, \tag{29}$$

Inflation and labor-market slack are measured at the metropolitan-area level r, while the expectation distribution is measured using respondents in survey region $R = g(r)$ assigned to metropolitan area r. The average firm expectation $E_{r,t}[\pi_{r,t+1}]$ is not directly observed. I use the mean one-year-ahead inflation expectation in Census region $R = g(r)$ as its empirical counterpart, denoted by $\pi^e_{R,t}$.

A.2 Overview

This extension examines how the relationship between expectation distributions and inflation differs across regions and crisis episodes. I link regional household expectations to metropolitan inflation and unemployment, controlling for metropolitan and calendar-month fixed effects. The resulting estimates use differences across regions within the same month. The analysis focuses on regional measurement, differences in distributional coefficients across episodes and locations, and the timing of the relationship with subsequent inflation.

A.3 Regional data and geographic assignment

The University of Michigan Surveys of Consumers distinguish Northeast, North Central, South and West. I use numerical one-year price-change responses (PX1) within each region and month. Regional distributional deviations are measured relative to each region's time-average reference density. I retain the estimated regional FPCA scores and their orientation throughout the extension. Regional mean expectations and conventional moments are calculated from finite numerical PX1 responses without survey weighting. The mean is the arithmetic average, and variance uses denominator $n-1$. Skewness and Pearson kurtosis use central moments with denominator n, standardized by the corresponding powers of the second central moment. All four regions use this common construction; records the reconciliation of the regional moment series.

The panel links metropolitan headline CPI inflation and unemployment rates to the expectation measures of the assigned survey region. The outcomes originate from the BLS CPI and Local Area Unemployment Statistics programs. Inflation is annualized monthly headline inflation, and unemployment enters in levels. The estimation crosswalk assigns Washington, D.C. to Northeast. Expectations are measured at the broader survey-region level and serve as mapping for the expectation distributions of the metropolitan areas assigned to that region.

The January 1990–January 2025 source panel contains 8,841 observations. Requiring the twelve-month unemployment lag and all regressors gives a common contemporaneous OLS/IV sample of 8,131 observations in 20 metropolitan areas and 409 months, January 1991–January 2025. St. Louis is excluded because its unemployment series is missing. Local-projection samples vary with the forecast horizon.

Figure A.1 displays the regional expectation densities.

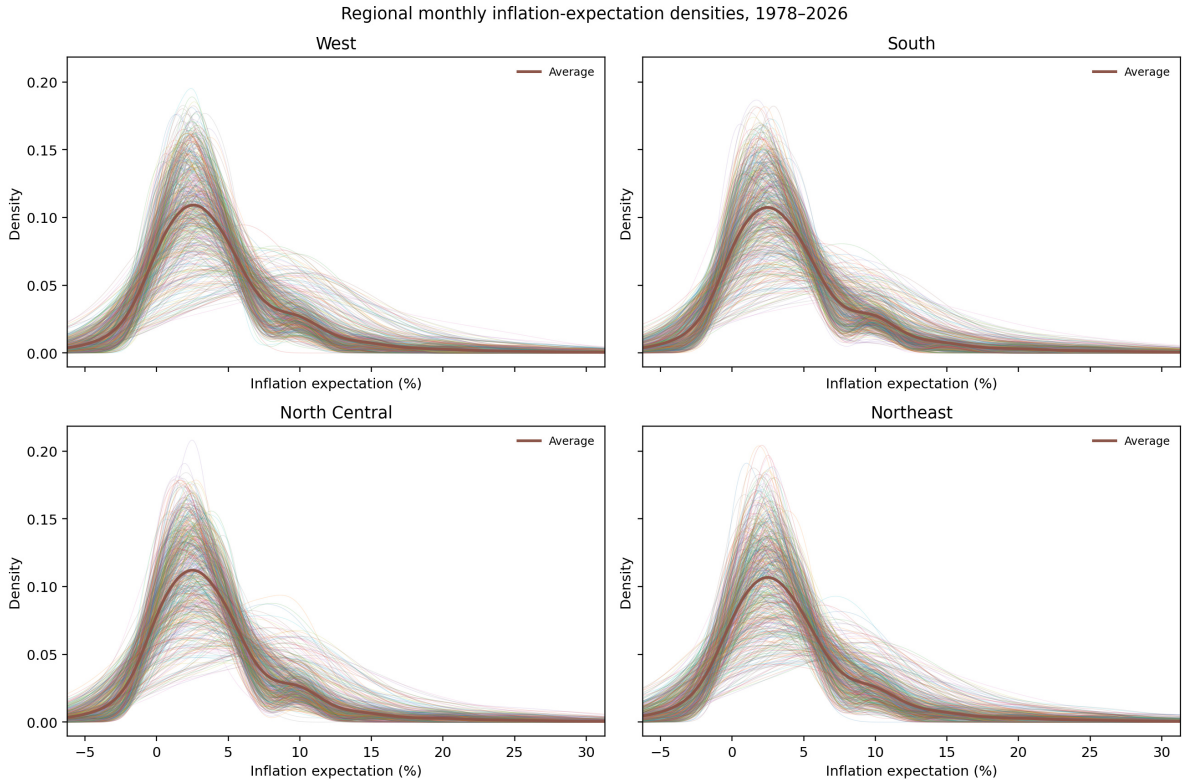


Figure A.1: Regional Densities of One-Year-Ahead Inflation Expectations

Panels identify West, South, Northeast, and North Central. Horizontal axes: individual one-year-ahead inflation expectation (PX1, %). Vertical axes: density. Black curves denote the displayed averages; the monthly curves are unchanged.

A.4 Regional empirical specifications

A.4.1 Pooled regional specification

Let i index metropolitan areas, $r(i)$ denote their assigned survey region, and t index months. The pooled regional specification is

$$\pi_{i,t} = \alpha_i + \tau_t + \beta_u u_{i,t} + \beta_\mu \mu_{r(i),t} + \boldsymbol{\theta}' \mathbf{F}_{r(i),t} + \boldsymbol{\delta}' \mathbf{M}_{r(i),t} + \varepsilon_{i,t}. \tag{30}$$

Here $\pi_{i,t}$ is annualized monthly headline CPI inflation, $u_{i,t}$ is the metropolitan unemployment rate, and $\mu_{r(i),t}$ is mean expected inflation. Metropolitan fixed effects α_i absorb persistent differences across locations; calendar-month fixed effects τ_t absorb common national developments. The distributional coefficients therefore describe associations between regional differences in expectations and relative metropolitan inflation within a month.

The vector of standardized FPCA scores is

$$\mathbf{F}_{r,t} = (d_{r,t}, s_{r,t}, \ell_{r,t})' = \left(\frac{FPCL_{1,r,t}}{\sigma_1}, -\frac{FPCL_{2,r,t}}{\sigma_2}, -\frac{FPCL_{3,r,t}}{\sigma_3} \right)'.$$

Higher values represent greater disagreement, a rightward shift, and greater left-tail risk, respectively. The standard deviations σ_k are the pooled source-panel values $(0.213893, 0.120088, 0.063783)$, calculated over January 1990–January 2025 and held

fixed across specifications, episodes and estimators. Each FPCA coefficient measures the associated change in inflation, in percentage points, for a one-standard-deviation movement in the factor. The vector $\mathbf{M}_{r,t}$ contains the conventional variance, skewness, and kurtosis measures.

I estimate an FPCA specification excluding $\mathbf{M}_{r,t}$, a moments specification excluding $\mathbf{F}_{r,t}$, and a combined specification including both. Unemployment and mean expectations enter each model. In the combined model, $H_0 : \boldsymbol{\theta} = \mathbf{0}$ tests whether the FPCA scores contribute information conditional on the moments; $H_0 : \boldsymbol{\delta} = \mathbf{0}$ tests the contribution of moments conditional on the FPCA scores.

A.4.2 Episode and regional interactions

For episode indicator D_t^E, I estimate

$$\begin{aligned}\pi_{i,t} = \alpha_i + \tau_t + \beta_u u_{i,t} + \beta_\mu \mu_{r(i),t} \\ + D_t^E \left(\boldsymbol{\theta}_E' \mathbf{F}_{r(i),t} + \boldsymbol{\delta}_E' \mathbf{M}_{r(i),t}\right) + \varepsilon_{i,t}.\end{aligned} \tag{31}$$

Broad COVID covers January 2020–January 2025; the acute inflation-surge window covers March 2021–June 2022. The broad Great Recession window covers December 2007–June 2009; the acute window covers September 2008–June 2009. Each episode model is estimated separately on the full comparison sample. Distributional coefficients are restricted to zero outside the selected episode. They measure within-episode associations, rather than changes from freely estimated pre-episode coefficients.

Regional heterogeneity is introduced by adding

$$D_t^E s_{r(i),t} \sum_{q \in \{\text{NE,S,W}\}} \eta_{q,E} \mathbf{1}\{r(i) = q\} \tag{32}$$

to equation (31). North Central is the reference region. Its rightward-shift coefficient is $\theta_{s,E}$; the coefficient in region q is $\theta_{s,E} + \eta_{q,E}$. Unemployment and the remaining included variables retain common coefficients across regions. The null $H_0 : \eta_{\text{NE},E} = \eta_{\text{S},E} = \eta_{\text{W},E} = 0$ tests equality of the four regional shift coefficients. Standard errors for regional totals use the covariance between the reference coefficient and its interaction.

A.4.3 Estimation and inference

Pooled OLS provides the contemporaneous benchmark. I also estimate the same specifications by two-stage least squares, instrumenting current unemployment with its twelve-month lag. Mean expectations and the distributional measures remain included regressors. The IV interpretation requires lagged unemployment to be uncorrelated with the structural error conditional on the regressors and fixed effects; it does not identify an exogenous expectations innovation.

OLS and IV use the common sample described in Section A.3. Availability of lagged unemployment restricts that comparison sample, but the lag is neither a regressor nor an instrument in OLS. Both estimators include metropolitan and calendar-month effects. Standard errors use metropolitan-clustered CR0 covariance estimates, with normal individual tests and chi-squared joint tests.

A.4.4 Regional local projections

To examine subsequent inflation, I estimate a separate projection at $h = 1, \ldots, 20$ months:

$$\begin{aligned}\pi_{i,t+h} = \alpha_{i,h} + \tau_{t,h} + \kappa_{r(i),h} D_t^C + \rho_h \pi_{i,t} \\ + \sum_{q=1}^{4} \mathbf{1}\{r(i) = q\} \left[\beta_{q,h}^P (1 - D_t^C) + \beta_{q,h}^C D_t^C\right] s_{r(i),t} \\ + \boldsymbol{\gamma}_h' \mathbf{z}_{i,t} + \boldsymbol{\psi}_h' D_t^C \mathbf{w}_{r(i),t} + \boldsymbol{\Phi}_h' \mathbf{x}_{i,t-1} + \varepsilon_{i,t+h}.\end{aligned} \tag{33}$$

Here D_t^C identifies broad COVID. Pre-COVID and COVID shift coefficients are estimated freely for each region. Region-by-COVID intercepts $\kappa_{r(i),h} D_t^C$ accommodate changes in regional average inflation, with North Central as the normalization.

The vector $\mathbf{z}_{i,t}$ contains current unemployment, mean expectations, disagreement, left-tail risk, and the three conventional moments. The vector $\mathbf{w}_{r(i),t}$ contains disagreement, left-tail risk, and the moments, allowing their coefficients to change during COVID. The lagged state vector $\mathbf{x}_{i,t-1}$ contains one monthly lag of inflation, unemployment, mean expectations, all three FPCA scores and the three moments.

The projections are estimated by OLS. Conditioning on current inflation separates the association with subsequent inflation from same-month co-movement. The coefficient $\beta_{q,h}^C$ measures the association between a one-SD rightward shift during COVID and annualized monthly inflation h months later; the outcome is not cumulative inflation. Exact calendar leads and lags use the January 1990–January 2025 source panel. Usable anchor dates begin in February 1990, and sample sizes vary with the availability of future outcomes.

Standard errors apply a Bartlett HAC estimator to monthly sums of regression scores with bandwidth $\max(12, h+1)$, accommodating cross-metropolitan dependence and serial correlation. Confidence intervals are pointwise and condition on the supplied FPCA scores. These projections describe conditional predictive associations; they do not identify causal effects of expectations or establish out-of-sample forecasting performance.

A.5 Regional results

A.5.1 Full-sample regional Phillips Curve

The full-period OLS comparisons in Table 8 show negative unemployment coefficients with Phillips Curve steepening from -0.274 to -0.280. Allowing the distributional shift coefficient to differ across regions changes this result: the expanded FPCA block rejects zero ($p = 0.009$), and equality of the regional shift coefficients is rejected ($p < 0.001$). The Southern shift interaction is positive, 0.660 (standard error 0.282). These comparisons motivate the episode-specific regional analysis.

A.6 Pooled full-sample

Table 8: Pooled Regional OLS: Full-Period Distributional Slopes

	(1) FPCA	(2) Moments	(3) Both	(4) Both + regional shift interactions
Unemployment	-0.276***	-0.274***	-0.276***	-0.280***
	(0.058)	(0.058)	(0.057)	(0.055)
Mean expectation	0.051	0.163	0.056	0.053
	(0.131)	(0.120)	(0.177)	(0.169)
High disagreement	0.325*	–	0.287	0.152
	(0.192)	–	(0.249)	(0.192)
Rightward shift	0.026	–	0.032	-0.071
	(0.097)	–	(0.103)	(0.246)
Left-tail risk	0.119	–	0.120	0.090
	(0.106)	–	(0.120)	(0.093)
Variance	–	0.0055*	0.0019	0.0057
	–	(0.0031)	(0.0048)	(0.0044)
Skewness	–	-0.0389	-0.0118	-0.0139
	–	(0.0469)	(0.0509)	(0.0518)
Kurtosis	–	0.0020752	0.0027477	0.0029183
	–	(0.0088057)	(0.0085124)	(0.0086794)
Rightward shift × Northeast	–	–	–	0.132
	–	–	–	(0.256)
Rightward shift × South	–	–	–	0.660**
	–	–	–	(0.282)
Rightward shift × West	–	–	–	-0.085
	–	–	–	(0.275)
FPCA block: p	0.222	–	0.607	0.009
Moment block: p	–	0.036	0.727	0.225
Regional equality: p	–	–	–	< 0.001
R^2	0.385	0.385	0.385	0.390
Metro and month effects	Yes	Yes	Yes	Yes
Estimator	OLS	OLS	OLS	OLS
Metropolitan clusters	20	20	20	20
Observations	8,131	8,131	8,131	8,131

Notes: Dependent variable: annualized monthly metropolitan headline CPI inflation. Pooled OLS with metropolitan and calendar-month fixed effects; no variable is instrumented. Estimation uses January 1991–January 2025 and the same 8,131 observations as the IV table. Twelve-month unemployment-lag availability restricts the comparison sample only; that lag is not an instrument or a regressor in OLS. Distributional slopes are estimated over the full period. FPCA coefficients are per one pooled SD; a rightward shift is $-FPCL2$. Column (4) uses North Central as the reference: add each regional interaction to the rightward-shift coefficient to obtain its total. Standard errors in parentheses use CR0 metropolitan clustering with normal pointwise tests, matching the IV table convention. FPCA block tests impose three restrictions, or six in column (4); the moment and regional-equality tests each impose three. D.C. retains its original Northeast assignment. * $p < 0.10$, ** $p < 0.05$, *** $p < 0.01$.

A.6.1 Distributional features during crisis periods

Table 9 reports the combined FPCA-and-moments IV specifications for the four episode windows. A one-SD rightward shift has a pooled regional coefficient of 0.867 (standard error 0.370) in broad COVID and 3.243 (1.437) in the acute inflation surge. Expressed in the leftward direction, the Great Recession coefficients are 1.083 (0.363) and 2.156 (0.541). These coefficients describe relative metropolitan inflation conditional on common monthly developments.

The right-tail coefficient is −0.686 (0.446) in broad COVID and −2.757 (0.913) in the acute surge; only the latter rejects zero at 5 percent. The Great Recession left-tail coefficients are 1.555 (0.554) and 1.181 (0.863), with only the broad-window estimate rejecting zero at 5 percent. The FPCA block rejects zero in acute COVID and both recession windows conditional on mean expectations and conventional moments, but does not reject

in pooled broad COVID ($p = 0.135$). Appendix A.8.3 reports the supplied broad-COVID OLS and IV comparisons and the broad- and acute-recession IV comparisons.

Table 9: Regional Episode Results: Shifts, Tails and Mean Expectations

Window	Broad COVID Jan. 2020– Jan. 2025	Acute COVID Mar. 2021– June 2022	Broad recession Dec. 2007– June 2009	Acute recession Sept. 2008– June 2009
Unemployment	-0.304***	-0.287***	-0.312***	-0.305***
	(0.088)	(0.086)	(0.090)	(0.091)
Mean expectation	0.110	0.121	0.203*	0.232**
	(0.100)	(0.105)	(0.105)	(0.106)
High disagreement	0.366	-1.282	1.217	0.817
	(0.694)	(1.576)	(0.993)	(1.651)
Rightward shift ($-\xi_2$)	0.867**	3.243**	–	–
	(0.370)	(1.437)	–	–
Leftward shift ($+\xi_2$)	–	–	1.083***	2.156***
	–	–	(0.363)	(0.541)
Right-tail risk ($+\xi_3$)	-0.686	-2.757***	–	–
	(0.446)	(0.913)	–	–
Left-tail risk ($-\xi_3$)	–	–	1.555***	1.181
	–	–	(0.554)	(0.863)
Variance	-0.002	0.116***	-0.122*	-0.106
	(0.009)	(0.044)	(0.068)	(0.084)
Skewness	-0.165	-0.528	-0.732	-1.453
	(0.162)	(0.760)	(0.459)	(1.268)
Kurtosis	-0.030	0.215	0.424*	-0.313
	(0.024)	(0.236)	(0.251)	(0.622)
FPCA block: p	0.135	0.003	0.003	< 0.001
Moment block: p	0.419	0.032	< 0.001	0.155
Metro and month effects	Yes	Yes	Yes	Yes
Observations	8,131	8,131	8,131	8,131

Notes: Combined FPCA-and-moments IV specifications, with unemployment instrumented by its twelve-month lag. All columns use the same comparison sample and fixed effects. Distributional slopes are restricted to zero outside the indicated window. Standard errors use metropolitan-cluster CR0 covariance; stars use normal pointwise tests.

Blue rows report a one-SD movement in the direction named: COVID uses $-\xi_2$ and $+\xi_3$, whereas the Great Recession uses $+\xi_2$ and $-\xi_3$. Dashes avoid reporting the same coordinate twice. A sign change is a relabeling of a coordinate, not a new regression. Coefficients are within-month regional associations, not realized changes in tail shares.

Red marks the conditional mean benchmark; it does not denote a zero effect. * $p < 0.10$, ** $p < 0.05$, *** $p < 0.01$.

A.6.2 Differences across regions

In broad COVID, the regional IV rightward-shift coefficients are 0.888 in North Central, 0.957 in Northeast, 2.080 in South and 0.328 in West. The South estimate is positive and precise (standard error 0.488), while West is imprecise (0.489). The acute COVID South estimate is 4.073 (1.285). OLS yields the same broad-COVID pattern, with a Southern coefficient of 2.079 (0.488). Equality of the four broad-COVID IV coefficients is rejected ($\chi^2(3) = 20.094$, $p < 0.001$).

The Great Recession places more weight on West and North Central. Their broad-window leftward-shift coefficients are 1.630 (0.510) and 1.318 (0.388), respectively; both reject zero at the 1 percent level. During the acute recession the West estimate is 1.715 (0.559) and North Central is 3.156 (0.788). The Southern recession coefficients are imprecise. The regions with the strongest conditional associations therefore differ across the two episodes. The complete regional comparison is in Table 10.

Table 10: Regional Shift Coefficients across Crisis Episodes

Total regional IV shift coefficients				
	Broad COVID	Acute COVID	Broad recession	Acute recession
Direction	Rightward	Rightward	Leftward	Leftward
North Central	0.888**	1.215	1.318***	3.156***
	(0.448)	(2.252)	(0.388)	(0.788)
Northeast	0.957**	-0.054	0.405	2.010**
	(0.414)	(0.800)	(0.354)	(0.910)
South	2.080***	4.073***	0.289	1.138
	(0.488)	(1.285)	(0.474)	(0.938)
West	0.328	1.029	1.630***	1.715***
	(0.489)	(1.597)	(0.510)	(0.559)
Equality of regions: p	< 0.001	0.009	< 0.001	0.006

Notes: Total regional coefficients from one joint IV regression per column. Standard errors include the covariance of the base coefficient and interaction. COVID uses rightward shift $-\xi_2$; recession columns use leftward shift $+\xi_2$. Coefficients are per common score SD. The other regressors and fixed effects remain as specified in equation (31). Episode dates are those in Table 9. Equality tests compare the four regional shift coefficients. * $p < 0.10$, ** $p < 0.05$, *** $p < 0.01$.

A.6.3 Subsequent regional inflation during COVID

Figure A.2 and Table 11 report local projections conditional on current inflation and the specified information set. The Southern coefficient is 1.103 at one month, 2.411 at two months and 2.171 at three months; each rejects zero at the 1 percent level. At two months, the other regional estimates range from 0.609 to 0.648. The Southern coefficient exceeds each other region after adjustment across the six regional pairs at that horizon. At three months, the South exceeds North Central and Northeast at the adjusted 5 percent level; the adjusted South–West p-value is 0.074. By six months the Southern estimate is weaker, 0.985 (standard error 0.597, $p = 0.099$), and it is imprecise at twelve months. The association is concentrated at short horizons.

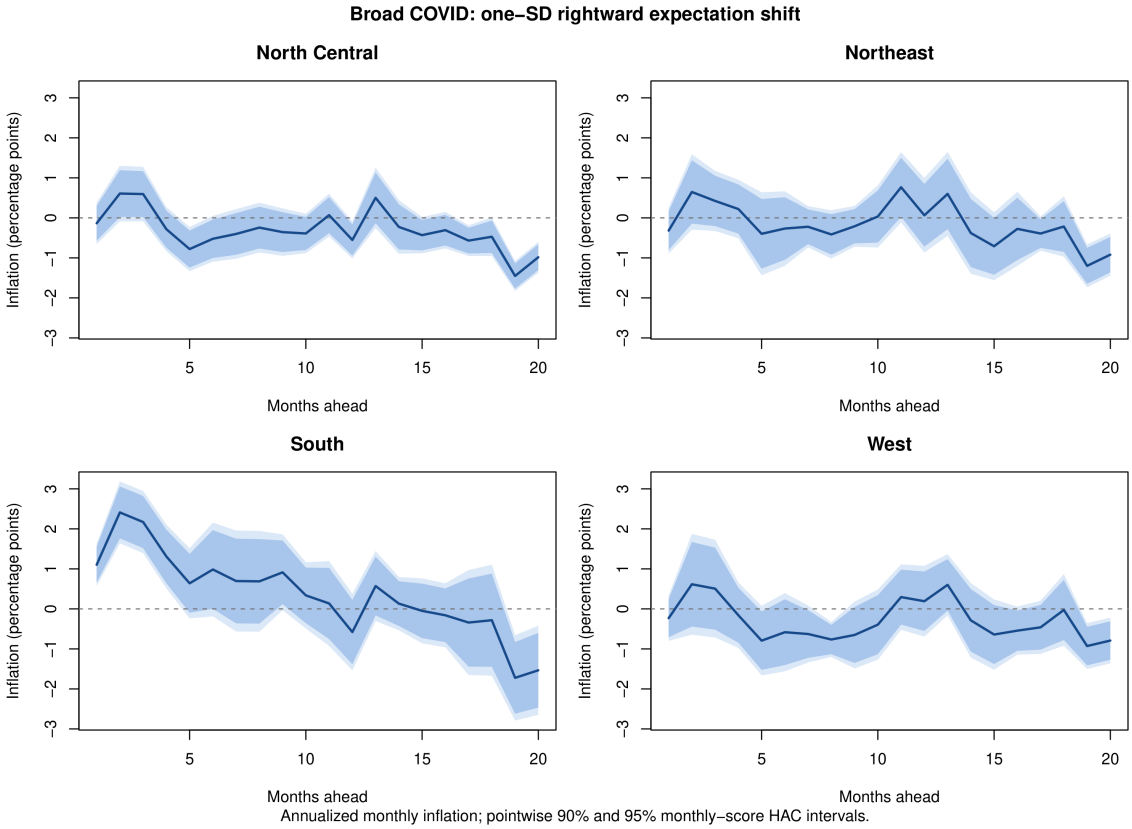


Figure A.2: Regional Predictive Local Projections during Broad COVID

Notes: Total COVID coefficients on a one-SD rightward shift, for annualized monthly metropolitan inflation one to twenty months ahead. Dark and light bands are pointwise 90 and 95 percent monthly-score HAC intervals, plotted from the reported coefficients and standard errors rounded to three decimal places. The specification is equation (33). The outcome is inflation at the stated horizon, not cumulative inflation. Full estimates and regional comparisons appear in Appendix A.7.

A.7 Local Projection estimates

The complete COVID response path is reported below. The pointwise bands condition on the supplied scores. Regional pairwise comparisons use the joint covariance matrix; Holm adjustments cover six pairs separately at each horizon and are not adjustments across all twenty horizons.

Table 11: Broad COVID: regional predictive local projections

	North Central	Northeast	South	West	N_h
1 month	-0.136	-0.319	1.103***	-0.232	8,332
	(0.264)	(0.293)	(0.270)	(0.289)	
2 months	0.609*	0.648	2.411***	0.616	8,312
	(0.355)	(0.480)	(0.394)	(0.642)	
3 months	0.595*	0.424	2.171***	0.507	8,292
	(0.347)	(0.382)	(0.396)	(0.623)	
4 months	-0.283	0.221	1.311***	-0.158	8,272
	(0.281)	(0.373)	(0.406)	(0.417)	
5 months	-0.779***	-0.398	0.639	-0.793*	8,252
	(0.281)	(0.529)	(0.446)	(0.443)	
6 months	-0.522*	-0.266	0.985*	-0.582	8,232
	(0.292)	(0.475)	(0.597)	(0.499)	
7 months	-0.401	-0.222	0.697	-0.627*	8,212
	(0.316)	(0.263)	(0.643)	(0.362)	
8 months	-0.243	-0.414	0.689	-0.765***	8,192
	(0.317)	(0.307)	(0.642)	(0.222)	
9 months	-0.355	-0.209	0.914*	-0.651	8,172
	(0.302)	(0.260)	(0.483)	(0.426)	
10 months	-0.389	0.034	0.338	-0.394	8,152
	(0.251)	(0.396)	(0.422)	(0.448)	
11 months	0.069	0.765*	0.136	0.295	8,132
	(0.273)	(0.448)	(0.540)	(0.417)	
12 months	-0.552**	0.065	-0.579	0.192	8,112
	(0.236)	(0.475)	(0.488)	(0.450)	
13 months	0.501	0.599	0.572	0.601	8,092
	(0.386)	(0.534)	(0.446)	(0.390)	
14 months	-0.226	-0.379	0.133	-0.286	8,072
	(0.342)	(0.518)	(0.339)	(0.474)	
15 months	-0.431*	-0.708	-0.049	-0.641	8,052
	(0.231)	(0.432)	(0.414)	(0.447)	
16 months	-0.307	-0.274	-0.159	-0.543*	8,032
	(0.232)	(0.473)	(0.408)	(0.306)	
17 months	-0.568***	-0.391*	-0.341	-0.460	8,012
	(0.195)	(0.217)	(0.669)	(0.339)	
18 months	-0.472*	-0.216	-0.282	-0.026	7,992
	(0.246)	(0.385)	(0.707)	(0.456)	
19 months	-1.451***	-1.199***	-1.723***	-0.928***	7,972
	(0.191)	(0.273)	(0.544)	(0.292)	
20 months	-0.983***	-0.919***	-1.533***	-0.791***	7,952
	(0.195)	(0.268)	(0.567)	(0.291)	

Notes: Each horizon is one joint regression for all four regions; entries are total regional coefficients, with monthly-score HAC standard errors in parentheses. The dependent variable is metropolitan inflation h months ahead. A unit increase is one pooled standard deviation of the rightward score $-\text{FPCL}_2$. Current inflation, the other specified current variables, one month of lagged states, metropolitan effects, anchor-month effects and region-by-COVID intercepts are included. N_h counts observations in the whole estimation sample, including pre-COVID and COVID. COVID anchor dates run from January 2020 to the last date with an observed outcome. The number of COVID months declines from 60 at $h = 1$ to 41 at $h = 20$. Inference uses Bartlett bandwidth $\max(12, h + 1)$ and normal critical values. $^{*}p < 0.10$, $^{**}p < 0.05$, $^{***}p < 0.01$; these are pointwise tests.

A.8 Additional Regional Analysis

A.8.1 Additional regional estimates

Table 12: Regional specification comparisons: OLS

	Mean	Moments	Fixed 3	Centered 3	Centered 6	Six + moments
Unemployment	-0.274***	-0.275***	-0.277***	-0.276***	-0.274***	-0.274***
	(0.045)	(0.045)	(0.045)	(0.045)	(0.045)	(0.045)
Mean PX1	0.146	0.103	0.006	0.054	0.134	0.161
	(0.105)	(0.127)	(0.140)	(0.142)	(0.146)	(0.151)
All shape terms: joint p	–	0.499	0.188	0.182	0.161	0.375
Centered PCs: joint p	–	–	–	0.182	0.161	0.286
Moments: joint p	–	0.499	–	–	–	0.864
Within R^2	0.0070	0.0072	0.0077	0.0076	0.0082	0.0083

Notes: All columns use the same 8,131 observations, metro and month fixed effects, and monthly-score HAC(12) inference. Moments are sample variance (denominator $N_{R,t}-1$), standardized skewness and Pearson kurtosis of individual PX1 responses. Fixed 3 uses the recovered original fixed-reference scores; centered scores are reconstructed from responses minus their region-month arithmetic mean. The final column conditions centered PCs and conventional moments on one another.

Table 13: Regional specification comparisons: lagged-unemployment IV

	Mean	Moments	Fixed 3	Centered 3	Centered 6	Six + moments
Unemployment	-0.309***	-0.310***	-0.310***	-0.309***	-0.307***	-0.307***
	(0.080)	(0.080)	(0.080)	(0.080)	(0.080)	(0.080)
Mean PX1	0.147	0.103	0.006	0.052	0.131	0.159
	(0.105)	(0.127)	(0.139)	(0.140)	(0.144)	(0.150)
All shape terms: joint p	–	0.490	0.177	0.175	0.159	0.371
Centered PCs: joint p	–	–	–	0.175	0.159	0.283
Moments: joint p	–	0.490	–	–	–	0.863
Within R^2	0.0069	0.0071	0.0076	0.0075	0.0081	0.0082

Notes: All columns use the same 8,131 observations, metro and month fixed effects, and monthly-score HAC(12) inference. Moments are sample variance (denominator $N_{R,t}-1$), standardized skewness and Pearson kurtosis of individual PX1 responses. Fixed 3 uses the recovered original fixed-reference scores; centered scores are reconstructed from responses minus their region-month arithmetic mean. The final column conditions centered PCs and conventional moments on one another.

A.8.2 Additional regional local projections

A separate metropolitan projection relates future local inflation to its Census region's fixed-reference shift score, while controlling for six centered regional components, mean PX1, current inflation, unemployment and distributional moments, their specified COVID interactions, and one lag of the state variables. Metropolitan and anchor-month fixed effects are included. At three months during COVID, the South coefficient is 1.452 (standard error 0.550), compared with 0.882 (0.443) for the Northeast, 0.616 (0.453) for North Central and 0.330 (0.600) for the West. These estimates concern metropolitan inflation, not the national outcome in the preceding comparison. The intervals are pointwise and the regressions do not identify exogenous expectation shocks.

Table 14: Regional heterogeneity in centered shape coefficients

	North Central	Northeast	South	West
$\xi_{1,R,t}$	-0.167	-0.286*	-0.105	-0.006
	(0.143)	(0.155)	(0.141)	(0.149)
$\xi_{2,R,t}$	-0.019	-0.115	0.238**	-0.275***
	(0.097)	(0.093)	(0.119)	(0.092)
$\xi_{3,R,t}$	0.070	-0.056	-0.199**	0.069
	(0.093)	(0.107)	(0.097)	(0.103)
$\xi_{4,R,t}$	-0.025	-0.209**	0.176*	0.120
	(0.092)	(0.100)	(0.098)	(0.098)
$\xi_{5,R,t}$	-0.142**	-0.209*	-0.054	-0.126
	(0.064)	(0.126)	(0.083)	(0.089)
$\xi_{6,R,t}$	-0.057	0.080	0.139	-0.038
	(0.068)	(0.122)	(0.136)	(0.117)
Six-PC joint p	0.166	0.108	0.092	0.029

Notes: One pooled OLS regression includes 24 region-specific PC coefficients, a common coefficient on the regional mean PX1, unemployment, and metro/month fixed effects. All scores use the same pooled basis and scale. Monthly-score HAC(12) standard errors allow contemporaneous dependence across all metros. The reported joint tests concern each region separately and are not adjusted for testing four regions; the West $p = 0.029$ does not survive a four-region Bonferroni correction.

Table 15: Regional shape coefficients during acute episodes

	COVID: change	COVID: total	GFC: change	GFC: total
$\xi_{1,R,t}$	-0.428	-0.618	2.073***	1.903***
	(0.507)	(0.485)	(0.589)	(0.584)
$\xi_{2,R,t}$	-0.684	-0.756	0.763*	0.672
	(0.809)	(0.812)	(0.434)	(0.427)
$\xi_{3,R,t}$	0.500*	0.475*	1.195***	1.182***
	(0.278)	(0.277)	(0.391)	(0.377)
$\xi_{4,R,t}$	-0.299	-0.269	1.752**	1.769***
	(0.618)	(0.611)	(0.684)	(0.686)
$\xi_{5,R,t}$	-0.686**	-0.791**	-1.243***	-1.353***
	(0.337)	(0.340)	(0.452)	(0.448)
$\xi_{6,R,t}$	-0.593*	-0.566*	-2.463***	-2.423***
	(0.310)	(0.300)	(0.525)	(0.521)
Six-PC joint p	< 0.001	< 0.001	< 0.001	< 0.001

Notes: Each episode is estimated separately over the full sample with all six PC main effects and their six episode interactions, mean PX1, unemployment, and metro/month fixed effects. Change is the interaction increment relative to observations outside that episode; total is the sum of main and interaction coefficients. Standard errors use monthly-score HAC(12). Acute COVID is March 2021–June 2022; acute GFC is September 2008–June 2009. The 16- and 10-month windows provide limited time-series information; asymptotic joint-test p-values should be treated cautiously.

Table 16: Regional uncertainty under alternative dependence assumptions

	Estimate	HAC(12) SE	HAC(24) SE	Region SE	Region p
$\xi_{1,R,t}$	-0.205	0.127	0.117	0.092	0.112
$\xi_{2,R,t}$	-0.085	0.066	0.063	0.033	0.083
$\xi_{3,R,t}$	-0.028	0.059	0.060	0.041	0.538
$\xi_{4,R,t}$	0.041	0.052	0.046	0.078	0.636
$\xi_{5,R,t}$	-0.111	0.052	0.048	0.035	0.052
$\xi_{6,R,t}$	0.019	0.055	0.057	0.053	0.738

Notes: Estimates are the same six-PC full-sample OLS coefficients. HAC aggregates score contributions by calendar month before applying the Bartlett kernel. Region SE clusters at the four Census regions and applies a 4/3 multiplier; the last column uses a t_3 reference. Four clusters provide a weak basis for cluster asymptotics, so this column is a sensitivity check. Metro-only clustering is retained in the replication records but is not the main inference method.

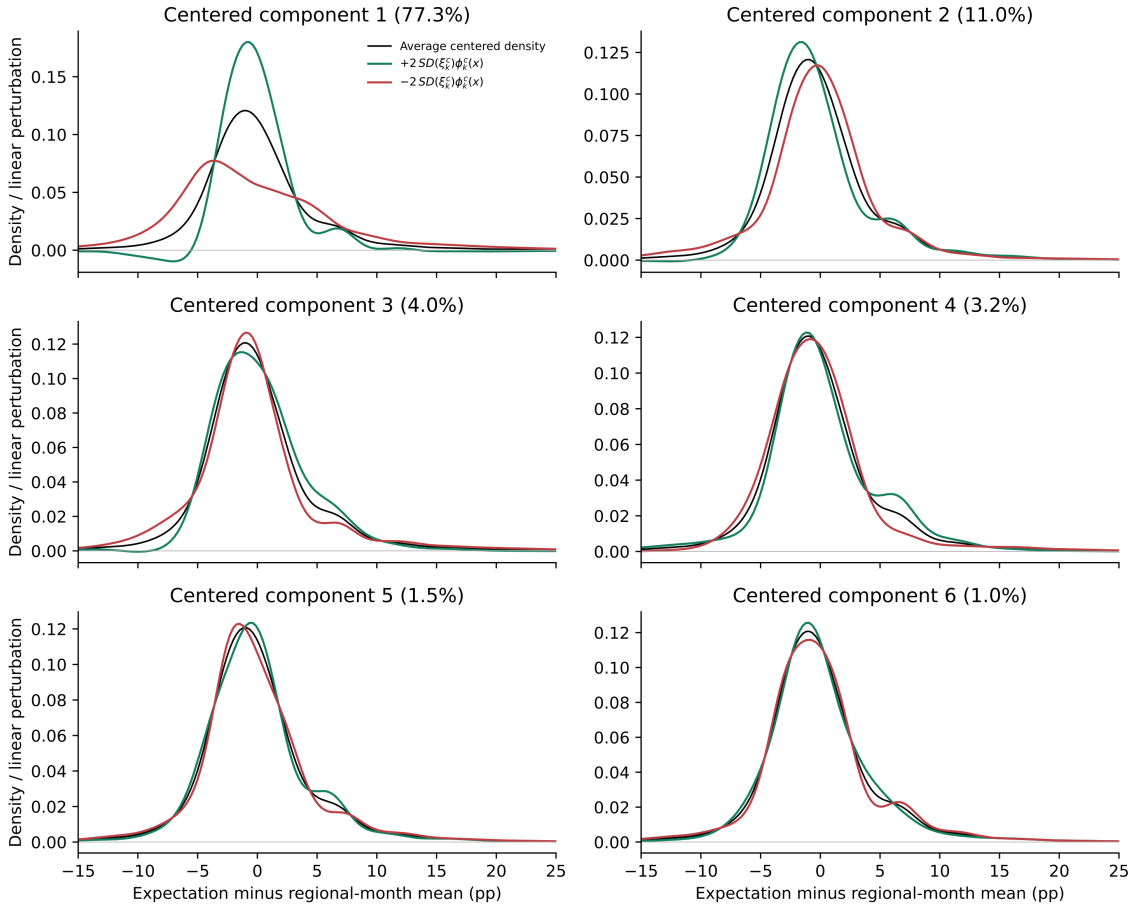


Figure A.3: Common regional mean-centered components. The black line is the pooled average centered density. Green and red lines add or subtract two pooled standard deviations of the corresponding score multiplied by its basis function. These linear perturbations illustrate a component direction and need not everywhere be nonnegative densities. Each region's density is centered on its own region-month arithmetic mean before FPCA.

Table 17: National inflation projections during COVID: aggregate and regional shifts

	$h = 1$	$h = 3$	$h = 6$	$h = 12$	$h = 20$
Aggregate	3.938	0.541	2.972	-2.986	-3.510
	(1.652)	(1.528)	(1.692)	(1.008)	(1.606)
North Central	0.953	1.817	1.685	-0.910	1.287
	(0.718)	(1.038)	(1.032)	(0.762)	(0.720)
Northeast	0.224	0.281	1.384	-2.056	0.718
	(0.782)	(0.630)	(0.972)	(1.343)	(0.551)
South	3.362	0.585	0.399	-2.233	-5.505
	(1.743)	(1.506)	(1.593)	(1.186)	(1.378)
West	0.106	-2.000	0.348	0.901	-0.624
	(0.628)	(1.115)	(1.584)	(1.171)	(0.487)
Four-region joint p	0.107	< 0.001	0.131	0.066	< 0.001
Joint p, Holm(20)	0.732	0.006	0.732	0.544	< 0.001

Notes: The outcome is national annualized monthly CPI inflation at horizon h. Each month appears once. The aggregate row comes from a separate aggregate-shift regression; all four regional shifts enter the regional regression jointly. Controls include current inflation and two inflation lags, unemployment gap, arithmetic mean PX1, PX5, six mean-centered aggregate PCs, and three conventional moments. Full-sample models retain all main effects and add COVID interactions; coefficients shown are the totals from March 2020 onward. Each fixed-reference shift is measured in its own pre-March-2020 standard deviation; recovered regional bases differ. Standard errors are Bartlett HAC with bandwidth $\max(12, h + 1)$. The final row adjusts the twenty horizon-specific four-region joint tests. Pointwise region estimates are not evidence of structural shocks or superior out-of-sample forecasts.

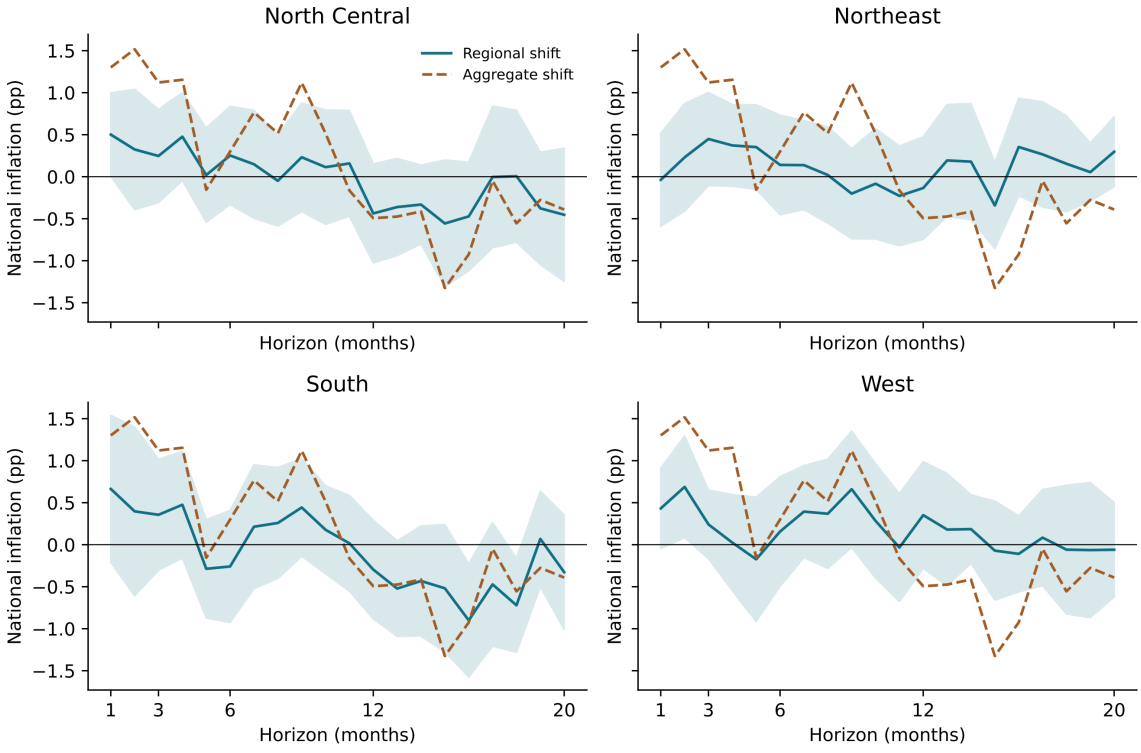


Figure A.4: Full-sample national-inflation projections using aggregate or jointly entered regional fixed-reference shift scores, conditional on the arithmetic mean and six mean-centered PCs. Shading shows regional pointwise 95 percent HAC intervals.

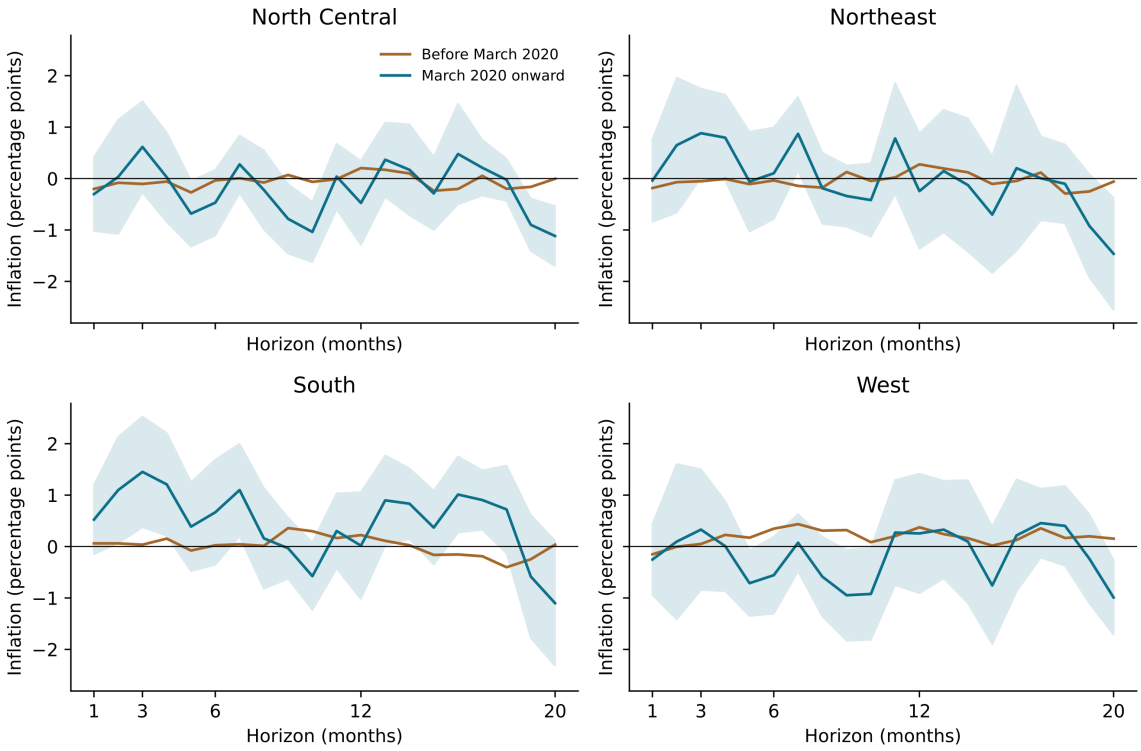


Figure A.5: Metropolitan inflation projections conditional on six centered regional PCs. The target is the recovered fixed-reference rightward-shift score; the blue line is the March 2020 onward coefficient and the brown line is the pre-COVID coefficient. Shading shows pointwise 95 percent monthly-score HAC intervals for the COVID path.

A.8.3 Complete Regional Model Comparisons

The supplied broad-COVID OLS and IV comparisons and the broad- and acute-recession IV comparisons are reported below.

Table 18: Broad COVID: Pooled Regional OLS

	(1) FPCA	(2) Moments	(3) Both	(4) Both + regional shift interactions
Unemployment	-0.271***	-0.272***	-0.270***	-0.276***
	(0.057)	(0.058)	(0.057)	(0.058)
Mean expectation	0.075	0.193**	0.109	0.069
	(0.092)	(0.089)	(0.100)	(0.106)
High disagreement	0.440	–	0.354	-0.312
	(0.432)	–	(0.700)	(0.846)
Rightward shift	0.923**	–	0.871**	0.891**
	(0.383)	–	(0.369)	(0.449)
Left-tail risk	0.705	–	0.695	0.591
	(0.450)	–	(0.449)	(0.407)
Variance	–	0.0019	-0.0019	0.0087
	–	(0.0050)	(0.0086)	(0.0113)
Skewness	–	-0.2268	-0.1671	-0.2717
	–	(0.1411)	(0.1627)	(0.1734)
Kurtosis	–	-0.0397343	-0.0307632	-0.0632172**
	–	(0.0264969)	(0.0243671)	(0.0272507)
Rightward shift × Northeast	–	–	–	0.064
	–	–	–	(0.515)
Rightward shift × South	–	–	–	1.188**
	–	–	–	(0.576)
Rightward shift × West	–	–	–	-0.561
	–	–	–	(0.587)
FPCA block: p	0.121	–	0.129	< 0.001
Moment block: p	–	0.192	0.417	0.101
Regional equality: p	–	–	–	< 0.001
R^2	0.386	0.385	0.386	0.389
Metro and month effects	Yes	Yes	Yes	Yes
Estimator	OLS	OLS	OLS	OLS
Metropolitan clusters	20	20	20	20
Observations	8,131	8,131	8,131	8,131

Notes: Dependent variable: contemporaneous annualized monthly metropolitan headline CPI inflation. Pooled OLS with metropolitan and calendar-month fixed effects; no variable is instrumented. Estimation uses January 1991–January 2025 and the same 8,131 observations as the IV table. Twelve-month unemployment-lag availability restricts the comparison sample only; that lag is not an instrument or a regressor in OLS. Distributional terms are interacted with January 2020–January 2025 and have zero slopes outside that window, matching the contemporaneous IV specification. FPCA coefficients are per one pooled SD; a rightward shift is $-FPCL2$. Column (4) uses North Central as the reference: add each regional interaction to the rightward-shift coefficient to obtain its total. Standard errors in parentheses use CR0 metropolitan clustering with normal pointwise tests, matching the IV table convention. FPCA block tests impose three restrictions, or six in column (4); the moment and regional-equality tests each impose three. D.C. retains its original Northeast assignment. * $p < 0.10$, ** $p < 0.05$, *** $p < 0.01$.

Table 19: Broad COVID: Distributional Shifts and Regional Heterogeneity

	(1) FPCA	(2) Moments	(3) Both	(4) Both + regional shift interactions
Unemployment	-0.305***	-0.307***	-0.304***	-0.292***
	(0.088)	(0.090)	(0.088)	(0.090)
Mean expectation	0.075	0.194**	0.110	0.069
	(0.092)	(0.090)	(0.100)	(0.106)
High disagreement	0.445	–	0.366	-0.308
	(0.430)	–	(0.694)	(0.841)
Rightward shift	0.920**	–	0.867**	0.888**
	(0.386)	–	(0.370)	(0.448)
Left-tail risk	0.696	–	0.686	0.587
	(0.446)	–	(0.446)	(0.405)
Variance	–	0.0018	-0.0020	0.0087
	–	(0.0050)	(0.0086)	(0.0113)
Skewness	–	-0.2255	-0.1651	-0.2711
	–	(0.1409)	(0.1623)	(0.1726)
Kurtosis	–	-0.0394423	-0.0304922	-0.0631141**
	–	(0.0265295)	(0.0243847)	(0.0271651)
Rightward shift × Northeast	–	–	–	0.068
	–	–	–	(0.512)
Rightward shift × South	–	–	–	1.192**
	–	–	–	(0.574)
Rightward shift × West	–	–	–	-0.560
	–	–	–	(0.586)
FPCA block: p	0.126	–	0.135	< 0.001
Moment block: p	–	0.193	0.419	0.099
All distributional terms: p	–	–	0.019	< 0.001
Regional equality: p	–	–	–	< 0.001
R^2	0.386	0.385	0.386	0.389
First-stage F	570.13	564.70	577.67	582.76
Metro and month effects	Yes	Yes	Yes	Yes
Metropolitan clusters	20	20	20	20
Observations	8,131	8,131	8,131	8,131

Notes: Annualized monthly headline CPI inflation. All regressions use January 1991–January 2025; distributional terms are interacted with January 2020–January 2025 and have zero slopes outside that window. Unemployment is instrumented with its twelve-month lag. FPCA coefficients are per common one-SD movement; $-FPCL2$ denotes a rightward shift. In column (4), North Central is the reference: the rightward-shift row is its coefficient, and the three regional interaction rows are differences from it. Total regional coefficients add the two relevant rows. The FPCA block test imposes three restrictions in columns (1) and (3), and six in column (4), including the regional interactions. Moment tests impose three restrictions. D.C. is assigned to the Northeast throughout. Standard errors clustered by metropolitan area are in parentheses. * $p < 0.10$, ** $p < 0.05$, *** $p < 0.01$.

Table 20: Great Recession: Broad and Acute Windows

	Broad: Dec. 2007–June 2009			Acute: Sept. 2008–June 2009		
	(1) FPCA	(2) Moments	(3) Both	(4) FPCA	(5) Moments	(6) Both
Unemployment	-0.308***	-0.309***	-0.312***	-0.306***	-0.306***	-0.305***
	(0.090)	(0.090)	(0.090)	(0.090)	(0.090)	(0.091)
Mean expectation	0.182*	0.203*	0.203*	0.217**	0.200*	0.232**
	(0.099)	(0.105)	(0.105)	(0.101)	(0.104)	(0.106)
High disagreement	-0.466	–	1.217	-0.594	–	0.817
	(0.510)	–	(0.993)	(0.995)	–	(1.651)
Rightward shift	-0.717***	–	-1.083***	-1.999***	–	-2.156***
	(0.235)	–	(0.363)	(0.609)	–	(0.541)
Left-tail risk	0.870	–	1.555***	0.652	–	1.181
	(0.548)	–	(0.554)	(1.000)	–	(0.863)
Variance	–	-0.0029	-0.1220*	–	-0.0426	-0.1061
	–	(0.0393)	(0.0685)	–	(0.0636)	(0.0843)
Skewness	–	-0.5490	-0.7321	–	-1.5253	-1.4531
	–	(0.4770)	(0.4592)	–	(1.2971)	(1.2683)
Kurtosis	–	0.1195791	0.4244008*	–	-0.6217414	-0.3127140
	–	(0.2558395)	(0.2507143)	–	(0.5778119)	(0.6222557)
FPCA block: p	0.022	–	0.003	0.004	–	< 0.001
Moment block: p	–	0.281	< 0.001	–	0.697	0.155
All distributional terms: p	–	–	< 0.001	–	–	< 0.001
R^2	0.386	0.385	0.387	0.386	0.385	0.387
First-stage F	559.01	553.02	544.96	561.58	544.33	535.50
Metro and month effects	Yes	Yes	Yes	Yes	Yes	Yes
Metropolitan clusters	20	20	20	20	20	20
Observations	8,131	8,131	8,131	8,131	8,131	8,131

Notes: Annualized monthly headline CPI inflation. The broad and acute interactions are estimated separately on the same January 1991–January 2025 panel. The broad window includes the NBER peak month. Distributional slopes are zero outside each indicated window. Unemployment is instrumented with its twelve-month lag. FPCA coefficients use the same one-SD scaling and orientation in both windows: high disagreement, rightward shift ($-FPCL2$), and left-tail risk. Each FPCA and moment block test imposes three restrictions; the combined test imposes six. Differences between the two point estimates are not a test of equality across the nested windows. D.C. is assigned to the Northeast throughout. Standard errors clustered by metropolitan area are in parentheses. * $p < 0.10$, ** $p < 0.05$, *** $p < 0.01$.

A.9 Robustness of the Mean-Centered Regional Estimates

Table 21 varies the HAC bandwidth, the estimation method and the regions used for identification. The six centered components are not jointly significant at the 5 percent level in the full sample under any reported bandwidth or after excluding any one Census region. The COVID interaction result is significant in the full panel but weakens when the South is excluded ($p = 0.099$) and disappears when the West is excluded ($p = 0.638$). This pattern indicates that the pooled COVID result depends on variation from the South and West; it does not establish that either region has an individually identified causal effect. The Great Recession interaction test remains below 0.05 in every leave-one-region-out regression, although inference is based on only nineteen episode months.

OLS and lagged-unemployment IV give similar conclusions. The HAC first-stage statistic for the six-component IV model is 89.39, indicating relevance of the twelve-month unemployment lag conditional on the included regressors; this statistic does not establish the exclusion restriction. Bartik estimates are not reported because the required instrument is absent from the recovered panel. Four-Census-region clustering is reported separately as an uncertainty sensitivity, with a t_3 reference for individual coefficients. With only four clusters, it is not used to validate a six-restriction joint test.

The episode regressions in the main text retain all full-sample component main effects and add episode interactions. The archived restricted design instead enters only components multiplied by the episode indicator, implicitly setting their coefficients to zero outside the episode. Re-estimating this restriction with the centered components is recorded in the replication outputs; its coefficients are episode-specific restricted slopes, not changes from an estimated outside-episode relationship. The main results use the unrestricted specification so that episode changes and episode totals have distinct interpretations.

Table 21: Regional robustness: temporal dependence and influential regions

Panel A: Joint tests of six centered components or six episode changes				
Specification	Estimator	HAC(6)	HAC(12)	HAC(24)
Full sample	OLS	0.188	0.161	0.090
Full sample	IV	0.188	0.159	0.087
COVID: coefficient changes	OLS	0.019	0.003	< 0.001
COVID: coefficient changes	IV	0.018	0.004	< 0.001
GFC: coefficient changes	OLS	< 0.001	< 0.001	< 0.001
GFC: coefficient changes	IV	< 0.001	< 0.001	< 0.001
Panel B: Leave-one-region-out OLS, HAC(12)				
Excluded region	Observations	Full sample	COVID change	GFC change
None	8,131	0.161	0.003	< 0.001
North Central	6,495	0.410	0.003	< 0.001
Northeast	6,905	0.138	< 0.001	< 0.001
South	6,086	0.233	0.099	0.037
West	4,907	0.107	0.638	< 0.001

Notes: Entries are joint-test p-values, except observation counts. All specifications include mean PX1, unemployment, metro fixed effects and month fixed effects. Episode models include all six factor main effects and six interactions. Leave-one-region-out estimates hold the original common basis and score scale fixed, remove all metros in one Census region, and re-estimate coefficients. The full-sample test concerns six PC coefficients; episode tests concern changes relative to observations outside the episode. March 2020–January 2025 defines COVID; December 2007–June 2009 defines the GFC.

B Mean-Centered FPCA Comparisons and Additional Aggregate Estimates

Back to appendix contents

B.1 Aggregate Phillips Curve: Mean-Centered Comparison

B.1.1 Mean Expectations and Distributional Information

Table 22 compares the mean-only specification, conventional higher moments, six mean-centered FPCA components, and their combination. The mean is the arithmetic monthly average of individual PX1 responses. The same controls, observations, and covariance estimator are used in all four columns.

Mean expectations remain informative when centered distributional features are included. The estimated mean coefficient is 1.204 in the benchmark, 1.523 with conventional moments, and 1.905 with six centered components. It remains statistically significant in all four columns. Thus, these estimates do not support a disappearance of the mean's association with inflation after conditioning on shape. Instead, mean expectations and distributional shape provide complementary information within the linear Phillips Curve.

The six centered components are jointly significant beyond the mean and common controls ($p = 0.00018$). Adding them raises R^2 from 0.405 to 0.434. This is additional in-sample explanatory content; it is not an out-of-sample forecasting result. The first and fifth components are individually significant in this specification, but interpretation centers on the joint block because the estimated basis represents a functional object and component signs are arbitrary normalizations.

B.1.2 Phillips-Curve Slope and Conventional Moments

The unemployment-gap coefficient is negative across specifications, but its magnitude and precision change. It is -0.249 in the mean-only model and -0.213 with six centered components; its HAC standard error rises from 0.110 to 0.160. The data therefore do not show that adding centered factors necessarily steepens the aggregate Phillips Curve. The six-factor estimate is not statistically different from zero at conventional levels under this covariance estimator.

Conventional moments and FPCA overlap in the information they summarize. The moments are jointly significant when added to the mean-only model ($p = 0.002$). When both representations enter, the six-factor block has $p = 0.113$ and the moments block has $p = 0.370$. These results support distributional information beyond the mean, but they do not establish that either representation independently dominates the other in the fully encompassing model.

The nonnested fitted-value comparison is more favorable to the functional representation: fitted values from the six-factor model add to the moments model ($p = 0.034$), whereas fitted values from the moments model do not add significantly to the six-factor model ($p = 0.353$). This test asks about the fitted linear combinations, rather than separately testing every additional coefficient. Its result should be read together with the encompassing block tests, rather than as evidence of universal superiority of FPCA.

B.1.3 Why Retain Six Components?

The first three components explain most density variation, but this does not ensure that they capture all inflation-relevant variation. Table 23 compares three and six on the same

Table 22: Aggregate Phillips Curve with the PX1 mean and six centered components

	Mean	+ Moments	+ Six factors	All
Unemployment gap	-0.249**	-0.270**	-0.213	-0.205
	(0.110)	(0.107)	(0.160)	(0.168)
Mean PX1	1.204***	1.523***	1.905***	1.849***
	(0.176)	(0.191)	(0.252)	(0.290)
$\xi_{1,t}$	–	–	1.006***	1.003
	–	–	(0.334)	(0.939)
$\xi_{2,t}$	–	–	0.029	0.233
	–	–	(0.134)	(0.265)
$\xi_{3,t}$	–	–	0.286	0.256
	–	–	(0.220)	(0.276)
$\xi_{4,t}$	–	–	0.242	0.044
	–	–	(0.226)	(0.289)
$\xi_{5,t}$	–	–	0.329**	0.292**
	–	–	(0.134)	(0.144)
$\xi_{6,t}$	–	–	0.085	0.059
	–	–	(0.188)	(0.173)
Variance	–	-0.030***	–	0.001
	–	(0.009)	–	(0.030)
Skewness	–	-0.225	–	-0.353
	–	(0.197)	–	(0.238)
Kurtosis	–	0.006	–	0.003
	–	(0.020)	–	(0.028)
Six factors jointly: p	–	–	< 0.001	0.113
Moments jointly: p	–	0.002	–	0.370
Factors 4–6: p	–	–	0.013	0.048
R^2	0.405	0.426	0.434	0.438

Notes: May 1990–January 2025, $N = 417$ in every column. The outcome is annualized monthly headline CPI inflation. Every specification includes an intercept, the unemployment gap, the arithmetic monthly PX1 mean, lagged mean PX5, the oil-supply news shock, and the monetary-policy shock. The six centered scores are standardized. Moments are raw-response variance, standardized skewness, and Pearson kurtosis. Bartlett HAC standard errors with twelve lags are in parentheses. Joint tests are asymptotic Wald tests. $^{*}p < 0.10$, $^{**}p < 0.05$, $^{***}p < 0.01$. Inference conditions on the estimated densities and basis.

sample. The three-component block has $p = 0.113$, while the additional fourth through sixth components have a joint p-value of 0.013 in the six-factor model. Conditional on conventional moments, the incremental three have $p = 0.048$. Low-variance directions can therefore matter for the dependent variable even when their contribution to density reconstruction is small.

Table 23: Three versus six mean-centered components

	Three	Six	Three + moments	Six + moments
Unemployment gap	-0.181	-0.213	-0.229	-0.205
	(0.127)	(0.160)	(0.158)	(0.168)
Mean PX1	1.700***	1.905***	1.714***	1.849***
	(0.288)	(0.252)	(0.344)	(0.290)
FPCA jointly: p	0.113	< 0.001	0.688	0.113
Factors 4–6: p	–	0.013	–	0.048
R^2	0.425	0.434	0.432	0.438

Notes: Same 417 observations, controls, score normalization, and HAC(12) inference as Table 22. "Factors 4–6" tests the incremental block conditional on components 1–3 and all other included regressors.

B.1.4 Comparison with Meeks–Monti

Meeks and Monti (2023) separate the mean forecast from the distribution around it. The present mean-centered specification follows that distinction. Their published forward-looking specifications use three functional components, while their monthly hybrid specification uses two; an earlier working-paper implementation considers six. I therefore compare three and six explicitly, rather than treating the factor count as identical across versions.

Table 24 applies a common monthly specification to the available January 1978–January 2025 data: inflation on the arithmetic PX1 mean, the unemployment gap, contemporaneous WTI price growth, an October–December 2008 indicator, and the specified functional scores. The comparison holds the sample and controls fixed while changing the representation. It adapts the benchmark's empirical logic; it is not an exact reproduction of the published sample and density estimator.

With six centered components, the mean coefficient is 1.607 and the factor block is jointly significant. With six level-density fixed-reference components, the mean coefficient is 0.165 and imprecisely estimated. The latter factors include movements in the level of the distribution and thus share more information with the mean. This distinction explains why evidence from a level-density representation cannot automatically be carried over to the mean-centered analysis. On the pre-COVID sample, the centered mean coefficient remains significant, and the six-component specification again contains information beyond the first three. The appendix reports that comparison separately.

B.1.5 Distributional Information across Episodes

The relevant distributional features vary across macroeconomic episodes. Table 25 reports coefficient totals for ordinary months, the broad COVID period beginning in March 2020, and earlier NBER recessions. The model retains baseline score effects and adds separate interaction increments. Each displayed total therefore measures the conditional relationship within that episode, not the increment alone.

Table 24: Adapted Meeks–Monti comparison on a common monthly sample

	Mean	Centered 3	Centered 6	Fixed-reference 6
Unemployment gap	-0.194**	-0.212**	-0.311***	-0.270***
	(0.088)	(0.102)	(0.101)	(0.097)
Mean PX1	1.369***	1.439***	1.607***	0.165
	(0.067)	(0.155)	(0.148)	(0.384)
FPCA jointly: p	–	0.135	< 0.001	0.003
Factors 4–6: p	–	–	< 0.001	0.028
R^2	0.610	0.613	0.626	0.623

Notes: January 1978–January 2025, $N = 565$. All columns include the same arithmetic PX1 mean, unemployment gap, WTI price growth, October–December 2008 indicator, and intercept. HAC(12) standard errors. "Fixed-reference" uses deviations of uncentered densities on a common wide 2,048-point grid; "centered" first subtracts the current arithmetic mean from individual responses. This adapted specification differs from the primary long-run-expectations-and-shocks specification and from the published Meeks–Monti estimator.

During the COVID period, the second, third, fourth, and sixth centered components have significant total coefficients. In earlier recessions the pattern differs, including a negative second-component coefficient. The six totals are jointly significant in both episodes. These results indicate state dependence in shape around the mean. They do not identify a pure rightward or leftward translation: that location information is carried by the separate mean and by the descriptive original-support density plots.

Table 25: Mean-Centered Aggregate Distributional Coefficients across Macroeconomic Episodes

	Ordinary months	Post-COVID	Earlier recessions
$\xi_{1,t}$	0.096	1.304	2.434*
	(0.424)	(0.863)	(1.479)
$\xi_{2,t}$	-0.866***	1.254***	-1.718***
	(0.286)	(0.377)	(0.658)
$\xi_{3,t}$	-0.020	1.824***	-0.748
	(0.244)	(0.656)	(0.720)
$\xi_{4,t}$	0.433**	1.325**	-1.001**
	(0.170)	(0.566)	(0.471)
$\xi_{5,t}$	0.516***	-0.219	0.468
	(0.147)	(0.735)	(0.671)
$\xi_{6,t}$	0.107	-1.816***	-0.021
	(0.169)	(0.560)	(0.458)
Six total coefficients: p	< 0.001	< 0.001	0.005

Notes: Total coefficients from one full-sample interaction regression with all baseline effects and common controls. COVID is March 2020–January 2025. Earlier recessions are July 1990–March 1991, March–November 2001, and December 2007–June 2009. Ordinary months exclude both groups. Standard errors include covariance between baseline and interaction estimates. HAC(12) inference is conditional on the basis; short regimes and multiple coefficient comparisons warrant caution.

Appendix D reports the robustness checks. The six-factor block remains informative beyond the mean under alternative HAC windows, KDE bandwidths, inflation lags, and

a cubic mean control. Its evidence is weaker before COVID and conditional on conventional moments. The contribution is consequently the additional and state-dependent information in the expectation distribution, with its limits made explicit.

B.2 Measurement and Distributional Summaries

The mean, central moments, and densities use the same valid individual PX1 responses. The national basis is estimated over January 1978–January 2025; the following descriptive tables use January 1990–January 2025, with the shorter available sample noted for lagged PX5. Tables 26–28 retain the units of the underlying observations. Centering each density removes a common translation but does not make its shape statistically unrelated to the mean over time.

Table 26: Aggregate variables: descriptive statistics

	N	Mean	SD	Minimum	Maximum
Annualized monthly CPI inflation	421	2.641	3.275	-21.437	16.409
Unemployment gap	421	0.616	1.543	-1.415	10.299
Mean PX1	421	3.750	1.037	0.730	8.358
Mean PX5, lag 1	417	3.569	0.727	2.546	5.674
Oil-supply news shock	421	-0.002	0.586	-3.027	1.893
Monetary-policy shock	421	0.000	0.052	-0.269	0.335
PX1 variance	421	26.372	22.576	7.683	137.069
PX1 skewness	421	1.423	1.133	-1.785	5.436
PX1 kurtosis	421	11.419	8.521	4.057	43.331

Notes: Monthly national data, January 1990–January 2025 (421 months). Lagged mean PX5 is available from May 1990 (417 months), which determines the common regression sample. CPI inflation equals $1200 \log(P_t/P_{t-1})$. Mean PX1 is the arithmetic average of individual one-year-ahead expectations. Mean PX5 is the arithmetic average of individual long-run expectations, lagged one month. Inflation and expectation means are in percentage points; variance is in squared percentage points, while skewness and kurtosis are dimensionless. Shock series retain their original units. SD denotes the sample standard deviation across months.

Table 27: Correlations among conventional PX1 moments

	Mean PX1	Variance	Skewness	Kurtosis
Mean PX1	1.000	0.573	0.339	0.129
Variance	0.573	1.000	0.320	0.363
Skewness	0.339	0.320	1.000	0.757
Kurtosis	0.129	0.363	0.757	1.000

Notes: Pearson correlations over January 1990–January 2025 ($N = 421$). The mean and conventional moments are calculated from the same individual PX1 responses. Skewness is the third central moment divided by variance to the power 3/2; kurtosis is the fourth central moment divided by variance squared.

Table 28: Correlations between centered components and conventional moments

	Mean PX1	Variance	Skewness	Kurtosis
$\xi_{1,t}$	-0.678	-0.865	-0.211	-0.252
$\xi_{2,t}$	0.545	0.123	0.511	0.290
$\xi_{3,t}$	-0.351	0.036	-0.051	0.326
$\xi_{4,t}$	-0.090	-0.190	-0.481	-0.388
$\xi_{5,t}$	-0.069	0.023	-0.126	-0.179
$\xi_{6,t}$	-0.012	-0.019	-0.109	-0.004

Notes: Pearson correlations over January 1990–January 2025 ($N = 421$). Scores use the full-history mean-centered basis and the same normalization as the mean-centered Phillips Curve. Centering removes a common translation of individual expectations, but it does not impose zero time-series correlation between the mean and changes in distributional shape. Score signs follow the eigenfunction normalization.

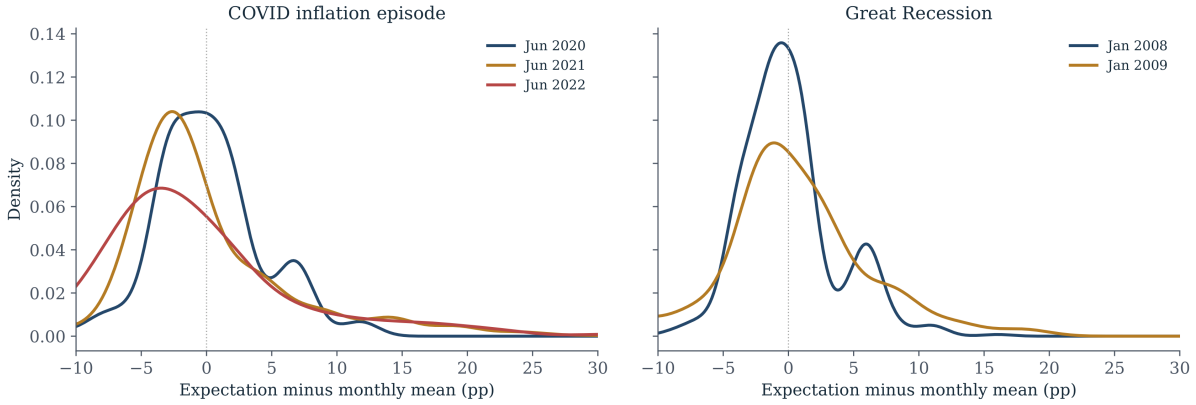


Figure B.1: Episode densities after subtracting the arithmetic PX1 mean. The horizontal axis measures expectations relative to the current monthly mean. These curves isolate differences in shape from movements in the mean.

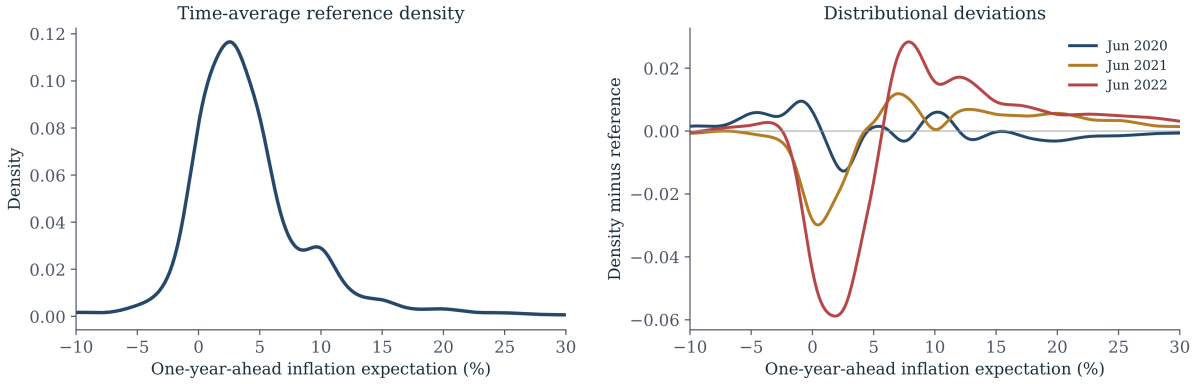


Figure B.2: Original-level densities and deviations from the time-average reference. The reference is a fixed sample average, not an identified expectation anchor or a maintained long-run equilibrium.

B.3 Additional Aggregate Estimates

The companion specifications retain the sample and controls of the corresponding mean-centered comparison table. Tables 29 and 30 report the coefficients on common controls and conventional homoskedastic inference. The mean-centered comparison uses HAC inference. Table 31 changes the sample for the adapted Meeks–Monti comparison and is distinct from the pre-COVID robustness regression using the primary PX5 and shock controls.

Table 29: Aggregate common-control coefficients

	Mean	+ Moments	+ Six factors	All
Long-run expectation, lag 1	0.075	0.625***	0.490	0.671**
	(0.173)	(0.217)	(0.360)	(0.279)
Oil-supply news shock	2.560***	2.515***	2.462***	2.452***
	(0.413)	(0.410)	(0.409)	(0.402)
Monetary-policy shock	0.715	1.185	0.615	0.315
	(2.311)	(2.232)	(1.922)	(1.841)
Constant	-2.001***	-4.113***	-6.137***	-6.127***
	(0.723)	(0.792)	(1.785)	(2.137)

Notes: Same models and sample as Table 22. HAC(12) standard errors. Coefficients retain the original units of the supplied shock series.

Table 30: Aggregate models with conventional OLS inference

	Mean	+ Moments	+ Six factors	All
Unemployment gap	-0.249***	-0.270***	-0.213**	-0.205*
	(0.081)	(0.082)	(0.108)	(0.109)
Mean PX1	1.204***	1.523***	1.905***	1.849***
	(0.129)	(0.159)	(0.247)	(0.281)
$\xi_{1,t}$	–	–	1.006***	1.003
	–	–	(0.247)	(0.609)
$\xi_{2,t}$	–	–	0.029	0.233
	–	–	(0.185)	(0.269)
$\xi_{3,t}$	–	–	0.286	0.256
	–	–	(0.184)	(0.293)
$\xi_{4,t}$	–	–	0.242	0.044
	–	–	(0.167)	(0.229)
$\xi_{5,t}$	–	–	0.329**	0.292**
	–	–	(0.140)	(0.148)
$\xi_{6,t}$	–	–	0.085	0.059
	–	–	(0.131)	(0.165)
Variance	–	-0.030***	–	0.001
	–	(0.008)	–	(0.023)
Skewness	–	-0.225	–	-0.353
	–	(0.186)	–	(0.240)
Kurtosis	–	0.006	–	0.003
	–	(0.027)	–	(0.032)
Six factors jointly: p	–	–	0.002	0.181
Moments jointly: p	–	0.002	–	0.422
Factors 4–6: p	–	–	0.076	0.190
R^2	0.405	0.426	0.434	0.438

Notes: Point estimates are identical to Table 22; standard errors and joint tests here use homoskedastic OLS assumptions. These results are an inference comparison, not the preferred covariance specification.

Table 31: Adapted Meeks–Monti comparison before COVID

	Mean	Centered 3	Centered 6	Fixed-reference 6
Unemployment gap	-0.196***	-0.333***	-0.371***	-0.332***
	(0.076)	(0.096)	(0.108)	(0.092)
Mean PX1	1.397***	1.140***	1.326***	0.474
	(0.063)	(0.140)	(0.140)	(0.298)
FPCA jointly: p	–	0.031	< 0.001	0.002
Factors 4–6: p	–	–	< 0.001	0.527
R^2	0.629	0.637	0.644	0.640

Notes: January 1978–December 2019, $N = 504$. Controls and density-comparison design follow Table 24; HAC(12) inference. This is an adapted monthly exercise, not a replication of the exact published estimator.

Table 32: Mean-Centered Episode Coefficient Totals Conditional on Conventional Moments

	Ordinary months	Post-COVID	Earlier recessions
$\xi_{1,t}$	0.527	1.358	9.456
	(1.073)	(1.121)	(6.009)
$\xi_{2,t}$	-0.849*	2.069***	2.236
	(0.475)	(0.526)	(2.639)
$\xi_{3,t}$	0.022	2.378***	1.279
	(0.393)	(0.659)	(1.689)
$\xi_{4,t}$	0.657**	0.384	-0.521
	(0.269)	(0.734)	(0.777)
$\xi_{5,t}$	0.504***	-0.980	0.208
	(0.168)	(0.602)	(0.602)
$\xi_{6,t}$	0.145	-2.043***	0.812
	(0.228)	(0.535)	(0.837)
Six total coefficients: p	< 0.001	< 0.001	< 0.001

Notes: Mean, common controls, six centered components, and conventional moments enter together, including baseline and episode interactions for the distributional measures. Episode dates and total-coefficient interpretation follow Table 25. HAC(12) standard errors.

C Additional Dynamic Evidence

Back to appendix contents

The supplementary figures report responses in small groups so that each shock and outcome can be read separately. The accompanying `VAR_Figure_Atlas.pdf` contains every response pair, grouped by shock with no more than three outcomes per page. Machine-readable impulse responses, model coefficients, covariance matrices, orthogonal shocks, forecast-error variance decompositions, and historical contributions accompany the figures.

Table 33: Coverage of the dynamic analysis

Exercise	Sample and factor construction	Specifications
Mean-centered recursive VAR	1990–January 2025; arithmetic mean, six centered scores	Macro-first and factors-first; one lag; two- and twelve-lag sensitivity
Component comparison	Same sample; three versus six centered scores	Common one-lag specification; six-factor matched-sample one-/two-lag comparison
Fixed-reference benchmark	1990–January 2025; three original scores	Original central-tendency series; arithmetic-mean counterpart; original recursive and reduced-form responses
Observed-shock projection	1978–January 2025	Original three-score and revised six-centered-score systems; monetary and oil series jointly
COVID recursive VAR	March 2020–January 2025	Frozen pre-COVID or archived full-sample basis; three original factors, one/two lags, both orderings; archived four-lag point responses; frozen centered-three counterpart
Factor-only VAR	1978–January 2025; four original scores	Standardized scores; two lags; recursive and reduced-form responses
COVID-only LP	March 2020–January 2025	Frozen pre-COVID basis; full-basis and long-run-control checks
Pooled predictive LP	1990–January 2025	Full-sample and COVID-total slopes; original three-factor and centered-six specifications

C.1 Inflation responses and recursive ordering

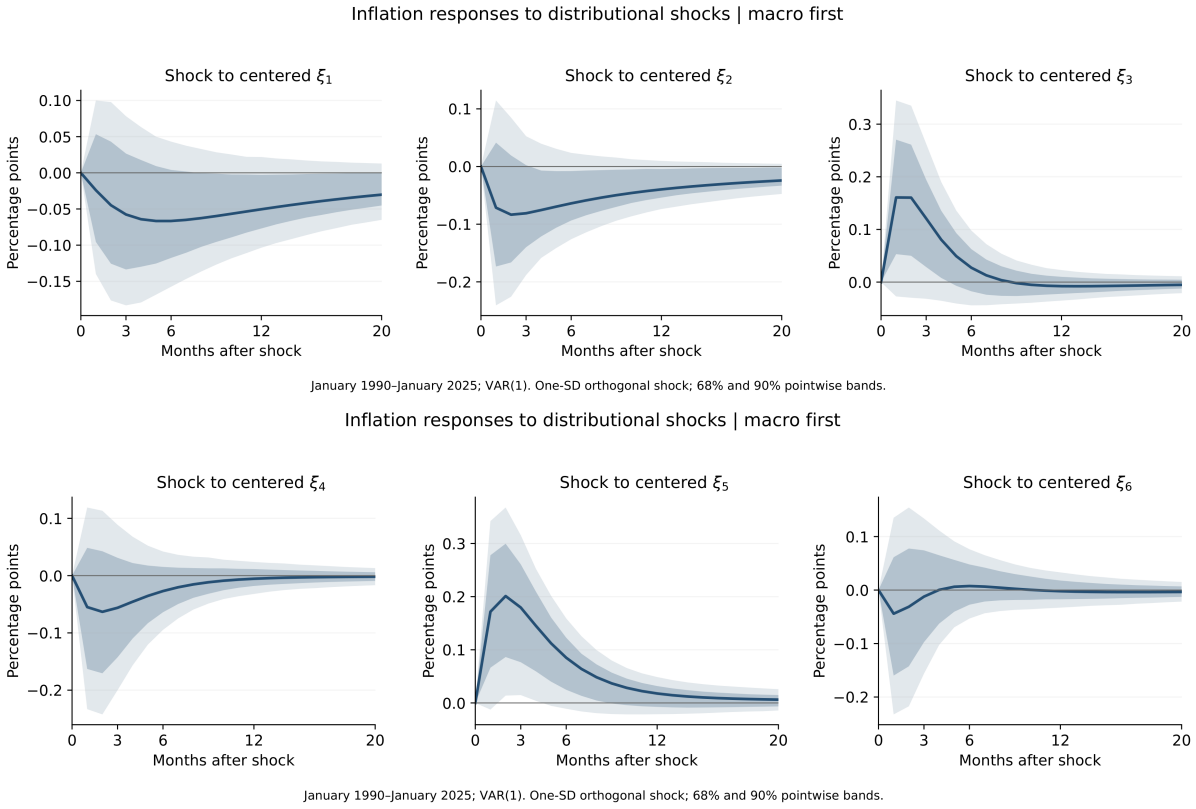


Figure C.1: Inflation responses to each centered-score shock: macroeconomic variables first
Notes: VAR(1), January 1990–January 2025. Each panel follows one positive one-standard-deviation orthogonal score shock. The response is annualized monthly CPI inflation in percentage points. Dark and light bands denote 68 and 90 percent pointwise residual-bootstrap intervals. The centered factors are numbered in variance order; the original left-/right-shift labels are not imposed on them.

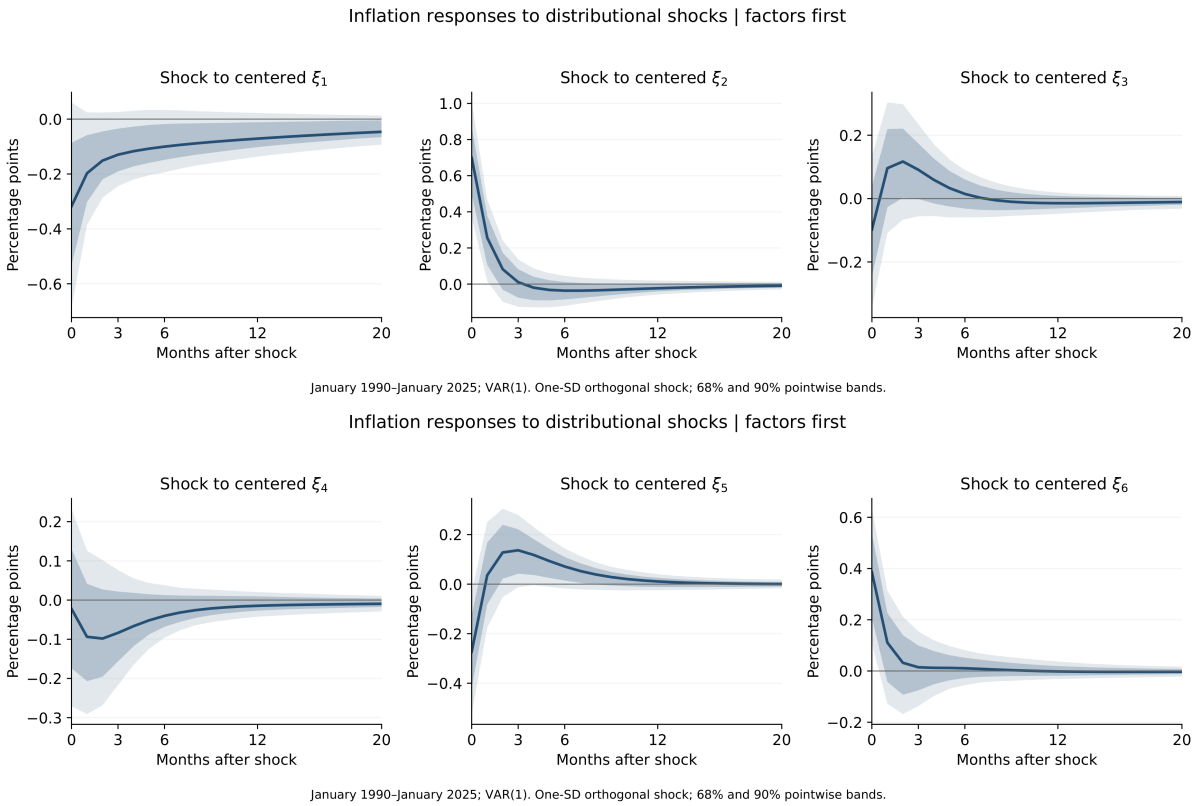


Figure C.2: Inflation responses to each centered-score shock: distributional scores first

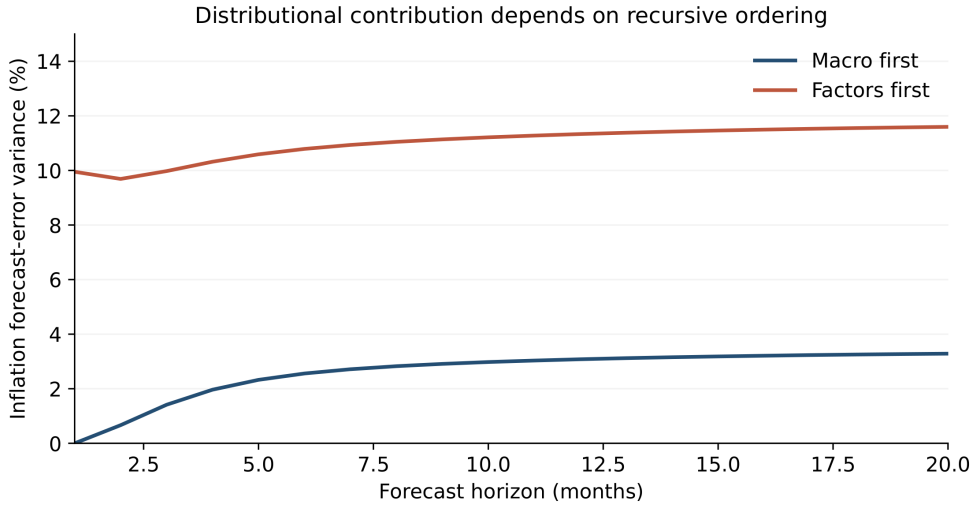


Figure C.3: Ordering sensitivity of the distributional share of inflation forecast-error variance
Notes: The six score-shock shares are summed. The zero one-month share in the macro-first model follows directly from its contemporaneous restrictions. Shares describe the fitted recursive systems and do not establish a causal contribution without those restrictions.

C.2 Responses associated with observed macroeconomic shocks

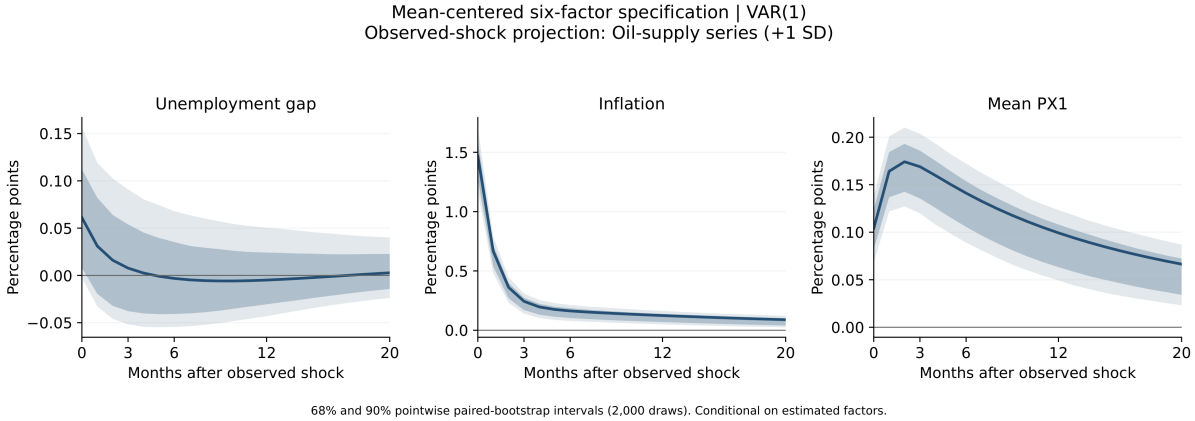


Figure C.4: Macroeconomic responses associated with the oil-supply-news series

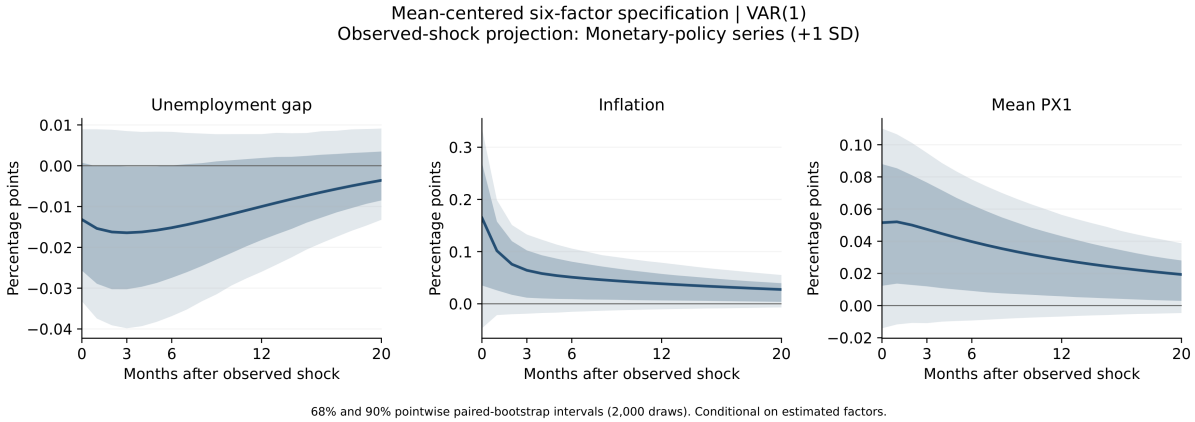


Figure C.5: Macroeconomic responses associated with the monetary-policy series

Notes: January 1978–January 2025; arithmetic mean PX1 and six centered scores. Reduced-form residuals are projected jointly on the two supplied observed series. Impacts are scaled by each series' sample standard deviation after lag trimming and propagated using the fitted VAR. Bands are pointwise percentiles of 2,000 paired residual-and-series bootstrap draws. These plots do not identify a complete structural shock system; no structural historical decomposition is attributed to these two series.

C.3 Predictive distributional effects during COVID

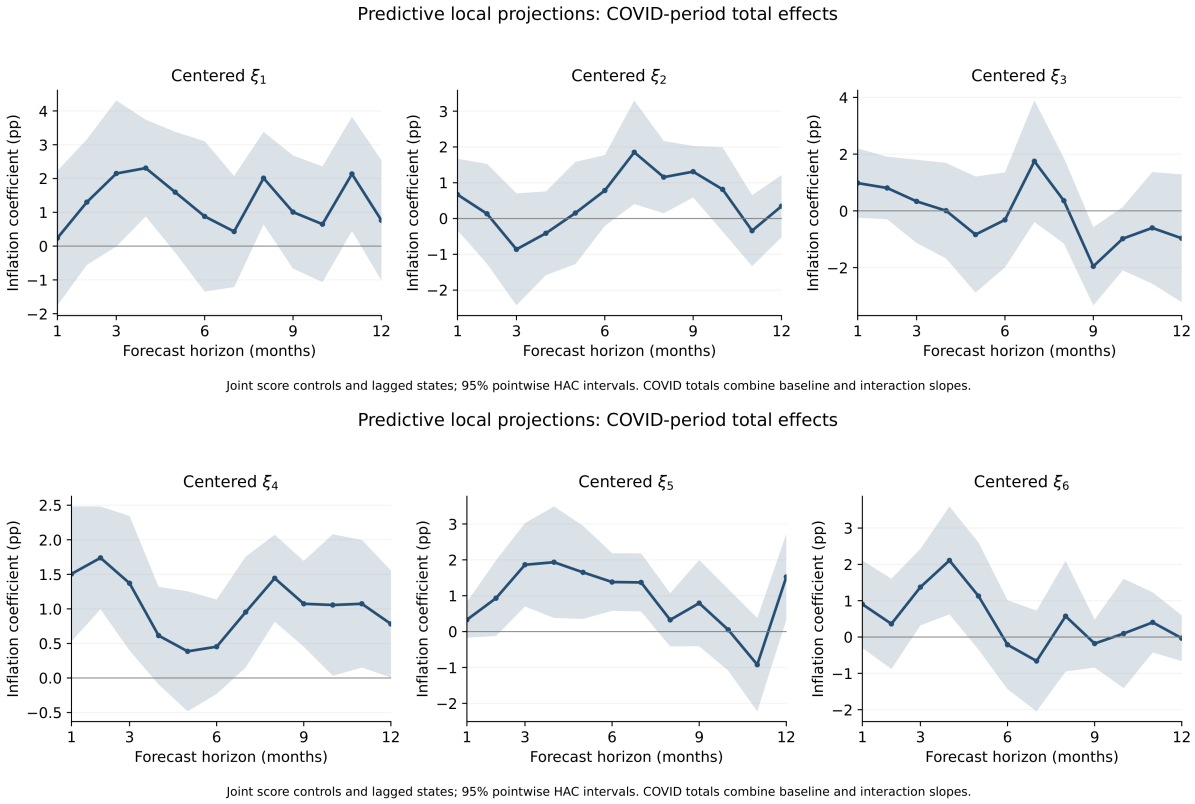


Figure C.6: COVID-total predictive coefficients for the six centered scores

Notes: Pooled full-sample local projections with COVID interactions, not regressions estimated only on the COVID subsample. Effects sum baseline and interaction coefficients. Intervals are 95 percent pointwise HAC intervals; the joint tests in Table 34 adjust across twenty horizons.

Table 34: Joint predictive content of six mean-centered scores

Horizon (months)	1	3	6	8	12
Full-sample joint p	0.062	0.196	0.248	0.421	0.093
COVID-total joint p	0.011	< 0.001	0.004	< 0.001	0.017
COVID-total Holm-adjusted p	0.032	< 0.001	0.016	< 0.001	0.034
COVID-increment Holm-adjusted p	< 0.001	< 0.001	< 0.001	< 0.001	0.082

Notes: Six-restriction Wald tests of the score coefficients jointly. COVID totals add baseline and March 2020–January 2025 interaction slopes; inference uses their full covariance. The COVID-increment row instead tests the six interaction increments jointly. The dependent variable is annualized monthly CPI inflation at $t+h$. Controls include current inflation, unemployment, arithmetic mean PX1, all six scores, the stored long-run expectation (verified as PX5 at $t-1$), and one lag of inflation, unemployment, mean PX1, and all scores. Bartlett HAC bandwidth is $\max(12, h+1)$, with $n/(n-k)$ correction and asymptotic chi-square reference. Holm adjustment covers all twenty horizons. Forecast-origin sample sizes decline from 416 at $h=1$ to 405 at $h=12$.

C.4 Historical shock contributions

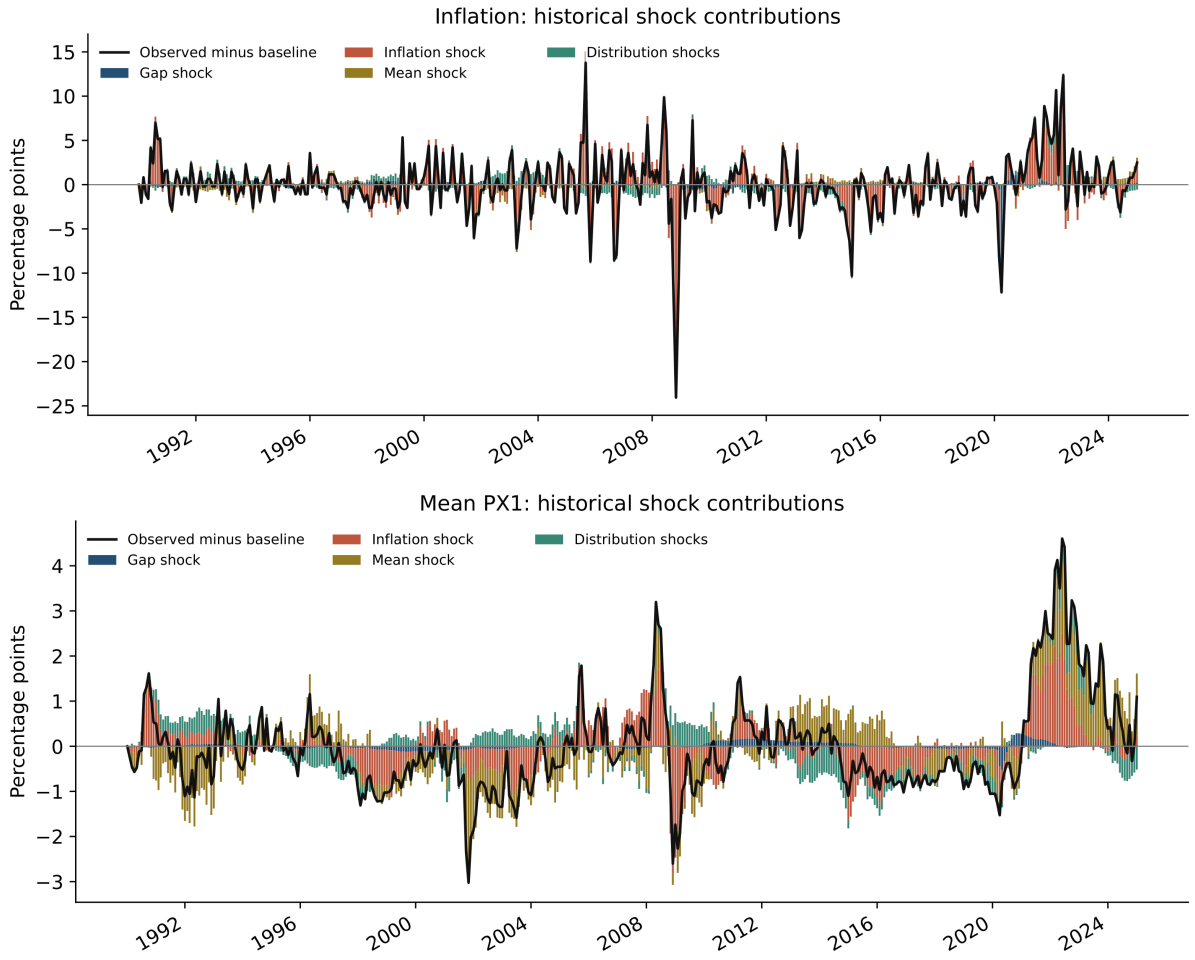


Figure C.7: Signed historical contributions to inflation and mean expectations

Notes: Main centered-six VAR(1), macroeconomic variables first. The six distributional contributions are grouped for display. The line is the observed series minus the fitted baseline due to initial conditions and the intercept; the colored contributions sum to this line. Complete individual contributions and the baseline are retained in the numerical output. These are signed historical contributions, not forecast-error variance shares.

D Robustness Checks

Back to appendix contents

Regional robustness checks are reported in Appendix A.9. The checks in this final appendix address specific sources of uncertainty: the representation of expectations, omitted inflation persistence and nonlinear mean effects, temporal dependence, regional concentration of identification, and restrictions used to interpret dynamic innovations. The checks use the actual arithmetic PX1 mean. Results that weaken an interpretation are reported alongside those that support it.

D.1 Robustness of the Mean-Centered Aggregate Results

Table 35 reports targeted changes to the number of components, the covariance estimator, the estimation period, and density construction. Every specification retains the same unemployment-gap and shock controls and the arithmetic mean of the individual PX1 responses. The first two columns of inference distinguish the information in the functional scores beyond the mean from their incremental information conditional on conventional moments.

The six-factor block remains jointly significant using HAC bandwidths of six and twenty-four months. Three components contain less information than six; the incremental test for components four through six in the main specification has $p = 0.013$. In the pre-COVID sample, with the density reference and basis estimated through December 2019, the six-score block has $p = 0.067$, compared with $p = 0.113$ after conditioning on moments. The mean PX1 coefficient remains positive.

Re-estimating the densities and all six components using bandwidths $0.75h$ and $1.25h$ gives joint score-block p-values of 0.0015 and below 0.001, respectively; conditional on moments, the corresponding values are 0.210 and 0.078. Restricting responses used for density construction to the pooled first and ninety-ninth percentiles gives $p = 0.003$ beyond the untrimmed mean and $p = 0.045$ conditional on moments. This exercise changes the tail information supplied to FPCA while preserving the main regression mean and moment controls. It is a sensitivity exercise, rather than the preferred treatment of the survey tails.

Allowing a cubic polynomial in mean PX1 yields a six-factor joint p-value below 0.001, or 0.062 conditional on conventional moments. Including the first two lags of inflation on the unchanged 417-month sample yields $p = 0.005$ and $p = 0.058$, respectively. These checks assess whether the distributional association is captured by nonlinearities in the mean or persistence in inflation.

The evidence therefore distinguishes information beyond the mean from an unrestricted claim that functional scores dominate all conventional moments. The latter conclusion is not supported uniformly across specifications. These exercises also retain the distinction between an association in the Phillips Curve and a structurally identified expectations shock. Reported inference conditions on the estimated densities and eigenfunctions; it does not incorporate uncertainty from estimating those objects.

Table 35: Aggregate Phillips Curve: targeted robustness checks

	N	Mean PX1	R^2	FPCA p	FPCA p, with moments
Mean-centered: six components	417	1.905	0.434	< 0.001	0.113
		(0.252)			
Three components	417	1.700	0.425	0.113	0.688
		(0.288)			
HAC(6)	417	1.905	0.434	0.005	0.329
		(0.298)			
HAC(24)	417	1.905	0.434	< 0.001	0.015
		(0.236)			
Original finite evaluation support	417	1.905	0.434	< 0.001	0.114
		(0.252)			
Pre-COVID sample and basis	356	1.556	0.417	0.067	0.113
		(0.272)			
Cubic polynomial in mean PX1	417	1.649	0.437	< 0.001	0.062
		(0.364)			
Inflation lags 1 and 2	417	1.403	0.555	0.005	0.058
		(0.252)			
Bandwidth 0.75h	417	1.927	0.435	0.001	0.210
		(0.278)			
Bandwidth 1.25h	417	1.847	0.432	< 0.001	0.078
		(0.238)			
Density responses trimmed at 1st/99th percentiles	417	1.856	0.437	0.003	0.045
		(0.356)			

Notes: OLS estimates. The mean coefficient and R^2 refer to the model including the functional scores without conventional moments. Parentheses report HAC standard errors. Joint tests are HAC Wald tests. Unless specified otherwise, the sample is May 1990–January 2025 and the HAC bandwidth is twelve months. The final column adds raw-response variance, standardized skewness and Pearson kurtosis. Bandwidth and response-trimming exercises re-estimate densities and the FPCA basis; all use 1,024 grid points. The cubic specification augments the mean with $(\mu_t - \bar{\mu})^2$ and $(\mu_t - \bar{\mu})^3$; its reported mean coefficient is the marginal effect at the sample mean. The lag specification includes both π_{t-1} and π_{t-2}. In the trimming exercise, the mean used to center the density is recalculated among retained responses, while the regression retains the original untrimmed mean and moment controls.

D.2 Robustness of the dynamic results

The dynamic checks vary the recursive ordering, the number of centered components, lag length, the basis-estimation period, and the covariance estimator used for predictive tests. The mean in every revised specification is the arithmetic average of individual monthly PX1 responses. The three-score COVID counterpart retains the original six-variable dimension, rather than inserting six shape factors into a 59-month system without a separate specification change.

Table 36 reports lag-length diagnostics for the full-sample nine-variable system. All fitted models are stable, with the largest companion-root modulus below one. Increasing the lag order does not eliminate the residual serial correlation detected by the adjusted Portmanteau test through 24 months. Consequently, the residual-bootstrap bands should be read as conditional on the fitted VAR, rather than as resolving its dynamic misspecification. The predictive local projections use HAC inference directly.

The conventional joint test of the six lagged scores in the VAR(1) inflation equation has $p = 0.312$, compared with $p = 0.032$ under HAC(12). At two lags, these values are 0.121 and 0.051. Longer-lag systems reject the joint null under both covariance choices, but the number of restrictions increases to 36 or 72, and the twelve-lag system estimates 109 parameters per equation. Its high-dimensional asymptotic HAC test should not be treated as decisive small-sample evidence. The reverse predictive test, from lagged inflation to the six scores in VAR(1), has HAC(12) $\chi^2(6) = 25.66$ and $p < 0.001$.

The estimated magnitude of the distributional contribution is also sensitive. At a twelve-month horizon its inflation forecast-error variance share is 3.1 percent in the main VAR(1), 4.9 percent in VAR(2), and 32.1 percent in VAR(12), all with macroeconomic variables ordered first. Reversing the contemporaneous ordering in VAR(1) raises the share to 11.3 percent. These comparisons show that the share attributed to shape innovations is not a stable structural estimate. The twelve-lag bootstrap retains 43 finite but unstable fitted draws among 2,000 replications, following the original retention convention; the numerical archive records this diagnostic.

Replacing six centered components with three reduces the twelve-month distributional share in the main ordering to 1.4 percent. The companion one-/two-lag comparison also uses matched dependent-variable dates, March 1990–January 2025. Separate COVID estimates compare the original full-sample basis with a basis frozen before COVID, and use both recursive orderings. The covariance, ordering, and sample checks therefore assess different sources of uncertainty rather than being interchangeable robustness exercises.

The predictive evidence is particularly strong in the COVID specification at the reported horizons. In the centered-six pooled local projections, the joint COVID-total tests at horizons one, three, six, eight, and twelve months remain significant after Holm adjustment across all twenty horizons. Full-sample joint tests do not reject at these displayed horizons. This evidence concerns conditional forecasting information in the shape of expectations and is compatible with feedback from inflation to expectations; it does not by itself demonstrate exogenous expectations formation. Re-estimating the centered-six projections with the reference density, eigenfunctions, and score scaling frozen at December 2019 gives the same conclusion for the displayed COVID-total tests: all five survive Holm adjustment across twenty horizons. This check removes post-COVID information from the construction of the predictive shape coordinates. Direct tests of the six interaction increments also reject unchanged slopes at one, three, six, and eight months after adjustment, while the twelve-month adjusted change test has $p = 0.082$.

Table 36: Lag length, residual dependence, and distributional predictive content

VAR lag order	1	2	6	12
Parameters per equation	10	19	55	109
Residual degrees of freedom	410	400	360	300
Largest companion-root modulus	0.944	0.961	0.989	0.993
Portmanteau(24) p	< 0.001	0.002	0.016	< 0.001
Score-lag block: conventional p	0.312	0.121	0.001	0.002
Score-lag block: HAC(12) p	0.032	0.051	< 0.001	< 0.001
Number of score-lag restrictions	6	12	36	72

Notes: Source sample January 1990–January 2025. The dependent-variable sample shortens with the lag order. The system contains the unemployment gap, annualized monthly CPI inflation, arithmetic mean PX1, and six mean-centered scores. Conventional tests use the equation's homoskedastic OLS covariance and an F reference; HAC tests use a Bartlett kernel with twelve lags, no finite-sample multiplier, and a chi-square reference. The adjusted Portmanteau statistic tests system residual autocorrelation through lag 24, with $9^2(24 - p)$ degrees of freedom. Stability does not imply serially uncorrelated residuals. Larger lag orders add both parameters and restrictions, making their nominal asymptotic tests less directly comparable.

E Historical Distributions

E.1 Monthly Densities across Historical Episodes

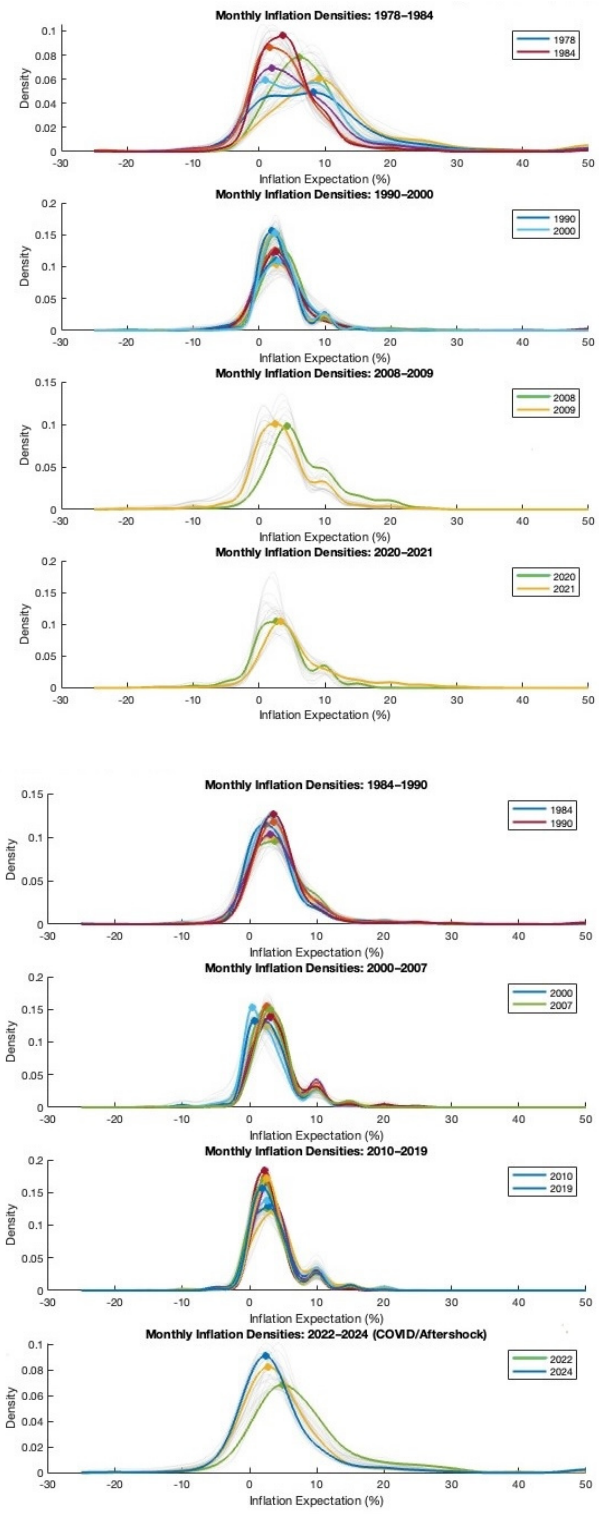


Figure E.1: Monthly Inflation-Expectation Densities across Historical Episodes

Each panel retains its original episode dates and comparison years. Horizontal axes: one-year-ahead inflation expectation (%). Vertical axes: density. Back to appendix contents.

References

Acosta, M., A. Ajello, M. Bauer, F. Loria, and S. Miranda-Agrippino (2025). *Financial Market Effects of FOMC Communication: Evidence from a New Event-Study Database*. Working Paper 2025-30. Revised August 2026. Federal Reserve Bank of San Francisco. DOI: 10.24148/wp2025-30.

Anderl, C. and G. M. Caporale (2024). "Functional Shocks to Inflation Expectations and Real Interest Rates and Their Macroeconomic Effects". In: *Review of World Economics* 160.4, pp. 1543–1575.

Armantier, O., G. Koşar, R. Pomerantz, D. Skandalis, K. Smith, G. Topa, and W. van der Klaauw (2021). "How Economic Crises Affect Inflation Beliefs: Evidence from the COVID-19 Pandemic". In: *Journal of Economic Behavior & Organization* 189, pp. 443–469.

Armantier, O., G. Koşar, J. Somerville, G. Topa, W. van der Klaauw, and J. C. Williams (2023). *The Curious Case of the Rise in Deflation Expectations*. Staff Report 1037. Originally October 2022; revised November 2023. Federal Reserve Bank of New York.

Ascari, G., P. Bonomolo, and A. Celani (Mar. 2024). *The Macroeconomic Effects of Inflation Expectations: The Distribution Matters*. Discussion Paper 18937. Centre for Economic Policy Research.

Ascari, G. and A. M. Sbordone (2014). "The Macroeconomics of Trend Inflation". In: *Journal of Economic Literature* 52.3, pp. 679–739.

Babb, N. R. and A. K. Detmeister (2017). *Nonlinearities in the Phillips Curve for the United States: Evidence Using Metropolitan Data*. Finance and Economics Discussion Series 2017-070. Board of Governors of the Federal Reserve System.

Bae, E., A. Hodge, and A. Weber (2024). *U.S. Inflation Expectations During the Pandemic*. Working Paper 2024/025. International Monetary Fund.

Barnichon, R. and A. H. Shapiro (2024). "Phillips Meets Beveridge". In: *Journal of Monetary Economics* 148. Supplement, p. 103660.

Barrales-Ruiz, J., A. Islam, M. Mohammed, and I. Panovska (2026). "From Beliefs to Prices: Analyzing How Inflation Expectations Affect the Inflation Distribution". In: *Journal of Economic Dynamics and Control* 186, p. 105318.

Beaudry, P., C. Hou, and F. Portier (2026). "Did Recent Inflation Reflect a Nonlinear Phillips Curve?" In: *American Economic Review: Insights*. Forthcoming.

Binder, C. (2020). "Coronavirus Fears and Macroeconomic Expectations". In: *Review of Economics and Statistics* 102.4, pp. 721–730.

Binder, C. and R. Kamdar (2022). "Expected and Realized Inflation in Historical Perspective". In: *Journal of Economic Perspectives* 36.3, pp. 131–156.

Binder, C. C., R. Kamdar, and J. M. Ryngaert (2024). "Partisan Expectations and COVID-Era Inflation". In: *Journal of Monetary Economics* 148. Supplement, p. 103649.

Bosq, D. (2000). *Linear Processes in Function Spaces: Theory and Applications*. New York: Springer.

Brandão-Marques, L., G. Gelos, D. J. Hofman, J. Otten, G. K. Pasricha, and Z. Strauss (2023). *Do Household Expectations Help Predict Inflation?* Working Paper 2023/224. International Monetary Fund.

Carroll, C. D. (2003). "Macroeconomic Expectations of Households and Professional Forecasters". In: *Quarterly Journal of Economics* 118.1, pp. 269–298.

Chang, M., X. Chen, and F. Schorfheide (2024). "Heterogeneity and Aggregate Fluctuations". In: *Journal of Political Economy* 132.12, pp. 4021–4067.

Chang, M. and F. Schorfheide (2024). *On the Effects of Monetary Policy Shocks on Income and Consumption Heterogeneity*. Working Paper 32166. National Bureau of Economic Research.

Chang, Y., F. Gómez-Rodríguez, and G. H. Hong (2022). *The Effects of Economic Shocks on Heterogeneous Inflation Expectations*. Working Paper 2022/132. International Monetary Fund.

Chang, Y., C. S. Kim, and J. Y. Park (2016). "Nonstationarity in Time Series of State Densities". In: *Journal of Econometrics* 192.1, pp. 152–167.

Chang, Y., S. Kim, and J. Y. Park (2025). *How Do Macroaggregates and Income Distribution Interact Dynamically? A Novel Structural Mixed Autoregression with Aggregate and Functional Variables*. CAMA Working Paper 7/2025. Centre for Applied Macroeconomic Analysis, Australian National University.

Cogley, T. and A. M. Sbordone (2008). "Trend Inflation, Indexation, and Inflation Persistence in the New Keynesian Phillips Curve". In: *American Economic Review* 98.5, pp. 2101–2126.

Coibion, O. and Y. Gorodnichenko (2015). "Information Rigidity and the Expectations Formation Process: A Simple Framework and New Facts". In: *American Economic Review* 105.8, pp. 2644–2678.

Coibion, O., Y. Gorodnichenko, and R. Kamdar (2018). "The Formation of Expectations, Inflation, and the Phillips Curve". In: *Journal of Economic Literature* 56.4, pp. 1447–1491.

Coibion, O., Y. Gorodnichenko, and S. Kumar (2018). "How Do Firms Form Their Expectations? New Survey Evidence". In: *American Economic Review* 108.9, pp. 2671–2713.

Coibion, O., Y. Gorodnichenko, and M. Weber (2022). "Monetary Policy Communications and Their Effects on Household Inflation Expectations". In: *Journal of Political Economy* 130.6, pp. 1537–1584.

D'Acunto, F., U. Malmendier, and M. Weber (2023). "What Do the Data Tell Us about Inflation Expectations?" In: *Handbook of Economic Expectations*. Academic Press. Chap. 5, pp. 133–161.

Doh, T. and A. L. Smith (2022). "A New Approach to Integrating Expectations into VAR Models". In: *Journal of Monetary Economics* 132, pp. 24–43.

Doser, A., R. Nunes, N. Rao, and V. Sheremirov (2023). "Inflation Expectations and Nonlinearities in the Phillips Curve". In: *Journal of Applied Econometrics* 38.4, pp. 453–471.

Fitzgerald, T., C. Jones, M. Kulish, and J. P. Nicolini (2024). "Is There a Stable Relationship between Unemployment and Future Inflation?" In: *American Economic Journal: Macroeconomics* 16.4, pp. 114–142.

Grishchenko, O. V. and L. Wilcox (2024). *Tale About Inflation Tails*. Finance and Economics Discussion Series 2024-028. Board of Governors of the Federal Reserve System.

Hall, P. and J. L. Horowitz (2007). "Methodology and Convergence Rates for Functional Linear Regression". In: *Annals of Statistics* 35.1, pp. 70–91.

Hazell, J., J. Herreño, E. Nakamura, and J. Steinsson (2022). "The Slope of the Phillips Curve: Evidence from U.S. States". In: *Quarterly Journal of Economics* 137.3, pp. 1299–1344.

Hooper, P., F. S. Mishkin, and A. Sufi (2020). "Prospects for Inflation in a High Pressure Economy: Is the Phillips Curve Dead or Is It Just Hibernating?" In: *Research in Economics* 74.1, pp. 26–62.

Hottman, C. and R. Reyes-Heroles (2023). *Globalization, Inflation Dynamics, and the Slope of the Phillips Curve*. Working paper, September 30.

Huber, F., M. Marcellino, and T. Tornese (2024). *The Distributional Effects of Economic Uncertainty*. arXiv preprint arXiv:2411.12655. DOI: 10.48550/arXiv.2411.12655.

Känzig, D. R. (2021). "The Macroeconomic Effects of Oil Supply News: Evidence from OPEC Announcements". In: *American Economic Review* 111.4, pp. 1092–1125. DOI: 10.1257/aer.20190964.

Kilian, L. and H. Lütkepohl (2017). *Structural Vector Autoregressive Analysis*. Cambridge University Press.

Łyziak, T., M. Pedersen, and E. Stanisławska (2025). "Consumer Inflation Expectations and Local Price Changes: Learning from Experience". In: *Journal of Macroeconomics* 86, p. 103725.

Łyziak, T. and X. S. Sheng (2023). "Disagreement in Consumer Inflation Expectations". In: *Journal of Money, Credit and Banking* 55.8, pp. 2215–2241.

Malmendier, U. and S. Nagel (2016). "Learning from Inflation Experiences". In: *Quarterly Journal of Economics* 131.1, pp. 53–87.

Mankiw, N. G. and R. Reis (2002). "Sticky Information Versus Sticky Prices: A Proposal to Replace the New Keynesian Phillips Curve". In: *Quarterly Journal of Economics* 117.4, pp. 1295–1328.

Mankiw, N. G., R. Reis, and J. Wolfers (2003). "Disagreement about Inflation Expectations". In: *NBER Macroeconomics Annual* 18, pp. 209–248.

McLeay, M. and S. Tenreyro (2020). "Optimal Inflation and the Identification of the Phillips Curve". In: *NBER Macroeconomics Annual* 34, pp. 199–255.

Meeks, R. and F. Monti (2023). "Heterogeneous Beliefs and the Phillips Curve". In: *Journal of Monetary Economics* 139, pp. 41–54.

Mirkov, N. and A. Steinhauer (2018). "Asymmetry of Individual and Aggregate Inflation Expectations: A Survey". In: *The Manchester School* 86.4, pp. 446–467.

Muth, J. F. (1961). "Rational Expectations and the Theory of Price Movements". In: *Econometrica* 29.3, pp. 315–335.

Park, J. Y. and J. Qian (2012). "Functional Regression of Continuous State Distributions". In: *Journal of Econometrics* 167.2, pp. 397–412.

Petersen, A. and H.-G. Müller (2016). "Functional Data Analysis for Density Functions by Transformation to a Hilbert Space". In: *The Annals of Statistics* 44.1, pp. 183–218.

Ramsay, J. O. and B. W. Silverman (2005). *Functional Data Analysis*. Second. New York: Springer.

Reis, R. (2021a). "Losing the Inflation Anchor". In: *Brookings Papers on Economic Activity*. Fall, pp. 307–361.

Reis, R. (2021b). *The People versus the Markets: A Parsimonious Model of Inflation Expectations*. Discussion Paper 15624. Centre for Economic Policy Research.

Reis, R. (2022). *The Burst of High Inflation in 2021–22: How and Why Did We Get Here?* Discussion Paper 17514. Centre for Economic Policy Research.

Rich, R. and J. Tracy (2021). "A Closer Look at the Behavior of Uncertainty and Disagreement: Micro Evidence from the Euro Area". In: *Journal of Money, Credit and Banking* 53.1, pp. 233–253.

Silverman, B. W. (1986). *Density Estimation for Statistics and Data Analysis*. London: Chapman and Hall.

Sims, C. A. (2003). "Implications of Rational Inattention". In: *Journal of Monetary Economics* 50.3, pp. 665–690.

Tsiaplias, S. (2020). "Time-Varying Consumer Disagreement and Future Inflation". In: *Journal of Economic Dynamics and Control* 116, p. 103903.

Weber, M., F. D'Acunto, Y. Gorodnichenko, and O. Coibion (2022). "The Subjective Inflation Expectations of Households and Firms: Measurement, Determinants, and Implications". In: *Journal of Economic Perspectives* 36.3, pp. 157–184.